

We thank Dr. Omid Alizadeh-Choobari and the three anonymous referees for their valuable comments and constructive suggestions on the manuscript. Below, we explain how the comments and suggestions are addressed and make note of the revision we made in the manuscript.

Referee #1

General comments:

- *Using various observational datasets, the present study has evaluated the performance of the quasi-global WRF-Chem model in terms of simulating both meteorological fields and aerosol properties over the Pacific region. Code modifications for a quasi-global WRF-Chem simulation were conducted at the Pacific Northwest National Laboratory (PNNL), and the modifications are planned to be incorporated in the future available release of WRF-Chem. The overall conclusion of the present study is that the model well simulated spatial and seasonal variability of both meteorological fields and aerosol properties across the Pacific region. Apart from running the WRF-Chem model on the quasi-global scale, which has already been conducted and its performance evaluated by Zhao et al. (2013b), the present study does not provide any new insights into the concept of transport of aerosols across the Pacific Ocean. Nevertheless, the observed datasets that have been gathered and the conducted numerical simulation have the potential to extend the current knowledge of the scientific community on the meteorological influences on transport of aerosols across the Pacific Ocean in different seasons. My general comment is major revision of the manuscript, both in the review provided in the introduction and in the analysis of the results. More details are provided below.*

We thank Dr. Omid Alizadeh-Choobari for a detail review. As we stated in the manuscript, “Although the quasi-global WRF-Chem simulation described by Zhao et al. (2013b) has been used to provide realistic chemical lateral boundary conditions for multiple regional modeling studies (e.g., Zhao et al., 2014; Fan et al., 2015), its evaluation has not been documented so far.” and “We focus on the simulation over the trans-Pacific transport region as a first step to evaluate the simulation for providing consistent lateral chemical boundaries for nested regional simulations used to investigate the impact of transported aerosols on regional air quality and climate.”, the purpose of this paper is to provide a documentation of evaluating the quasi-global WRF-Chem simulations particularly for trans-Pacific transport, which is important and was not done in Zhao et al. (2013b) that focused on the sensitivity of modeling dust to size distributions. The text is revised as the reviewer suggested. We are following-up on using the quasi-global simulations for providing boundary conditions to higher resolution simulations to study the impacts of trans-Pacific aerosols on clouds and precipitation in the western U.S.

Specific comments:

- *The first paragraph of the introduction section discusses about the trans-Pacific transport of aerosols which has already been well known, and with much more details have been already discussed in previous articles. Seasonal variations in aerosol optical depth across the Pacific that have been later discussed in Section*

4.2.1 do not add any new insights into the current understanding of the subject. What is more important and should be discussed in the introduction and later on in the results section of the manuscript are different meteorological mechanisms that are responsible for both emission (particularly for natural aerosols such as dust) and transport of aerosols in different seasons. In this way, part of the strong seasonal variations in aerosol optical depth that have been presented in Figs. 4 and 5 can be explained. For example, as discussed by Alizadeh-Choobari et al. (2014) both shifting and strength of the prevailing wind over the Pacific Ocean are responsible for the transport pathway of aerosols and the extent that they can travel. In addition, as depending on the season, aerosols are transported at different elevations across the Pacific Ocean, the meteorological conditions behind such seasonal variations can be fully discussed. As an example, such factors for May 2007 are discussed by Uno et al. (2009).

As we stated in the manuscript, “We focus on the simulation over the trans-Pacific transport region as a first step to evaluate the simulation for providing consistent lateral chemical boundaries for nested regional simulations used to investigate the impact of transported aerosols on regional air quality and climate.” Hence the purpose of the seasonal analysis is to evaluate the quasi-global simulations of aerosols using WRF-Chem that can further provide chemical boundary conditions for nested regional simulations rather than focusing on investigating the mechanisms driving the seasonal variations of aerosols, which has been well examined in previous studies as the reviewer also mentioned. We highlighted the potential aerosol impact on the air quality and climate over the western U.S. in the introduction because the next step of research is to use this quasi-global WRF-Chem simulation to drive the nested simulations over the western U.S. for understanding the trans-Pacific aerosols’ impact there. Now we add more discussion of the previous studies about the trans-Pacific aerosols in the introduction, “Previous studies have shown that aerosols outflowed from the Asian continent can be transported by the mid-latitude prevailing westerlies across the Pacific Ocean and ultimately reach the west coast of North America and beyond, and its efficiency is the largest in spring (e.g., Takemura et al., 2002; Chin et al., 2007; Yu et al., 2008; Uno et al., 2009, 2011; Alizadeh-Choobari et al., 2014). Takemura et al. (2002) found that the contribution of anthropogenic aerosols to the total aerosol optical thickness is comparable to that of dust during the transport over the North Pacific in spring. Chin et al. (2007) found that the long-range transported dust brought 3 to 4 times more fine particles than anthropogenic pollutants to the total surface fine particles over the U.S. on annual average with a maximum influence in spring and over the northwestern U.S. Yu et al. (2008) estimated that about 25% of the Asian outflow reaches the west coast of North America, which is about 15% of the total North American emissions, and the transport fluxes are largest in spring and smallest in summer. Uno et al. (2011) also revealed that the dust trans-Pacific path sometimes could be split into two branches: a southern path to

the central U.S. and a northern path that is trapped and stagnant for a longer time and finally subsides over the northwestern U.S.”

We did briefly explain the underlying mechanisms of seasonal variation in the manuscript “Previous studies found that trans-Pacific transport of air pollutants is most efficient in MAM due to active cyclonic activity and that pollutants are lifted to the free troposphere where they can be rapidly transported across the Pacific by strong westerlies (e.g., Forster et al., 2004; Liang et al., 2004; Heald et al., 2006; Yu et al., 2008).” We also associated the model biases with meteorological processes, e.g., “The model generally underestimates the retrieved AOD over the North Pacific with the annual mean value of 0.13 that is lower than the retrieved values of 0.15 (MODIS) and 0.16 (MISR). This negative bias is mainly due to the underestimation of the oceanic AOD to the south of 20°N, which may be due to underestimation of marine emissions (Yu et al., 2003) and/or overestimation of aerosol wet removal associated with the positive bias in precipitation (Fig. 3). The discrepancy may also be due to higher uncertainty at low aerosol level (Levy et al., 2013) and cloud contamination in the retrievals that leads to an overestimation of AOD in some regions of the North Pacific (e.g., Zhang and Reid, 2006).”

- ***The averaged methods that have been used in the study caused the observed and simulated data to be missing over large areas in summer. This has led to the wrong conclusion that summer is the cleanest season in Regions 2 and 3 (lines 355 and 406, and Fig. 5), while in reality this is not the case.***

First, we sampled observations and simulations at the same time and location. Although this sampling method results in some missing data due to cloud impact on satellite retrievals, it reduces the sampling discrepancy in space and time between satellites and simulations and assures a fair comparison. Second, our results about seasonal variation of aerosols over Pacific from either satellite retrievals or simulations are generally consistent with previous studies (e.g., Fig. 3 and 4 in Yu et al., 2008, and Fig. 3 in Yu et al., 2012) using satellites and models that also show the smallest aerosol amounts in summer on average. We clarify this in the manuscript now “This seasonal variation is generally consistent with previous studies (Yu et al., 2008, 2012), although our sampling method results in more missing data from satellite retrievals in JJA than other seasons.”

Yu, H. B., L. A. Remer, M. Chin, H. S. Bian, R. G. Kleidman, and T. Diehl: A satellite-based assessment of transpacific transport of pollution aerosol, *J. Geophys. Res.*, 113, D14S12, doi:10.1029/2007JD009349, 2008.

Yu, H., L. A. Remer, M. Chin, H. Bian, Q. Tan, T. Yuan, and Y. Zhang: Aerosols from Overseas Rival Domestic Emissions over North America, *Science*, 337, 566-569, 2012.

- ***As the authors mentioned, there have been some modifications to run the WRF-Chem model on the quasi-global scale. Please briefly discuss these changes in the***

model description as this is a quite new aspect and novelty of the present study.

To configure the quasi-global WRF-Chem simulation, we modified the treatment of the chemical boundary conditions to use periodic boundary conditions in the zonal direction while the boundary treatment in the meridional direction is based on prescribed conditions. We also modified other parts of the model such as the oceanic emission schemes and convective transport scheme of tracers to produce more reasonable aerosol distributions globally. We now highlight these changes in the revised manuscript “Code modifications include changes to the chemical boundary treatment using periodic boundary conditions in the zonal direction for quasi-global WRF-Chem simulation. Other changes to the model include the oceanic (sea salt and dimethyl sulfide) emission schemes and the convective transport and removal scheme of tracers that play a significant role in quasi-global WRF-Chem simulations of aerosols.”

- ***Due to many writing problems, the manuscript should undergo a language revision.***

We made corrections to English writing.

- ***Last paragraph in page 5: The work of Alizadeh-Choobari et al. (2015) can be cited and discussed here. They conducted the WRF-Chem model to study the global distribution of mineral dust and its radiative forcing on the global scale.***

We apologize for missing the discussion of Alizadeh-Choobari et al. (2015), which is very relevant to our study. We have included it in the revision. In addition, we actually tried the WRF-Chem configuration adopted by Dr. Alizadeh-Choobari for global simulations, but we found the specific configuration only runs stably in global simulations with simple chemistry as used in Alizadeh-Choobari et al. (2015). This may be due to convergence issue of solving chemical reactions near the relatively pristine polar regions. However, more sophisticated chemistry is needed for the purpose of our studies on not only dust but also other anthropogenic aerosols. Therefore, a more stable quasi-global WRF-Chem configuration is used in our studies. We added more discussion about this in the revised manuscript “Alizadeh-Choobari et al. (2015) conducted a global WRF-Chem simulation of dust and its radiative forcing, which was configured with dust aerosol only without other aerosols and chemistry. However, WRF-Chem global simulation with sophisticated chemistry including anthropogenic and natural aerosols could not run stably due potentially to convergence issue of solving chemical reactions near the relatively pristine polar regions. Given the need of sophisticated chemistry to simulate not only dust but also other anthropogenic aerosols, a more stable near global coverage WRF-Chem configuration is used in this study to circumvent this technical difficulty to characterize the trans-Pacific transport of aerosols.”

Technical corrections:

- **Line 23: Write the WRF-Chem in full as it appears the first time in abstract.**

Done.

- **Line 25: Add “the” before “first time”**

Done.

- **Line 57 and in other parts of the manuscript: Add “the” before “Pacific Ocean”**

Done.

- **It is better to remove lines 127 to 131. The version of WRF-Chem can be mentioned in Section 2.1.**

Revised.

- **Line 147: You have mentioned that “cloud-ice-borne aerosols are not explicitly treated in the model”. Is it parameterized? Please specify that.**

Now we clarify it in the text “Cloud-ice-borne aerosols through ice nucleation of aerosols are not considered in the model, but the removal of aerosols by the droplet freezing process is considered.”

- **Line 325: Remove “of” before “2010-2014” here and throughout the manuscript.**

Done.

- **Line 338: Discuss possible explanation for the overestimation of model simulation in the specified regions.**

The overestimation of precipitation over the ITCZ may be due to biases from the convective parameterizations in producing tropical precipitation in WRF. More discussion about this is now added into the manuscript “The excessive precipitation over the tropical Pacific may be due to biases from the convective parameterizations in producing tropical precipitation in WRF, such as overestimation of precipitation efficiency from simple treatment of cloud microphysical processes in convective clouds, and biases in the prescribed temperature and humidity reference profiles (e.g., Fonseca et al., 2015; Hagos et al., 2016). Short sensitivity experiments we performed show that the WRF simulated tropical precipitation is sensitive to the choice of convective parameterizations (not shown).”

- **Line 548: You mean “the total aerosol amount”?**

We mean the total dust amount consisting of transpacific dust and local dust.

- **Line 593: remove “for first time”**

This is to emphasize that the evaluation is done for the first time, as we also state in the

abstract. Now we follow your suggestion as in abstract to change it as “for the first time”.

Anonymous Referee #2

General comments:

- *This paper presents a nice evaluation of a quasi-global WRF-Chem model in simulating trans-pacific transport of aerosol. Multiple satellites and in-situ observations are used to evaluate spatial, temporal and vertical distribution of aerosol simulations. Aerosol species over the West US and their contributions from local emissions are also discussed. This paper is well written and very useful for other researchers. I only have a few minor comments that should be addressed prior to publications.*

We thank the reviewer for a detailed review. Both text and figures are revised as the reviewer suggested.

Minor comments:

- **L170: Could you specify what kind of technical difficulties in running global WRF-Chem?**

Before configuring the quasi-global WRF-Chem simulations, we experimented with WRF-Chem configurations for global simulations, and found that only global simulations without sophisticated chemistry as adopted by Alizadeh-Choobari et al. (2015) can run stably. The reason may be due to convergence issue of solving chemical reactions near the relatively pristine polar regions. However, sophisticated chemistry is needed to simulate not only dust but also other anthropogenic aerosols. Therefore, a more stable quasi-global WRF-Chem configuration is used in our studies. We now add more discussion about this in the revised manuscript “Alizadeh-Choobari et al. (2015) conducted a global WRF-Chem simulation of dust and its radiative forcing, which was configured with dust aerosol only without other aerosols and chemistry. However, WRF-Chem global simulation with sophisticated chemistry including anthropogenic and natural aerosols could not run stably due potentially to convergence issue of solving chemical reactions near the relatively pristine polar regions. Given the need of sophisticated chemistry to simulate not only dust but also other anthropogenic aerosols, a more stable near global coverage WRF-Chem configuration is used in this study to circumvent this technical difficulty to characterize the trans-Pacific transport of aerosols.”

- **L283-286: Is CALIOP data collocated with model simulations? Please clarify.**

Yes. Now we clarify it in the manuscript “The model results are sampled for averaging at the locations and times where and when retrievals are available.”

- **L387-389: What’s the mean values for model simulations?**

The mean values from the model simulation are the same as those from the AERONET data. Now we clarify it as “The model reproduces exactly these values at the three sites

with correlation coefficients of 0.45, 0.65, and 0.64, respectively.”

- ***L441: “followed by DJF”?***

Revised.

- ***Figure 15: This figure needs some improvement. The dots are not easy to see.***

Now we revised the figure responding to the comments from other reviewers. Figure 15 now shows the monthly comparison between observation and simulation. The quality is improved.

Anonymous Referee #3

General comments:

- *This manuscript presents the model evaluation of 5-year quasi-global WRF-Chem simulations using various surface and satellite observational and reanalysis datasets. Despite the lack of direct aerosol measurement data especially over East Asia and Pacific Ocean, authors are able to use available satellite or ground-based retrieved aerosol optical properties such as AOD, AAOD, and EAE to compare with simulations and draw the conclusion that WRF-Chem model can well simulate the spatial and seasonal variability of aerosol properties and transport and evolution of aerosols over the trans-Pacific domain during the 5-year time period. This manuscript is generally well written with many interesting analyses. It's definitely of scientific interest to the research community and I would recommend it to be accepted after a minor revision.*

We thank the reviewer for a detailed review. Both text and figures are revised as the reviewer suggested.

Specific comments:

- *Lines 110-111: Using in-situ observational aerosol (including dust) data to evaluate the simulations especially over pollutant source regions such as East Asia for the trans-Pacific domain is critical to demonstrate the model's capability in accurately simulating aerosol transport/evolution. There are actually a few regular networks from China, Japan, and Korea that provide long-term observational or observational-derived data for PM_{2.5} or PM₁₀ to the public. However it takes some efforts in order to collect those data and might be out of the scope of work to the authors. At least I would like to see this lack of evaluation using in-situ data to be acknowledged as a limitation in the summary section.*

We used mostly space and ground based remote sensing data to evaluate the simulations because we cannot obtain the public-released observations of PM over East Asia for the simulation period. Although we are aware of the data from the Acid Deposition Monitoring Network in East Asia (EANET), they provide measurements only up to 2008, which may not be suitable for evaluating our simulations for 2010-2014. To the best of our knowledge, there are no publicly available in-situ observations that can be used to evaluate our simulated aerosols over East Asia. We thank the reviewer for pointing out possible sources of data that may be obtained from researchers in East Asia through collaboration, which would be included in our future studies. We have acknowledged this in the introduction “For lack of in-situ observations over East Asia and the Pacific Ocean for our simulation period, evaluation is performed mainly using reanalysis and satellite retrieval (e.g., CALISPO, MODIS, and MISR) datasets, along with available ground-based observations from AERONET and IMPROVE in the region.” and in the summary, we add “Evaluation of model results with in-situ observations would be informative. In-

situ data even for specific events are valuable especially over Asia and the Pacific where public data are currently sparse or inaccessible, although some observations may be obtained through collaborations.”

- ***Lines 338-339: What may cause this large overprediction for precipitation (authors didn't show any statistics, however from the plots alone it seems that the overprediction is more than 50% for some seasons)?***

The overestimation of precipitation over the ITCZ may be due to biases in the convective parameterizations that produce a large fraction of tropical precipitation in WRF. More discussion about this is now added into the manuscript “The simulation reasonably reproduces the spatial and seasonal variations of precipitation, with spatial correlation coefficients of 0.89, 0.81, 0.81, and 0.84 for DJF, MAM, JJA, and SON, respectively. The simulation overestimates annual mean precipitation averaged over the North Pacific (3.1 mm day⁻¹ from GPCP versus 4.2 mm day⁻¹ from WRF-Chem). The overestimation (more than 50%) is particularly large over the Inter-Tropical Convergence Zone (ITCZ) and the western tropical Pacific located south of 20°N and the major pathway of trans-Pacific transport. The excessive precipitation over the tropical Pacific may be due to biases from the convective parameterizations in producing tropical precipitation in WRF, such as overestimation of precipitation efficiency from simple treatment of cloud microphysical processes in convective clouds, and biases in the prescribed temperature and humidity reference profiles (e.g., Fonseca et al., 2015; Hagos et al., 2016). Short sensitivity experiments we performed show that the WRF simulated tropical precipitation is sensitive to the choice of convective parameterizations (not shown).”

- ***Line 344: WRF-Chem provides AOD on several wavelengths, none of which are exactly 550 (for AERONET and MODIS) or 500 nm (for OMI). I am curious if any interpolation has been done to match with satellite or ground-based retrievals?***

Yes, interpolations were performed across several wavelengths. Now we clarify it in the manuscript “The WRF-Chem simulated AOD at 600 nm and 400 nm are used to derive the AOD at 550 nm (using the Angström exponent).” and “The model simulated AAOD at 600 nm and 400 nm are used to derive the AAOD at 500 nm (using the Angström exponent).”

- ***Lines 366-367: There are large discrepancies between MODIS and MISR AOD over western U.S. What are the exact causes? Could authors provide the retrieval uncertainties between two retrievals? Also it seems that high AOD values over western U.S. is collocated with some dust source regions. I would like to see some linkage between the dust performance of the model and AOD here over western U.S.***

Although the MODIS retrieval of high AOD over the western U.S. is sometimes

collocated with the dust source regions, the magnitude of AOD is significantly overestimated because of large uncertainties in the assumed surface reflectance in semi-arid regions (Remer et al., 2005; Levy et al., 2013). In comparison, the MISR observations in the western U.S. show better quality presumably because of the MISR multi-angle capability, allowing for a better characterization of surface reflectance. Now this is clarified in the manuscript “**The MODIS retrieval shows higher AOD over the semi-arid regions (e.g., Northwest China and the southwestern U.S.) than the MISR retrieval; however the MODIS retrieved AOD magnitude over these regions is significantly overestimated because of its large uncertainties in the assumed surface reflectance in semi-arid regions (Remer et al., 2005; Levy et al., 2013). In comparison, the MISR observations in the western U.S. show better quality presumably because of the multi-angle capability that allows for a better characterization of surface reflectance.**”

- ***Figure 8: It should be filled dots instead of black dots. Are there any meaning of the positioning of triangles and circles in addition to representing MODIS and WRF-Chem, since the positioning looks to me quite random?***

Corrected. The triangles and circles represent the mean values, which is clarified now.

- ***Lines 428-429: The larger EAE over West Pacific reflects smaller aerosol sizes and should be due to that large particles have been deposited (through either dry or wet deposition) during the long-range transport.***

It is true that EAE could become larger because larger particles are removed preferentially during the transport from Asia continent to West Pacific. However, in our study, EAE is reduced after long-range transport from the West Pacific to the East Pacific. The latter region should have larger particles deposited than the former one. This decrease of EAE is likely from the larger fractional contribution of sea salt particles in the latter region.

- ***Line 438: Again any interpolation here?***

Yes, we did. Now we clarify it. See the response to your previous comment.

- ***Lines 556-557: Uncertainties in the model treatment of aerosol thermodynamics/dynamics (e.g., condensation) may also significantly contribute to the nitrate biases.***

Now we revise it as “**The simulation has relatively larger positive biases (a factor of 2) in months (February, March, October, and November) between the cold and warm seasons, which may reflect model deficiency in aerosol thermodynamics (i.e., the partitioning of nitrate aerosol to the gas phase in these months is too slow in the model).**”

- ***Line 583: Are biogenic emissions from MEGAN? This information should be***

added in the model description.

Now we add “Biogenic emissions are calculated following Guenther et al. (1994).”

Technical notes:

- *Figure 5: The variation bar is out of bound in the figure for MODIS in some seasons. This should be fixed. Similar issues also occur in Figures 8 and 9.*

Corrected.

- *Line 409: higher AOD than MISR.*

Corrected.

- *Line 544: sulfate.*

Corrected.

Anonymous Referee #4

General comments:

- *This study evaluated a fully coupled meteorology-chemistry model (WRF-Chem) configured to conduct quasi-global simulation for years of 2010-2014 using multiple observation datasets. The evaluation has been focused on the simulation over the trans-Pacific transport region.*

After going through the manuscript, though a lot of analysis and comparison have been done between model and observation, I still have some concerns regarding the simulation and results, especially the relative old anthropogenic emission inventory and the way to including biomass burning emissions. Also, as an evaluation paper, I did not see to much quantitative analysis and conclusions when compare the differences between model and observation. In some places, the scientific points are not well presented, and some presentations and conclusions are more or less like an assumption description or arbitrary statement, which need to provide enough evidences or references to convince the reader.

I recommend this paper for publication in GMD after major revision if the authors satisfactorily address all the comments and questions.

We thank the reviewer for a detailed review. More clarification about the experiment set-up and quantitative analysis are added. Both text and figures are revised as the reviewer suggested. More detailed responses are provided in the following.

Specific comments:

- *Section 2.3, the emissions data is a very important input data for the part of chemical transport model. I am surprised that that the author did not use the recently updated anthropogenic emission inventory, e.g. the HTAP v2.1, which has been widely used from last year in a lot of model, including WRF-Chem. Even for the emissions over Asia and US, the MEIC (<http://www.meicmodel.org/dataset-mix.html>) and NEI 2010 are also the updated version compare to the emission inventory used in the manuscript. When the evaluated results show big differences between model and observations, how do the authors quantify how much is due to emission uncertainty and how much is due to model performance in simulating the long-range transport? So I strongly recommend the authors to use the recent anthropogenic emissions or the updated version.*

We didn't use the latest global emission dataset HTAP because the experiments were conducted before the dataset was publicly released (Janssens-Maenhout et al., 2015). However, as we described in the manuscript, the two key regions (East Asia and the U.S.) where we investigated the impact of trans-Pacific aerosol to the West U.S. are updated with recently available dataset. Now we correctly stated that the anthropogenic emissions over the U.S. are from NEI 2011. In the manuscript, we also clarified that “Over East Asia, the Asian emission inventory described by Zhang et al. (2009) at 0.5°x0.5°

horizontal resolution for 2006 is used except that BC, OC, and sulfate emissions over China are from the China emission inventory for 2010 described by Lu et al. (2011) at a 0.1°x0.1° horizontal spatial resolution and a monthly temporal resolution for the simulation period.” We thank the reviewer for bringing to our attention the MEIC inventory and we notice that this is also a relatively new dataset (Li et al., 2016) in review status. Li et al. (2016) also adopted the emission inventory in Lu et al. (2011) for India, and estimated Asian emission growth rates from 2006 to 2010 as follows: -8.0% for SO₂, +19% for NO_x, +4% for CO, +15% for NMVOC, +2% for NH₃, -3% for PM₁₀, -2% for PM_{2.5}, +6 % for BC, +2 % for OC. The most significant changes are for NO_x and NMVOC that exceed 10% difference. Both HTAP and MEIC emission inventories will be used in our future studies.

We now add some discussion about uncertainties associated with anthropogenic emissions in the summary “Last but not least, the model biases against observations may be also partly contributed by uncertainties in the emissions. Some recently updated anthropogenic emissions (e.g., Janssens-Maenhout et al., 2015; Li et al., 2016) and other biomass burning emissions with higher temporal and spatial resolutions (e.g., Wiedinmyer et al., 2011) may be used in future studies to investigate the impact of emission uncertainties on trans-Pacific aerosols over the West U.S.”

- ***Section 2.3: I am wondering how did the authors include the GFED3 biomass burning emission into the model? Normally, the standard WRF-Chem code uses PREP- CHEM-SOURCE to generate and include the GFED3 biomass burning emission in the forecast. However, it can only generate the emission rate of the first simulation day (month) if the authors did not cycle the chemistry in the simulation everyday (every month). Otherwise, the authors should modify the code update (read) the GFED3 biomass burning every day (every month). Actually, the GFED3 has daily data, why did the author only include the monthly data when compared with the daily observation (IMPROVE data).***

The GFEDv3 monthly biomass burning emission fluxes are read in every day with our code modification. We now clarify it in the manuscript “Biomass burning emissions are obtained from the Global Fire Emissions Database, Version 3 (GFEDv3) with monthly temporal resolution (van der Werf et al., 2010) and vertically distributed following the injection heights suggested by Dentener et al. (2006) for the Aerosol Comparison between Observations and Models (AeroCom) project. The WRF-Chem code is modified to update the biomass burning emissions every day.” We now also add the discussion about uncertainties associated with emissions in the summary (see the response to the comment above). Since we focus more on evaluating the monthly, seasonal, and annual variation of transpacific aerosols in this study, the simulation results are now compared with monthly IMPROVE observations in Figure 15. More quantitative discussion is also added (see the response to other comments).

- **Section 4, Figure 2, 3, 4: Please show the difference between model and observation, especially with quantitative presentation (e.g. percentage differences).**

We keep Figure 2 as is because the simulation captures the wind circulation quite well as we clarify now with more quantitative discussion “Strong westerly winds occur over the North Pacific throughout the seasons with a peak (up to 12 m/s; 5.48 m/s on spatial average) in boreal winter (DJF) followed by boreal spring (MAM) (4.46 m/s on spatial average). The winds are weakest in boreal fall (SON) (4.1 m/s on spatial average). In general, the model can well reproduce the spatial pattern of winds across the Pacific with wind speeds of 4.1-5.41 m/s averaged spatially for the four seasons, with a spatial correlation coefficient of 0.98 throughout the seasons.”

Figure 3 is now revised to show the difference between the simulations and observations. More quantitative discussion is also added in the manuscript “The simulation reasonably reproduces the spatial and seasonal variations of precipitation with spatial correlation coefficients of 0.89, 0.81, 0.81, and 0.84 for DJF, MAM, JJA, and SON, respectively. The simulation overestimates annual mean precipitation averaged over the North Pacific (3.1 mm day⁻¹ and 4.2 mm day⁻¹, respectively, from GPCP and WRF-Chem). The overestimation (more than 50%) is particularly over the Inter-Tropical Convergence Zone (ITCZ) and the western tropical Pacific that are south to the 20°N and the major pathway of trans-Pacific transport. The excessive precipitation over the tropical Pacific may be due to biases from the convective parameterizations in producing tropical precipitation in WRF, such as overestimation of precipitation efficiency from simple treatment of cloud microphysical processes in convective clouds, and biases in the prescribed temperature and humidity reference profiles (e.g., Fonseca et al., 2015; Hagos et al., 2016). Short sensitivity experiments we performed show that the WRF simulated tropical precipitation is sensitive to the choice of convective parameterizations (not shown)”

The quantitative comparison of Figure 4 is partly shown in Figure 5. Now we add more quantitative discussion about Figure 4 as “The WRF-Chem simulation generally well captures the observed spatial and seasonal variability of AOD across the Pacific with the spatial correlation coefficients of 0.63-0.76 for the four seasons against the MISR retrievals. The model generally underestimates the retrieved AOD over the North Pacific (0°-60°N, 120°E-120°W) with an annual mean value of 0.11, which is lower than the retrieved values of 0.14 (MODIS) and 0.15 (MISR). Over the region north of 20°N (20°N-60°N, 120°E-120°W), the simulation produces an average AOD of 0.14 that is more consistent with the retrieved values of 0.15 (MODIS) and 0.16 (MISR). This negative bias of the oceanic AOD south of 20°N may be due to underestimation of marine emissions (Yu et al., 2003) and/or overestimation of aerosol wet removal associated with the positive bias in precipitation (Fig. 3).” For the discussion of Figure 5, text has been revised as “The retrievals show clearly that AOD peaks in MAM followed by DJF in all the regions across the Pacific. The simulated annual mean AOD of 0.21,

0.16, and 0.09 over the West, Central, and East Pacific, respectively, successfully reproduce the observed values of 0.22, 0.16, and 0.10 from MODIS and 0.21, 0.16, and 0.10 from MISR. The simulation also captures the seasonal variability with the maximum AOD in MAM followed by DJF. In general, the MODIS and MISR retrievals and simulation consistently show that AOD is reduced from the West Pacific to the East Pacific.”

- ***P18, L398: The MODIS overestimation is compared to AERONET? Please quantify their differences.***

Yes, the MODIS retrievals overestimate AOD against the AERONET retrievals. More quantitative discussion is now added in the manuscript “Over East Asia, the MISR and AERONET retrievals agree well with the annual mean of 0.37 and 0.33, respectively. Their monthly variation correlates with a coefficient of 0.8. The MODIS retrievals with the annual mean of 0.48 generally overestimate AOD against the AERONET retrievals and correlate with the AERONET retrieved monthly AOD with a coefficient of 0.67. The simulation reproduces the AERONET observed AOD variability with an annual mean of 0.38 and a monthly correlation coefficient of 0.74.”

- ***P19, L403: Are there any references about the domination of sea-salt aerosol?***

Yes, Smirnov et al. (2003) also concluded that sea-salt aerosol dominates AOD over this Pacific island in the cold season. The manuscript is revised with more clarification and quantitative discussion as “Over the island of Pacific (the Midway_Island site), retrievals from AERONET, MODIS, and MISR are generally consistent with each other on annual mean with values of 0.14, 0.13, and 0.14, respectively. The MISR retrievals correlate well with the AERONET retrievals in monthly variation with a coefficient of 0.70, which is 0.42 for MODIS, showing a minimum in summer months. The simulated annual mean AOD of 0.14 well reproduces the AERONET retrieval. The model also captures the AERONET retrieved monthly variation of AOD with a correlation coefficient of 0.64. The simulation shows that this monthly variation is largely determined by the variation of sea-salt aerosol (e.g., Smirnov et al., 2003) and Asian pollutant outflow.”

- ***P19, Figure 7: Please explain the underestimate in in July and August over the West US.***

Now we add the discussion about this in Section 4.2.1 “Over the western U.S., the MISR and MODIS retrievals well capture the monthly variation of AERONET retrievals with correlation coefficients of ~0.9, but MISR and MODIS retrieve an annual mean AOD of 0.12 and 0.20, respectively, which are higher than the AERONET retrieval of 0.07, particularly in March-October. The simulated annual mean AOD of 0.07 reproduces the AERONET retrieval. The simulation also correlates well with the AERONET retrievals with a coefficient of 0.76 in monthly variation. Both the AERONET retrieval and

simulation show that the largest AOD occurs in the spring months, which has significant contribution from the dust aerosol transported across the Pacific (to be discussed in Section 4.5). The simulation compares more consistently with the AERONET retrieval than with the MISR and MODIS retrievals in terms of magnitude, which suggests that the difference between the MODIS and MISR retrievals and the simulation over the western U.S. shown in Figure 4, is largely due to uncertainties associated with the satellite retrievals. The simulation underestimates the AERONET retrieved AOD in July-September. This underestimation may come from the model significant negative biases in carbonaceous aerosols in the warm season (to be discussed in Section 4.5).” and in Section 4.5 “The observed OC still shows the peak concentration of $1.27 \mu\text{g m}^{-3}$ in JJA, and the model significantly underestimates the peak OC concentration with a value of $0.20 \mu\text{g m}^{-3}$. The negative bias of OC over the Southwest seems not to be related to the underestimation of biomass burning because BC is reasonably simulated. This seasonal variability may be determined by the secondary production of OC, which peaks in JJA because photochemistry is more active and emissions of biogenic VOCs are higher in the warm season. The underestimation of secondary organic aerosol (SOA) may be due to uncertainty of biogenic emissions (Zhao et al., 2016) and the outdated SOA mechanism used in the current version of WRF-Chem (Shrivastava et al., 2011).”

- ***P20, L442-444: Any explanations about this conclusion?***

More quantitative discussion and explanation are added “The simulated seasonal mean AAOD of 0.015 over the West Pacific agrees reasonably well with the OMI retrieval of 0.014 in DJF but is higher in the other three seasons, with the largest difference in JJA. The significantly lower AAOD in seasons other than DJF from the OMI retrieval is also shown in the comparison with the AERONET retrieval (to be discussed with Fig. 10). Over the Central Pacific, the simulated seasonal mean AAOD of 0.014 and 0.006 in MAM and SON, respectively, generally reproduces the retrieved AAOD of 0.017 and 0.005, but the model overestimates (underestimates) the retrieved values in JJA (DJF) with 0.008 (0.005) from the simulation and 0.004 (0.009) from the retrieval. This difference may reflect the model deficiency in simulating Asian BC outflow over the Pacific in JJA and DJF, but may also result from retrieval uncertainties. The OMI retrievals may have difficulty in distinguishing the ocean color effects from those of low aerosol concentrations in the UV spectral range and ignoring the less-sufficient amounts of absorbing aerosols (Veihelmann et al., 2007; Torres et al., 2013). Jethva et al. (2014) found that the most important source of uncertainty in OMI AAOD is the effect of sub-pixel cloud contamination related to the sensor’s coarse spatial resolution, which causes AAOD underestimations for cases of low aerosol load. Over the East Pacific, the simulated seasonal mean AAOD of 0.0035, 0.0091, 0.0048, and 0.0042 for DJF, MAM, JJA, and SON, respectively, are generally consistent with the retrieved values of 0.005, 0.007, 0.0012, and 0.003, which shows the maximum value in MAM. The most

significant difference occurs in JJA. Similar as over the Central Pacific, the underestimation of retrieved AAOD over the clean region may contribute to the difference. The retrievals and simulation show large variability of AAOD, and they generally agree within the 10th and 90th percentiles of each other. AAOD is larger over the West Pacific than the Central and East Pacific, which is consistent with the AOD pattern. The simulation shows that AAOD peaks in MAM followed by JJA over the three sub-regions, which may be due to the stronger outflow of dust and anthropogenic pollutants in the two seasons.”

- ***L444-447: I don't think so. I did not see that the model is able to reproduce the seasonal variation well. Again, please provide quantitative value using statistic method to convince the readers.***

The manuscript is revised with more quantitative discussion and explanation. See the response to the comment above.

- ***L468-L470, the seasonal variation of anthropogenic BC emission overs Asian is not such significant to make this big differences, which can be found in either INTEX-B or MEIC emission inventory.***

The manuscript is revised as “The simulation generally captures the observed monthly variability with the minimum AAOD of 0.035 and 0.032 in July from the simulation and the AERONET retrieval, respectively, and the maximum of 0.055 and 0.054 in October, respectively. The model overestimates AAOD in the warm months (May-September) with the mean values of 0.046 and 0.036 from the simulation and retrieval, respectively, and underestimates AAOD in December and January with the mean values of 0.037 and 0.043, respectively. The model positive (negative) biases in AAOD in the warm (cold) months may be partly related to the constant anthropogenic BC emissions applied throughout the seasons, but previous studies have shown that anthropogenic BC emissions over China may have seasonal variation, with roughly 6% versus 13% of the annual total BC emission in summer and winter, respectively, estimated in Lu et al. (2011).”

- ***L471-474: I don't understand the point.***

It is revised as “The lower OMI AAOD over East Asia may also indicate its negative biases over the West Pacific (Fig. 9) where the air is significantly affected by the East Asian outflow. The biases in the OMI algorithm of retrieving SSA over East Asia may be also applied over the West Pacific.”

- ***Figure 11: there are big differences if the authors quantify them, especially under 1km. It is not such subjective to get this conclusions.***

We revised the manuscript with more quantitative discussion about the comparison as

“The model generally reproduces the aerosol extinction vertical variation with correlation coefficients of 0.95-0.97. The simulated aerosol extinction coefficients are consistent with the retrievals around 0.5-1 km with difference within 15%. The difference increases in the free troposphere and below 0.5 km. The simulation is higher than the retrieval in the free troposphere (e.g., about a factor of 2 around 4 km), which may be due to the reduced sensitivity of CALIOP to tenuous aerosol layers above 4 km (Yu et al., 2010). The lower (up to 30% lower) simulated extinction coefficients below 0.5 km in all three sub-regions may indicate negative biases in estimating marine aerosol emissions and excessive wet scavenging of the model, as shown in Fig. 4. The in-situ measurements over the region are needed for further validating both remote sensing data and the simulation.”

- ***L496: Is it Figure 11?***

It should be Figure 12 that shows the simulated vertical distributions of aerosol mass and its composition fraction.

- ***Figure 12: Any references to show similar vertical distribution?***

We are not aware of any references over this investigated region.

- ***L502-507: Which is the major factor, the retrieval bias in observation data of CALIPSO or the emission uncertainty in the inventory? This conclusion looks like assumption without any strong evidence support.***

Without in-situ measurements that are generally more accurate than remote sensing data, it is difficult to further validate the simulation and the CALIOP retrieval. We now clarify this in the manuscript as “In-situ measurements over the region are needed for further validating both remote sensing data and the simulation.” In addition, we revised the manuscript with more quantitative discussion about the comparison (see the response to the comment above).

- ***Section 4.5: Please use the general model evaluation method or figure (Taylor diagram) to provide quantitatively values before getting the conclusions.***

Figure 15 is now revised to show comparison between the monthly values from the simulation results and the IMPROVE observations. Section 4.5 is now significantly revised with more quantitative discussion and explanation of the comparison.

- ***L570: It is better to compare the GFED3 with other biomass burning emission, e.g. FINN, or refer the published results to get this conclusion. Also, about the underestimate of BC and OC, please see my comment 2 about including biomass burning into the model.***

We modified the WRF-Chem code to read in the GFEDv3 biomass burning emissions

daily (see our response to your comments above). We also compare the GFED and FINN emission inventories. Now we add more discussion in the manuscript “At the Northwest sites, the observed BC and OC show significant seasonal variation with the highest surface concentration in June-September (JJAS). The sensitivity simulation shows that the peak is dominated by the North American emission that is contributed by biomass burning with a maximum in JJAS (Chin et al., 2007). The simulation captures this seasonality to some extent with monthly correlation coefficients of 0.74 and 0.69 for BC and OC, respectively. However, the simulation significantly underestimates the JJAS peak with $0.05 \mu\text{g m}^{-3}$ and $0.49 \mu\text{g m}^{-3}$ BC and $0.5 \mu\text{g m}^{-3}$ and $4.5 \mu\text{g m}^{-3}$ OC from the simulation and retrieval, respectively. This significant negative bias in the model is likely from uncertainties in the GFEDv3 biomass burning inventory for the simulation period. The monthly mean emissions at a relatively coarse horizontal resolution may not be able to capture the strong local fire events. Mao et al. (2011) pointed out that the GFED inventory may underestimate the magnitude of biomass burning emissions in the western U.S. due to the issue of detecting small fires, for example, from prescribed and agricultural burning (e.g., Randerson et al., 2012; Giglio et al., 2010). Mao et al. (2014) estimated that the biomass burning BC emissions inverted from the IMPROVE observations can be a factor of 5 higher than the GFED inventory in July-September over the Western U.S.. Another biomass burning emission inventory FINN (Fire INventory from Ncar) (Wiedinmyer et al., 2011) also shows a factor of 3 higher BC emissions than the GFED inventory over the Northwest U.S. (100°W - 125°W and 40°N - 50°N) in September 2011 (not shown).”

We also add the discussion about uncertainties associated with emissions in the Summary section “Last but not least, the model biases against observations may be also partly contributed by the uncertainties in emissions. Some recently updated anthropogenic emissions (e.g., Janssens-Maenhout et al., 2015; Li et al., 2016) and other biomass burning emissions with higher temporal and spatial resolutions (e.g., Wiedinmyer et al., 2011) may be used in future studies to investigate the impact of emission uncertainties on trans-Pacific aerosols over the West U.S.”

1 | **Trans-Pacific transport and evolution of aerosols: Evaluation of quasi-**
2 | **global WRF-Chem simulation with multiple observations**

3 | ^{1,2}Zhiyuan Hu, ²Chun Zhao, ¹Jianping Huang, ²L. Ruby Leung, ²Yun Qian, ^{3,4}Hongbin
4 | Yu, ⁵Lei Huang, ⁵Olga V. Kalashnikova

5 |
6 | ¹Key Laboratory for Semi-Arid Climate Change of the Ministry of Education, Lanzhou
7 | University, Gansu, China

8 | ²Atmospheric Sciences and Global Change Division, Pacific Northwest National
9 | Laboratory, Richland, WA, USA

10 | ³Earth System Science Interdisciplinary Center, University of Maryland, MD, USA

11 | ⁴Earth Science Division, NASA Goddard Space Flight Center, MD, USA

12 | ⁵Jet Propulsion Laboratory, California Institute of Technology and NASA, Pasadena, CA,
13 | USA

14 |
15 |
16 |
17 | Manuscript for submission to *WRF-Chem special issue in Geosci. Model Dev.*

18 |
19 |
20 | *Corresponding authors:

21 | Chun Zhao, phone: (509) 371-6372; email: chun.zhao@pnnl.gov

Chun Zhao 4/12/2016 11:07 AM

Deleted: pacific

24 **Abstract**

25 | A fully coupled meteorology-chemistry model (WRF-Chem, the Weather
26 | Research and Forecasting model coupled with chemistry) has been configured to conduct
27 | quasi-global simulation for the 5 years of 2010-2014 and evaluated with multiple
28 | observation datasets for the first time. The evaluation focuses on the simulation over the
29 | trans-Pacific transport region using various reanalysis and observational datasets for
30 | meteorological fields and aerosol properties. The simulation generally captures the
31 | overall spatial and seasonal variability of satellite retrieved aerosol optical depth (AOD)
32 | and absorbing AOD (AAOD) over the Pacific that is determined by the outflow of
33 | pollutants and dust and the emissions of marine aerosols. The assessment of simulated
34 | extinction Angstrom exponent (EAE) indicates that the model generally reproduces the
35 | variability of aerosol size distributions as seen by satellites. In addition, the vertical
36 | profile of aerosol extinction and its seasonality over the Pacific are also well simulated.
37 | The difference between the simulation and satellite retrievals can be mainly attributed to
38 | model biases in estimating marine aerosol emissions as well as the satellite sampling and
39 | retrieval uncertainties. Compared with the surface measurements over the western U.S.,
40 | the model reasonably simulates the observed magnitude and seasonality of dust, sulfate,
41 | and nitrate surface concentrations, but significantly underestimates the peak surface
42 | concentrations of carbonaceous aerosol likely due to model biases in the spatial and
43 | temporal variability of biomass burning emissions and secondary organic aerosol (SOA)
44 | production. A sensitivity simulation shows that the trans-Pacific transported dust, sulfate,
45 | and nitrate can make significant contribution to surface concentrations over the rural
46 | areas of the western U.S., while the peaks of carbonaceous aerosol surface concentrations

Chun Zhao 4/12/2016 11:07 AM
Deleted: In general, precipitation and winds are well simulated by the model.

Chun Zhao 4/12/2016 11:07 AM
Deleted: outflows

Chun Zhao 4/12/2016 11:07 AM
Deleted: that are dominated by marine aerosols near the surface and the outflow of pollutants and dust above 4 km

Chun Zhao 4/12/2016 11:07 AM
Deleted: reproduces

54 are dominated by the North American emissions. Both the retrievals and simulation show
55 small interannual variability of aerosol characteristics for 2010-2014 averaged over three
56 Pacific sub-regions. The evaluation in this study demonstrates that the WRF-Chem quasi-
57 global simulation can be used for investigating trans-Pacific transport of aerosols and
58 providing reasonable inflow chemical boundaries for the western U.S. to further
59 understand the impact of transported pollutants on the regional air quality and climate
60 with high-resolution nested regional modeling.

61

62

63 1 Introduction

64 Aerosols, including from natural and anthropogenic sources in Europe, North
65 Africa, and East Asia, can be transported across the Pacific Ocean thousands of miles
66 downwind to North America and even beyond. Previous studies using ground-based and
67 satellite measurements and numerical models have estimated about 7-10 days of travel
68 time for aerosols to traverse the Pacific Ocean (Eguchi et al., 2009). Previous studies
69 have shown that aerosols outflowed from the Asian continent could be transported by the
70 mid-latitude prevailing westerlies across the Pacific Ocean and ultimately reach the west
71 coast of North America and beyond, and its efficiency is the largest in spring (e.g.,
72 Takemura et al., 2002; Chin et al., 2007; Huang et al., 2008; Yu et al., 2008; Uno et al.,
73 2009, 2011; Alizadeh-Choobari et al., 2014). Takemura et al. (2002) found that the
74 contribution of anthropogenic aerosols to the total aerosol optical thickness is comparable
75 to that of dust during the transport over the North Pacific in spring. Chin et al. (2007)
76 found that the long-range transported dust brought 3 to 4 times more fine particles than
77 anthropogenic pollutants to the total surface fine particles over the U.S. on annual
78 average with a maximum influence in spring and over the northwestern U.S. Yu et al.
79 (2008) estimated that about 25% of the Asian outflow reaches the west coast of North
80 America, which is about 15% of the total North American emissions, and the transport
81 fluxes are largest in spring and smallest in summer. Uno et al. (2011) also revealed that
82 the dust trans-Pacific path sometimes could be split into two branches: a southern path to
83 the central U.S. and a northern path that is trapped and stagnant for a longer time and
84 finally subsides over the northwestern U.S.

Chun Zhao 4/12/2016 11:07 AM

Deleted: These transported aerosols can play an important role in atmospheric composition (Yu et al., 2008), air quality (

88 | These trans-Pacific aerosols can play an important role in atmospheric
89 | composition (e.g., Yu et al., 2008), air quality (e.g., Jaffe et al., 1999; VanCuren, 2003;
90 | Heald et al., 2006; Chin et al., 2007; Fischer et al., 2009; Yu et al., 2012; Tao et al.,
91 | 2016), and regional weather and climate (e.g., Lau et al., 2008; Eguchi et al., 2009; Yu et
92 | al., 2012; Creamean et al., 2013; Fan et al., 2014; Huang et al., 2006, 2014) over the U.S.
93 | West Coast. At the surface, Heald et al. (2006) found that Asian anthropogenic aerosol
94 | plume increased aerosol concentrations in elevated regions of the northwestern U.S. by
95 | 0.16 $\mu\text{g m}^{-3}$ in spring 2001. Chin et al. (2007) also found that long-range transported dust
96 | increased the annual mean fine particle concentrations by 0.5-0.8 $\mu\text{g m}^{-3}$ over the western
97 | U.S., with a maximum enhancement in spring. The trans-Pacific transported aerosols can
98 | also significantly absorb and scatter solar radiation (Yu et al., 2012; Fast et al., 2014; Tao
99 | et al., 2016), and serve as cloud condensation nuclei and ice nuclei that affect winter
100 | storms in the western U.S. (Sassen, 2002; Ault et al., 2011; Creamean et al., 2013; Fan et
101 | al., 2014). Deposition of the transported aerosols on/into snowpack in elevated regions
102 | (Hadley et al., 2010) may also accelerate snowmelt and influence the regional
103 | hydrological cycle and climate over the western U.S. (Qian et al., 2009 and 2015; Painter
104 | et al., 2010). Hence it is important to quantify the trans-Pacific transport of aerosols and
105 | how they evolve over the long distance.

106 | Previous studies have used global models to quantify the long-range transport of
107 | aerosols to the western U.S. (e.g., Fairlie et al., 2007; Heald et al., 2006; Chin et al.,
108 | 2007; Hadley et al., 2007). However, simulations were performed at relatively coarse
109 | resolutions (typically 1-2 degrees) that cannot fully resolve the large geographical
110 | variability of aerosols over the western U.S. with complex topography (Zhao et al.,

Chun Zhao 4/12/2016 11:07 AM

Deleted: concentration

112 2013a). Coarse resolution simulations also lack the capability to fully resolve aerosol-
113 cloud-precipitation interaction. Some studies have reported regional simulations at
114 relatively high resolutions over the western U.S. (e.g., Zhao et al., 2013a; Fan et al.,
115 2014; Fast et al., 2014). However, most of them either used sparse in-situ observations to
116 provide lateral boundary conditions that are only suitable for idealized or short-term
117 sensitivity studies, or used simulations from global models with inconsistent physics and
118 chemistry schemes to provide lateral boundary conditions, which introduce biases in
119 estimating the contribution and effect of trans-Pacific transported aerosols.

120 To investigate the impact of trans-Pacific transported aerosols on regional air
121 quality and climate of the U.S. West Coast, a multi-scale modeling framework including
122 global simulation at coarse resolutions that captures the large-scale circulation and
123 provides consistent chemical lateral boundaries for nested regional simulation at high
124 resolutions is needed. WRF-Chem, the Weather Research and Forecasting (WRF) model
125 (Skamarock et al., 2008) coupled with a chemistry component (Grell et al., 2005), is such
126 a modeling framework. As a state-of-the-art model, WRF-Chem supports nested
127 simulations, and includes complex aerosol processes and interactions between aerosols
128 and radiation, clouds, and snow albedo (Zhao et al., 2014). The model has been used
129 extensively to study aerosols and their impacts on air quality and climate at regional
130 scales (e.g., Fast et al., 2006, 2009; Gustafson et al., 2007; Qian et al., 2010; Gao et al.,
131 2011, 2014; Shrivastava et al., 2011; Chen et al., 2013, 2014; Zhao et al., 2010, 2011,
132 2012, 2013a; 2014). Zhao et al. (2013b) is the first study to use WRF-Chem for quasi-
133 global (180° W-180° E, 60° S-70° N) simulations at a resolution of 1° × 1° to examine
134 uncertainties in simulating global dust mass balance and radiative forcing.

Chun Zhao 4/12/2016 11:07 AM

Deleted: US

Chun Zhao 4/12/2016 11:07 AM

Deleted: provide

137 Although the quasi-global WRF-Chem simulation described by Zhao et al. (2013b)
138 has been used to provide realistic chemical lateral boundary conditions for multiple
139 regional modeling studies (e.g., Zhao et al., 2014; Fan et al., 2015), its evaluation has not
140 been documented so far. In this study, the WRF-Chem simulation for 2010-2014 is
141 evaluated extensively using observational data. For lack of in-situ observations over East
142 Asia and ~~the~~ Pacific Ocean during ~~our~~ simulation period, evaluation is performed mainly
143 using reanalysis and satellite retrieval (e.g., CALISPO, MODIS, and MISR) datasets,
144 along with some available ground-based observations from AERONET and IMPROVE
145 in the region. We focus on the simulation over the trans-Pacific transport region as a first
146 step to evaluate the simulation for providing consistent lateral chemical boundaries for
147 nested regional simulations used to investigate the impact of transported aerosols on
148 regional air quality and climate. Spatial evolution of aerosols during the trans-Pacific
149 transport as well as their seasonal and annual variability simulated by WRF-Chem will
150 also be characterized.

151 In the following sections, the detailed setup of WRF-Chem will be described in
152 Section 2. In Section 3 ground-based measurements and satellite retrievals will be
153 presented. In Section 4, we evaluate the WRF-Chem simulated spatial distributions and
154 seasonal and annual variability of aerosols across the Pacific with the observations. The
155 conclusion can be found in Section 5.

156

157 **2 Model description**

158 [2.1 WRF-Chem](#)

Chun Zhao 4/12/2016 11:07 AM

Deleted: the

Chun Zhao 4/12/2016 11:07 AM

Moved (insertion) [1]

160 In this study, WRF-Chem (3.5.1), updated by scientists at Pacific Northwest National
161 Laboratory (PNNL), is used.

162 The MOSAIC (Model for Simulation Aerosol Interactions and Chemistry) aerosol
163 module (Zaveri et al., 2008) coupled with the CBM-Z (carbon bond mechanism)
164 photochemical mechanism (Zaveri and Peters, 1999) in WRF-Chem is selected in this
165 study. MOSAIC uses a sectional approach to represent aerosol size distributions with
166 four or eight discrete size bins in the current version of WRF-Chem (Fast et al., 2006).
167 All major aerosol components including sulfate (SO_4^{2-}), nitrate (NO_3^-), ammonium (NH_4^+),
168 black carbon (BC), organic matter (OM), sea-salt, and mineral dust are simulated in the
169 model. The MOSAIC aerosol scheme includes physical and chemical processes of
170 nucleation, condensation, coagulation, aqueous phase chemistry, and water uptake by
171 aerosols. Dry deposition of aerosol mass and number is simulated following the approach
172 of Binkowski and Shankar (1995), which includes both turbulent diffusion and
173 gravitational settling. Wet removal of aerosols by grid-resolved stratiform clouds and
174 precipitation includes in-cloud removal (rainout) and below-cloud removal (washout) by
175 impaction and interception, following Easter et al. (2004) and Chapman et al. (2009).
176 Cloud-ice-borne aerosols through ice nucleation of aerosols are not considered in the
177 model, but the removal of aerosols by the droplet freezing process is considered.
178 Convective transport and wet removal of aerosols by cumulus clouds follow Zhao et al.
179 (2013b).

180 Aerosol optical properties such as extinction, single scattering albedo (SSA), and
181 asymmetry factor for scattering are computed as a function of wavelength for each model
182 grid box. Aerosols are assumed internally mixed in each bin (i.e., a complex refractive

Chun Zhao 4/12/2016 11:07 AM

Deleted: and briefly described in Section 2.1. Section 2.2 discusses the setup of model simulations for this study. In Section 2.3, the emissions used in the simulations are described, including anthropogenic and biomass burning emissions, and mineral dust and sea-salt emissions. .

Chun Zhao 4/12/2016 11:07 AM

Moved up [1]: 2.1 WRF-Chem .

Chun Zhao 4/12/2016 11:07 AM

Deleted: explicitly treated

192 index is calculated by volume averaging for each bin for each chemical constituent of
193 aerosols). The Optical Properties of Aerosols and Clouds (OPAC) data set (Hess et al.,
194 1998) is used for the shortwave (SW) and longwave (LW) refractive indices of aerosols,
195 except that a constant value of $1.53+0.003i$ is used for the SW refractive index of dust
196 following Zhao et al. (2010, 2011). A detailed description of the computation of aerosol
197 optical properties in WRF-Chem can be found in Fast et al. (2006) and Barnard et al.
198 (2010). Aerosol radiative feedback is coupled with the Rapid Radiative Transfer Model
199 (RRTMG) (Mlawer et al., 1997; Iacono et al., 2000) for both SW and LW radiation as
200 implemented by Zhao et al. (2011). The optical properties and direct radiative forcing of
201 individual aerosol species in the atmosphere are diagnosed following the methodology
202 described in Zhao et al. (2013a). Aerosol-cloud interactions were included in the model
203 by Gustafson et al. (2007) for calculating the activation and resuspension between dry
204 aerosols and cloud droplets.

205 2.2 Numerical experiments

206 Following Zhao et al. (2013b), we use a quasi-global channel configuration with
207 periodic boundary conditions in the zonal direction and 360×145 grid cells (180° W- 180°
208 E, 67.5° S- 77.5° N) to perform simulation at 1° horizontal resolution over the period
209 2010-2014. Alizadeh-Choobari et al. (2015) conducted a global WRF-Chem simulation
210 of dust and its radiative forcing, which was configured with dust aerosol only without
211 other aerosols and chemistry. However, WRF-Chem global simulation with sophisticated
212 chemistry including anthropogenic and natural aerosols could not run stably due
213 potentially to convergence issue of solving chemical reactions near the relatively pristine
214 polar regions. Given the need of sophisticated chemistry to simulate not only dust but

Chun Zhao 4/12/2016 11:07 AM
Deleted: of 2010-2014. This circumvents some technical difficulties in running global WRF-Chem in v3.5.1 for a near global coverage

219 | also other anthropogenic aerosols, a more stable near global coverage WRF-Chem
220 | configuration is used in this study to circumvent this technical difficulty to characterize
221 | the trans-Pacific transport of aerosols. The simulation is configured with 35 vertical
222 | layers up to 50 hPa. The meteorological initial and lateral meridional boundary
223 | conditions are derived from the National Center for Environmental Prediction final
224 | analysis (NCEP/FNL) data at 1° horizontal resolution and 6 h temporal intervals. The
225 | modeled wind components u and v and atmospheric temperature are nudged towards the
226 | NCEP/FNL reanalysis data throughout the domain with a nudging timescale of 6 h in all
227 | cases (Stauffer and Seaman, 1990). This provides a more realistic simulation of large-
228 | scale circulation, which is important for modeling long-range transport. The chemical
229 | initial and meridional boundary conditions are taken from the default profiles in WRF-
230 | Chem, which are the same as those used by McKeen et al. (2002) and are based on
231 | averages of mid-latitude aircraft profiles from several field studies over the eastern
232 | Pacific Ocean. The impact of chemical boundary conditions on the simulated results is
233 | negligible (Zhao et al. 2013b). This study uses a set of selected schemes for model
234 | physics, including the MYJ (Mellor–Yamada–Janjic) planetary boundary layer scheme,
235 | Noah land surface scheme, Morrison 2-moment microphysics scheme, Kain-Fritsch
236 | cumulus scheme, and RRTMG longwave and shortwave radiation schemes.

237 | **2.3 Emissions**

238 | Anthropogenic emissions are obtained from the REanalysis of the TROspheric
239 | (RETRO) chemical composition inventories (<http://retro.enes.org/index.shtml>) except
240 | over East Asia and the United States. Over the U.S., the National Emission Inventory
241 | (NEI) 2011 is used. Over East Asia, the Asian emission inventory described by Zhang et

Chun Zhao 4/12/2016 11:07 AM

Deleted: 1°

Chun Zhao 4/12/2016 11:07 AM

Deleted: 2005 (WRF-Chem user guide from
http://ruc.noaa.gov/wrf/WG11/Users_guide.pdf
D)

246 al. (2009) at 0.5°x0.5° horizontal resolution for 2006 is used except that BC, OC, and
247 sulfate emissions over China are from the China emission inventory for 2010 described
248 by Lu et al. (2011) at a 0.1°x0.1° horizontal spatial resolution and a monthly temporal
249 resolution for the simulation period. Biogenic emissions are calculated following
250 Guenther et al. (1994). Biomass burning emissions are obtained from the Global Fire
251 Emissions Database, Version 3 (GFEDv3) with monthly temporal resolution (van der
252 Werf et al., 2010) and vertically distributed following the injection heights suggested by
253 Dentener et al. (2006) for the Aerosol Comparison between Observations and Models
254 (AeroCom) project. The WRF-Chem code is modified to update the biomass burning
255 emissions every day. Sea-salt emission follows Zhao et al. (2013a), which is based on
256 Gong (2003) to include correction of particles with radius less than 0.2 μm and Jaegle et
257 al. (2011) to include the sea-salt emission dependence on sea surface temperature.
258 Vertical dust emission fluxes are calculated with the Goddard Chemical Aerosol
259 Radiation Transport (GOCART) dust emission scheme (Ginoux et al., 2001), and the
260 emitted dust particles are distributed into the MOSAIC aerosol size bins following a
261 theoretical expression based on the physics of scale-invariant fragmentation of brittle
262 materials derived by Kok (2011). For MOSAIC 8-bin, dust particles are emitted into
263 eight size bins with mass fractions of 10⁻⁶%, 10⁻⁴%, 0.02%, 0.2%, 1.5%, 6%, 26%, and
264 45%, respectively. Although the main purpose of this study is to evaluate the WRF-Chem
265 simulation, a sensitivity simulation, in which dust, fire, and anthropogenic emissions over
266 North America (10°N-70°N and 170°W-60°W) are removed, is also conducted to
267 understand the contribution of trans-Pacific transported aerosols to the surface aerosol
268 concentrations over the western U.S.

270

271 **3 Aerosol Observations**

272 **3.1 Satellite Retrievals**

273 **3.1.1 MODIS**

274 The Moderate Resolution Imaging Spectroradiometer (MODIS) instrument
275 onboard the NASA EOS Terra satellite observes Earth in 36 spectral bands from 0.4 to
276 14.4 μm , and provides nearly daily global coverage with local equatorial overpass time of
277 about 10:30 ~~AM~~ since 2000 (King et al., 1999). The “dark target” algorithm has been
278 developed to retrieve AOD and size parameters (Angstrom exponent, effective radius,
279 and fine-mode fraction) over waters and vegetated lands (Kaufman et al., 1997; Remer et
280 al., 2005). The “deep blue” algorithm has been implemented to retrieve AOD over bright
281 land initially, which then has also been extended to vegetated land (Hsu et al., 2006,
282 2013). MODIS aerosol products have been widely used to characterize the regional,
283 seasonal, and global distribution of aerosol and its components (Yu et al., 2003, 2009;
284 Chin et al., 2004; Kaufman et al., 2005a), estimate aerosol radiative forcing (Yu et al.,
285 2004; Remer and Kaufman, 2006), and study aerosol-cloud interactions (Kaufman et al.,
286 2005b; Koren et al., 2005; Yu et al., 2007). In this study, MODIS data from the collection
287 5.1 are used. We use the “deep blue” AOD over land and the “dark target” AOD over
288 ocean, both at 550 nm and at $1^\circ \times 1^\circ$ horizontal resolution. Also, we use the “dark target”
289 over-ocean extinction Angstrom exponent (EAE) over the 470-660 nm wavelength range
290 to evaluate model simulations of particle size information (Anderson et al., 2005; Remer
291 et al., 2005; Levy et al., 2013).

292 **3.1.2 MISR**

Chun Zhao 4/12/2016 11:07 AM

Deleted: am

294 The Multi-angle Imaging SpectroRadiometer (MISR) instrument onboard the
295 Terra spacecraft crosses the equator at ~10:30 AM local time since 1999. It observes
296 continuously in four narrow spectral bands centered at 446, 558, 672 and 866 nm using
297 nine separate cameras oriented along the orbital track with surface viewing zenith angles
298 ranging from $\pm 70.5^\circ$ (Diner et al., 1998). Aerosol retrievals are performed on 16×16
299 patches of 1.1 km sub-regions, yielding an aerosol product at 17.6×17.6 km spatial
300 resolution, referred to as a “Level 2” product (Martonchik et al., 2002). MISR Level 2
301 aerosol products have been described in Kahn et al (2009). The latest version (Version 22)
302 of MISR aerosol product also provides the fraction of AOD due to “fine” (particle radii
303 $< 0.35 \mu\text{m}$), “medium” (particle radii between 0.35 and $0.7 \mu\text{m}$) and “large” (particle
304 radii $> 0.7 \mu\text{m}$) particles as well as the fraction of AOD due to “spherical” and
305 “nonspherical” particles at the four MISR spectral bands. Here, we compare the MISR
306 AOD at 550 nm from Version 22 of Level 2 with the model results.

307 3.1.3 OMI

308 OMI onboard the NASA Aura satellite has a daily global coverage, and crosses
309 the equator at 1:45 PM local time. The nadir horizontal resolution of OMI is $24 \times 13 \text{ km}^2$.
310 In this study the OMAERUV Level 2 Collection 003 V1.4.2 product (Jethva et al., 2014)
311 is used as an independent data set providing SSA that is derived based on the reflectances
312 measured by the OMI instrument at $0.39 \mu\text{m}$. The information on aerosol absorption in
313 OMI measurements comes, to a large extent, from the interaction with Rayleigh
314 scattering in the UV spectral region (Torres et al., 2013). The retrieved parameters are
315 also reported at $0.38 \mu\text{m}$ and $0.50 \mu\text{m}$. Current OMI AOD has positive biases likely due
316 to a combination of factors including cloud contamination, surface albedo effects,

Chun Zhao 4/12/2016 11:07 AM

Deleted: μm

Chun Zhao 4/12/2016 11:07 AM

Deleted: μm

Chun Zhao 4/12/2016 11:07 AM

Deleted: μm

320 radiometric calibrations, and misidentified aerosol type (Ahn et al., 2008). Therefore, in
321 this study, OMI AAOD at 500 nm is reconstructed using the WRF-Chem simulated 500
322 nm AOD and OMI SSA at 500 nm with the formula of $AAOD_{OMI}=AOD_{MODEL}\times(1-$
323 $SSA_{OMI})$.

324 | 3.1.4 CALIPSO

325 In this study, we use aerosol extinction profiles retrieved by the Cloud-Aerosol
326 Lidar with Orthogonal Polarization (CALIOP) onboard the Cloud-Aerosol Lidar and
327 Infrared Pathfinder Satellite Observation (CALIPSO) satellite. The CALIPSO satellite
328 was launched into a Sun-synchronous orbit on 28 April 2006. CALIOP is a dual-
329 wavelength polarization lidar and is designed to acquire vertical profiles of attenuated
330 backscatter from a near nadir-viewing geometry during both day and night phase (Winker
331 | et al., 2007; [Liu et al., 2004, 2008](#); [Hu et al., 2007, 2009](#)). In this study, the aerosol
332 extinction profiles at a nominal horizontal resolution of 5 km from the CALIPSO Level 2
333 profile products are used to evaluate the model. We focus on the CALIOP nighttime
334 observations in cloud-free condition, because nighttime observations have higher
335 accuracy than daytime observations (Winker et al., 2009).

336 The cloud-aerosol discrimination (CAD) score, which is an indicator that
337 measures confidence level of the discrimination between clouds (positive value) and
338 aerosols (negative value), is used to help screen out aerosol profiles that contain cloud
339 signals. We include the aerosol data with CAD score between -20 and -100, the same as
340 Yu et al., (2010, 2015). The other screening is to exclude aerosol layers where the
341 retrieval algorithm has to adjust the initially selected lidar ratio that is based on the type
342 and subtype of the aerosol layer to be analyzed. It should be noted that when the aerosol

Chun Zhao 4/12/2016 11:07 AM

Deleted:

Chun Zhao 4/12/2016 11:07 AM

Deleted:).

345 extinction is not detected by CALIOP, we set its value and also the corresponding model
346 result equal to zero, and then we compare CALIOP extinction profiles with the model
347 and analyze the seasonal variation.

348 **3.2 Ground-based observations**

349 **3.2.1 AERONET**

350 The AErosol RObotic NETwork (AERONET) is a globally distributed remote
351 sensing network for aerosol monitoring from ground stations (Holben et al., 1998).
352 AERONET uses the Cimel sun/sky photometer that measures AOD in 16 spectral
353 channels (340-1640 nm). The measurements provide products every 15 minutes during
354 daytime. In addition, an inversion algorithm is used for the retrieval of aerosol size
355 distribution, complex refractive index, single-scattering albedo, and phase function
356 (Dubovik and King, 2000; Dubovik et al., 2002). The spectral AOD from AERONET has
357 an accuracy of ± 0.01 (Eck et al., 1999; Holben et al., 2001). In the analysis presented in
358 this paper, the cloud screened and quality assured level 2.0 products are used. AERONET
359 products do not measure at wavelength $0.55 \mu\text{m}$, so we calculate them through using the
360 Angstrom exponent and the values at two nearest wavelengths $0.5 \mu\text{m}$ and $0.675 \mu\text{m}$. The
361 AERONET sites are located along the trans-Pacific transport pathways, so the products
362 are important for evaluating the model results. Five sites over East Asia, one island site
363 | over [the](#) North Pacific, and four sites over the western U.S. are selected for comparison as
364 shown in Figure 1.

365 **3.2.2 IMPROVE**

366 The Interagency Monitoring for Protected Visual Environments (IMPROVE)
367 network was initiated in 1985 by U.S. federal agencies including EPA, National Park

368 Services, Department of Agriculture-Forest Service, and other land management agencies
369 as a part of the EPA Regional Haze program (Malm et al., 1994). The network monitors
370 the visibility conditions and changes in national parks and wilderness areas on a long-
371 term basis. The detail sample collection and analytical methodology have been given by
372 Hand et al., (2011), and the data can be downloaded from
373 (<http://views.cira.colostate.edu/fed/DataWizard/Default.aspx>). There are 15 sites (Fig. 1)
374 along the west coast selected to compare with the surface aerosols of the model. In this
375 study, the mass concentrations of sulfate, nitrate, EC, OC, and dust in PM_{2.5} (particulate
376 matter with aerodynamic diameter less than 2.5 μm) are used to evaluate the model. The
377 fine dust is calculated following the formula (Malm et al., 1994; Zhao et al., 2013a):

$$378 \quad \text{PM}_{2.5}\text{-Dust} = 2.2[\text{Al}] + 2.49[\text{Si}] + 1.63[\text{Ca}] + 2.42[\text{Fe}] + 1.94[\text{Ti}]$$

379 Where [Al], [Si], [Ca], [Fe], and [Ti] represent the mass concentration of aluminum,
380 silicon, calcium, iron, and titanium, respectively.

381

382 4 Results

383 4.1 Wind fields and precipitation

384 Winds and precipitation are two crucial meteorological factors playing important
385 roles in aerosol emission, transport, and removal. The seasonal mean wind fields at 850
386 hPa averaged for the period 2010-2014 from the WRF-Chem simulation are compared
387 with the Modern-Era Retrospective analysis for Research and Applications (MERRA)
388 reanalysis data (Rienecker et al., 2011) (Fig. 2). Strong westerly winds occur over the
389 North Pacific throughout the seasons with a peak (up to 12 m/s; 5.48 m/s on spatial
390 average) in boreal winter (DJF) followed by boreal spring (MAM) (4.46 m/s on spatial

Chun Zhao 4/12/2016 11:07 AM

Deleted: was

Chun Zhao 4/12/2016 11:07 AM

Deleted: of

Chun Zhao 4/12/2016 11:07 AM

Deleted: Figure

Chun Zhao 4/12/2016 11:07 AM

Deleted:).

395 average). The winds are weakest in boreal fall (SON) (4.1 m/s on spatial average). In
396 general, the model can well reproduce the spatial pattern of winds across the Pacific with
397 wind speeds of 4.1-5.41 m/s averaged spatially for the four seasons, with a spatial
398 correlation coefficient of 0.98 throughout the seasons. Figure 3 shows the spatial
399 distribution of seasonal mean precipitation from the Global Precipitation Climatology
400 Project (GPCP) observation (Huffman et al., 2001) averaged for the period 2010-2014
401 and the difference in the WRF-Chem simulation. Over East Asia, precipitation reaches a
402 maximum during the boreal summer (JJA) followed by MAM. In the North Pacific basin,
403 the largest precipitation occurs in DJF along the storm tracks with the maximum
404 westerlies. Over the U.S. west coast, precipitation peaks during DJF and reaches a
405 minimum in JJA. The simulation reasonably reproduces the spatial and seasonal
406 variations of precipitation with spatial correlation coefficients of 0.89, 0.81, 0.81, and
407 0.84 for DJF, MAM, JJA, and SON, respectively. The simulation overestimates annual
408 mean precipitation averaged over the North Pacific (3.1 mm day⁻¹ and 4.2 mm day⁻¹,
409 respectively, from GPCP and WRF-Chem). The overestimation (more than 50%) is
410 particularly over the Inter-Tropical Convergence Zone (ITCZ) and the western tropical
411 Pacific that are south to the 20°N and the major pathway of trans-Pacific transport. The
412 excessive precipitation over the tropical Pacific may be due to biases from the convective
413 parameterizations in producing tropical precipitation in WRF, such as overestimation of
414 precipitation efficiency from the simple treatment of cloud microphysical processes in
415 convective clouds, and biases in the prescribed temperature and humidity reference
416 profiles (e.g., Fonseca et al., 2015; Hagos et al., 2016). Short sensitivity experiments we

Chun Zhao 4/12/2016 11:07 AM
Deleted: and its seasonality

Chun Zhao 4/12/2016 11:07 AM
Deleted: and WRF-Chem simulation

Chun Zhao 4/12/2016 11:07 AM
Deleted: of

Chun Zhao 4/12/2016 11:07 AM
Deleted: variation

Chun Zhao 4/12/2016 11:07 AM
Deleted: ,

Chun Zhao 4/12/2016 11:07 AM
Deleted: in some regions,

Chun Zhao 4/12/2016 11:07 AM
Deleted: of

Chun Zhao 4/12/2016 11:07 AM
Deleted:

425 performed show that the WRF simulated tropical precipitation is sensitive to the choice
426 of convective parameterizations (not shown).

427

428 **4.2 Aerosol optical depth**

429 4.2.1 Spatial and temporal variation

430 Figure 4 shows the spatial distributions of seasonal mean AOD at 550 nm across
431 the Pacific from Asia to North America averaged for 2010-2014 from the retrievals of
432 MODIS and MISR onboard Terra and the corresponding WRF-Chem simulation. The
433 WRF-Chem simulated AOD at 600 nm and 400 nm are used to derive the AOD at 550
434 nm (using the Angström exponent). In order to reduce the sampling discrepancy between
435 the two retrievals, the daily results from the two satellite retrievals and simulation are
436 sampled and averaged at the same time and location. This way of averaging leads to the
437 blank areas of missing values, which are relatively large in JJA. Satellite retrievals show
438 consistent spatial pattern with the spatial correlation coefficients of 0.65-0.88 for the four
439 seasons. The MODIS retrieval shows higher AOD over the semi-arid regions (e.g.,
440 Northwest China and the southwestern U.S.) than the MISR retrieval; however the
441 MODIS retrieved AOD magnitude over these regions is significantly overestimated
442 because of its large uncertainties in the assumed surface reflectance in semi-arid regions
443 (Remer et al., 2005; Levy et al., 2013). In comparison, the MISR observations in the
444 western U.S. show better quality presumably because of the multi-angle capability that
445 allows for a better characterization of surface reflectance. Both retrievals indicate that
446 AOD is high over the Asian continent and gradually decreases across the Pacific. High
447 AOD coincides with the sub-tropical jet (30°N-50°N, Fig. 2) over the Pacific and results

Chun Zhao 4/12/2016 11:07 AM

Deleted: Satellite retrievals show

449 from wind-induced increase in sea-salt loading and the Asian pollutant outflow. Seasonal
450 variation of aerosols across the Pacific is evident, with peak AOD over the western
451 Pacific in MAM and minimum AOD in JJA and SON. This seasonal variation is
452 generally consistent with previous studies (Yu et al., 2008, 2012), although our sampling
453 method results in more missing data from satellite retrievals in JJA than other seasons.
454 Previous studies found that trans-Pacific transport of air pollutants is most efficient in
455 MAM due to active cyclonic activity and that pollutants are lifted to the free troposphere
456 where they can be rapidly transported across the Pacific by strong westerlies (e.g., Forster
457 et al., 2004; Liang et al., 2004; Heald et al., 2006; Yu et al., 2008).

Chun Zhao 4/12/2016 11:07 AM

Deleted: it

458 The WRF-Chem simulation generally well captures the observed spatial and
459 seasonal variability of AOD across the Pacific, with the spatial correlation coefficients of
460 0.63-0.76 for the four seasons against the MISR retrievals. The model generally
461 underestimates the retrieved AOD over the North Pacific (0°-60°N, 120°E-120°W) with
462 an annual mean value of 0.11, which is lower than the retrieved values of 0.14 (MODIS)
463 and 0.15 (MISR). Over the region north of 20°N (20°N-60°N, 120°E-120°W), the
464 simulation produces an average AOD of 0.14 that is more consistent with the retrieved
465 values of 0.15 (MODIS) and 0.16 (MISR). This negative bias of the oceanic AOD south
466 of 20°N may be due to underestimation of marine emissions (Yu et al., 2003) and/or
467 overestimation of aerosol wet removal associated with the positive bias in precipitation,
468 (Fig. 3). The discrepancy may also be due to the higher uncertainty at low aerosol level
469 (Levy et al., 2013) and cloud contamination in the retrievals that leads to an
470 overestimation of AOD in some regions of the North Pacific (e.g., Zhang and Reid, 2006).
471 The model also simulates lower AOD over the continent of North America compared

Chun Zhao 4/12/2016 11:07 AM

Deleted: .

Chun Zhao 4/12/2016 11:07 AM

Deleted: to the

Chun Zhao 4/12/2016 11:07 AM

Deleted: 20°N, which

Chun Zhao 4/12/2016 11:07 AM

Deleted: .

477 with satellite retrievals. The difference between the simulation and retrievals may be due
478 to the uncertainty in satellite retrievals over the continents (e.g., Liu et al., 2004; Levy et
479 al., 2010).

480 Since this study focuses on the trans-Pacific transport and evolution of aerosols,
481 the Pacific is further divided into three sub-regions (Region 1: 20°N-50°N and 120°E-
482 140°E; Region 2: 20°N-50°N and 140°E-140°W; Region 3: 20°N-50°N and 140°W-
483 120°W) representing the West Pacific, the Central Pacific, and the East Pacific shown as
484 the black boxes in Figure 4 for analysis. Figure 5 shows the seasonal mean 550 nm AOD
485 over the three sub-regions from the MISR and MODIS retrievals and the corresponding
486 WRF-Chem simulation at the pass time of MISR and MODIS, respectively, averaged for
487 2010-2014. The retrievals show clearly that AOD peaks in MAM followed by DJF in all
488 the regions across the Pacific. The simulated annual mean AOD of 0.21, 0.16, and 0.09
489 over the West, Central, and East Pacific, respectively, successfully reproduce the
490 observed values of 0.22, 0.16, and 0.10 from MODIS and 0.21, 0.16, and 0.10 from
491 MISR. The simulation also captures the seasonal variability with the maximum AOD in
492 MAM followed by DJF. In general, the MODIS and MISR retrievals and simulation
493 consistently show that AOD reduces from the West Pacific to the East Pacific. The
494 interannual variability of AOD over the three sub-regions is small for 2010-2014
495 indicated by the retrievals and simulation (not shown).

496 Available observations from several AERONET sites (Fig. 1) over East Asia, the
497 Pacific, and the western U.S. are also compared with the model simulation. Figure 6
498 shows the comparison of observed and simulated AOD at three representative
499 AERONET sites for 2010-2014 over East Asia, an island of the Pacific, and the western

Chun Zhao 4/12/2016 11:07 AM
Deleted: It shows

Chun Zhao 4/12/2016 11:07 AM
Deleted: successfully reproduces

Chun Zhao 4/12/2016 11:07 AM
Deleted: observed

Chun Zhao 4/12/2016 11:07 AM
Deleted: .

Chun Zhao 4/12/2016 11:07 AM
Deleted: are consistent

Chun Zhao 4/12/2016 11:07 AM
Deleted: , which is also indicated by the simulation

Chun Zhao 4/12/2016 11:07 AM
Deleted: US

508 | U.S. coast. The observations and simulation agree well at all three sites, and both reflect
509 | the AOD gradient from East Asia to the western U.S. as shown in Figure 4. Observed
510 | AOD is the highest with a mean value of 0.31 at the SACOL site over East Asia and
511 | reduces to 0.075 at the Midway_Island site, and 0.045 at the Frenchman_Flat site. The
512 | model reproduces exactly these values at the three sites with correlation coefficients of
513 | 0.45, 0.65, and 0.64, respectively. About 90% of simulated AOD is within a factor of 2 of
514 | the AERONET measurements.

Chun Zhao 4/12/2016 11:07 AM
Deleted: US

515 | Figure 7 further shows the monthly variation of AOD averaged at the AERONET
516 | sites over East Asia, the Pacific island, and the West U.S. (as shown in Fig. 1) from the
517 | AERONET observations, MODIS and MISR retrievals, and WRF-Chem simulation. For
518 | the simulated AOD, contributions by dust, BC, OC, sulfate, and other aerosols are also
519 | shown. Over East Asia, the MISR and AERONET retrievals agree well with the annual
520 | mean of 0.37 and 0.33, respectively. Their monthly variation correlates with a coefficient
521 | of 0.8. The MODIS retrievals with the annual mean of 0.48 generally overestimate AOD,
522 | against the AERONET retrievals and correlate with the AEROENT retrieved monthly
523 | AOD with a coefficient of 0.67. The simulation reproduces the AERONET observed
524 | AOD variability with an annual mean of 0.38 and a monthly correlation coefficient of
525 | 0.74. Model results show that anthropogenic aerosols dominate the AOD from summer to
526 | winter while dust can significantly contribute to the AOD in spring. Over the island of
527 | Pacific (the Midway_Island site), retrievals from AERONET, MODIS, and MISR are
528 | generally consistent with each other on annual mean with values of 0.14, 0.13, and 0.14,
529 | respectively. The MISR retrievals correlate well with the AERONET retrievals in
530 | monthly variation with a coefficient of 0.70, which is 0.42 for MODIS, showing a

Chun Zhao 4/12/2016 11:07 AM
Deleted: 75

Chun Zhao 4/12/2016 11:07 AM
Deleted: 63

Chun Zhao 4/12/2016 11:07 AM
Deleted: US

Chun Zhao 4/12/2016 11:07 AM
Deleted: in

Chun Zhao 4/12/2016 11:07 AM
Deleted: .

Chun Zhao 4/12/2016 11:07 AM
Deleted: .

Chun Zhao 4/12/2016 11:07 AM
Deleted: simulation on

Chun Zhao 4/12/2016 11:07 AM
Deleted: of AOD, primarily

540 minimum in summer months. The simulated annual mean AOD of 0.14 well reproduces
541 the AERONET retrieval. The model also captures the AERONET retrieved monthly
542 variation of AOD with a correlation coefficient of 0.64. The simulation shows that this
543 monthly variation is largely determined by the variation of sea-salt aerosol (e.g., Smirnov
544 et al., 2003) and Asian pollutant outflow. The trans-Pacific transported aerosols (other
545 than sea-salt), show strong monthly variation with a maximum in April and a minimum in
546 July. Over the western U.S., the MISR and MODIS retrievals well capture the monthly
547 variation of AERONET retrievals with correlation coefficients of ~0.9, but MISR and
548 MODIS retrieve an annual mean AOD of 0.12 and 0.20, respectively, which are higher
549 than the AERONET retrieval of 0.07, particularly in March-October. The simulated
550 annual mean AOD of 0.07 reproduces the AERONET retrieval. The simulation also
551 correlates well with the AERONET retrievals with a coefficient of 0.76 in monthly
552 variation. Both the AERONET retrieval and simulation show that the largest AOD occurs
553 in the spring months, which has significant contribution from the dust aerosol transported
554 across the Pacific (to be discussed in Section 4.5). The simulation compares more
555 consistently with the AERONET retrieval than with the MISR and MODIS retrievals in
556 terms of magnitude, which suggests that the difference between the MODIS and MISR
557 retrievals and the simulation over the western U.S. shown in Figure 4 is largely due to
558 uncertainties associated with the satellite retrievals. The simulation underestimates the
559 AERONET retrieved AOD in July-September. This underestimation may come from the
560 model significant negative biases in carbonaceous aerosols in the warm season (to be
561 discussed in Section 4.5).

Chun Zhao 4/12/2016 11:07 AM
Deleted: , which shows a minimum in summer months.

Chun Zhao 4/12/2016 11:07 AM
Deleted: also

Chun Zhao 4/12/2016 11:07 AM
Deleted: Over the western U.S., both retrievals and simulation show

Chun Zhao 4/12/2016 11:07 AM
Deleted: section

Chun Zhao 4/12/2016 11:07 AM
Deleted: MODIS retrieved lower AOD than MISR, and both retrievals are significantly higher than that from the AERONET retrieval in March-October, while the

Chun Zhao 4/12/2016 11:07 AM
Deleted: is

Chun Zhao 4/12/2016 11:07 AM
Deleted: consistent

Chun Zhao 4/12/2016 11:07 AM
Deleted: US shown in Fig. 4 is due to uncertainty in satellite retrievals.

577 4.2.2 Wavelength dependence

578 The wavelength dependence of AOD that can be represented by the extinction
579 Angstrom exponent (EAE) is an indicator of aerosol particle size (Angstrom, 1929;
580 Schuster et al., 2006). In general, relatively small values of EAE indicate that aerosol size
581 distributions are dominated by coarse aerosols typically associated with dust and sea-salt,
582 while relatively large values of EAE indicate fine aerosols usually contributed by
583 anthropogenic pollution and biomass burning. Figure 8 shows the seasonal mean EAE
584 averaged for 2010-2014 from the MODIS retrievals and the WRF-Chem simulation over
585 the three sub-regions. The retrievals show clearly that the seasonal median EAE values
586 peak at 1.25, 0.74, and 0.89 in JJA and reach a minimum of 0.68, 0.20, and 0.21 in DJF
587 in three sub-regions of the West, Central, and East Pacific, respectively. This seasonality
588 reflects the fact that photochemistry is most active in JJA to produce fine aerosol particles
589 such as sulfate. In general, the simulation successfully reproduces the observed EAE
590 seasonality, with the JJA maximum of 1.09, 0.82, and 0.79 and the DJF minimum of 0.83,
591 0.42, and 0.35 in the three sub-regions, respectively. The retrievals and simulation also
592 show that the values of EAE are greater in the West Pacific than in the Central and East
593 Pacific. This pattern may reflect the dominance of the Asian pollutant outflow on the
594 aerosol size distributions over the West Pacific, while the relatively large-size particles of
595 sea-salt dominates in the other two regions. Again, the annual variability of EAE over the
596 three sub-regions is small (not shown).

597

598 **4.3 Aerosol absorption optical depth**

Chun Zhao 4/12/2016 11:07 AM

Deleted: all

Chun Zhao 4/12/2016 11:07 AM

Deleted: .

601 Light absorbing aerosols such as BC and dust play an important role in the
602 atmosphere to absorb radiation and change the heating profiles in the atmosphere.
603 Aerosol absorption optical depth (AAOD) is an important parameter for evaluating the
604 model performance in simulating light absorbing aerosols. Figure 9 shows the seasonal
605 mean AAOD at 500 nm averaged for 2010-2014 and over the three sub-regions from the
606 OMI retrieval and the WRF-Chem simulation. The model simulated AAOD at 600 nm
607 and 400 nm are used to derive the AAOD at 500 nm (using the Angström exponent).
608 Both retrievals and simulation show small interannual variability (not shown). The
609 simulated seasonal mean AAOD of 0.015 over the West Pacific agrees reasonably well
610 with the OMI retrieval of 0.014 in DJF but is higher in the other three seasons, with the
611 largest difference in JJA. The significantly lower AAOD in seasons other than DJF from
612 the OMI retrieval is also shown in the comparison with the AERONET retrieval (to be
613 discussed with Fig. 10). Over the Central Pacific, the simulated seasonal mean AAOD of
614 0.014 and 0.006 in MAM and SON, respectively, generally reproduces the retrieved
615 AAOD, of 0.017 and 0.005, but the model overestimates (underestimates) the retrieved
616 values in JJA (DJF) with 0.008 (0.005) from the simulation and 0.004 (0.009) from the
617 retrieval. This difference may reflect the model deficiency in simulating Asian BC
618 outflow over the Pacific in JJA and DJF, but may also result from retrieval uncertainties.
619 The OMI retrievals may have difficulty in distinguishing the ocean color effects from
620 those of low aerosol concentrations in the UV spectral range and ignoring the less-
621 sufficient amounts of absorbing aerosols (Veihelmann et al., 2007; Torres et al., 2013).
622 Jethva et al. (2014) found that the most important source of uncertainty in OMI AAOD is
623 the effect of sub-pixel cloud contamination related to the sensor's coarse spatial

Chun Zhao 4/12/2016 11:07 AM

Deleted: retrievals

Chun Zhao 4/12/2016 11:07 AM

Deleted: Both the retrievals and simulation show that AAOD peaks in MAM followed by JJA over the three sub-regions, which may be due to the stronger outflow of dust and anthropogenic pollutants in the two seasons. The simulated AAOD over

Chun Zhao 4/12/2016 11:07 AM

Deleted: . Over

Chun Zhao 4/12/2016 11:07 AM

Deleted: simulation

Chun Zhao 4/12/2016 11:07 AM

Deleted: , except overestimating (underestimating)

Chun Zhao 4/12/2016 11:07 AM

Moved (insertion) [2]

Chun Zhao 4/12/2016 11:07 AM

Deleted:). Over

636 resolution, which causes AAOD underestimations for cases of low aerosol load. Over the
637 East Pacific, the simulated seasonal mean AAOD of 0.0035, 0.0091, 0.0048, and 0.0042
638 for DJF, MAM, JJA, and SON, respectively, are generally consistent with the retrieved
639 values of 0.005, 0.007, 0.0012, and 0.003, which shows the maximum value in MAM.
640 The most significant difference occurs in JJA. Similar as over the Central Pacific, the
641 underestimation of retrieved AAOD over the clean region may contribute to the
642 difference. The retrievals and simulation show large variability of AAOD, and they
643 generally agree within the 10th and 90th percentiles of each other. AAOD is larger over
644 the West Pacific than the Central and East Pacific, which is consistent with the AOD
645 pattern. The simulation shows that AAOD peaks in MAM followed by JJA over the three
646 sub-regions, which may be due to the stronger outflow of dust and anthropogenic
647 pollutants in the two seasons.

648 The AERONET retrieval products (version 2) also provide AAOD values but
649 only at the sites and time when the total AOD exceeds a threshold value of 0.4 at 440 nm
650 because the AERONET inversion algorithms require a high signal-to-noise ratio to
651 retrieve some optical products such as AAOD. The total AOD values over the Central
652 Pacific and the western U.S. are less than this threshold value most of the time, and only
653 AAOD values retrieved at the East Asian sites are available and reliable. Figure 10 shows
654 the monthly variation of AAOD averaged at the AERONET sites over East Asia (Fig. 1)
655 from the AERONET observation, OMI retrieval, and WRF-Chem simulation. The
656 AERONET retrieval shows the monthly variation of AAOD over East Asia with
657 relatively lower values in JJA probably due to wet removal of aerosols by precipitation
658 and mixing with clean marine air during the East Asian summer monsoon (Zhao et al.,

Chun Zhao 4/12/2016 11:07 AM
Deleted: AAOD is

Chun Zhao 4/12/2016 11:07 AM
Deleted: with some overestimation in JJA.

Chun Zhao 4/12/2016 11:07 AM
Formatted: Not Superscript/ Subscript

Chun Zhao 4/12/2016 11:07 AM
Formatted: Not Superscript/ Subscript

Chun Zhao 4/12/2016 11:07 AM
Deleted: US

Chun Zhao 4/12/2016 11:07 AM
Deleted: observations

Chun Zhao 4/12/2016 11:07 AM
Deleted: retrievals

Chun Zhao 4/12/2016 11:07 AM
Deleted: retrievals show

2010). The simulation generally captures the observed monthly variability, with the minimum AOD of 0.035 and 0.032 in July from the simulation and the AERONET retrieval, respectively, and the maximum of 0.055 and 0.054 in October, respectively. The model overestimates AAOD in the warm months (May-September) with the mean values of 0.046 and 0.036 from the simulation and retrieval, respectively, and underestimates AAOD in December and January with the mean values of 0.037 and 0.043, respectively. The model positive (negative) biases in AAOD in the warm (cold) months may be partly related to the constant anthropogenic BC emissions applied throughout the seasons, but previous studies have shown that anthropogenic BC emissions over China may have seasonal variation, with roughly 6% versus 13% of the annual total BC emission in summer and winter, respectively, estimated in Lu et al. (2011). The simulation shows that AAOD over East Asia is dominated by BC and is partly contributed by dust. Other aerosols contribute to small amount of AAOD due to the internal mixing of aerosols in the atmosphere (Zhao et al., 2013a). The OMI retrieved AAOD is lower than that from AERONET and WRF-Chem, particularly in JJA and SON. The lower OMI AAOD over East Asia may also indicate its negative biases over the West Pacific (Fig. 9) where the air is significantly affected by the East Asian outflow. The biases in the OMI algorithm of retrieving SSA over East Asia may be also applied over the West Pacific.

4.4 Aerosol vertical distributions

Column integrated properties of aerosol (e.g., AOD and AAOD) provide useful information in regard to atmospheric aerosol loading but little information on the vertical

Chun Zhao 4/12/2016 11:07 AM
Deleted: , but overestimate AAOD in the warm months such as August and September. The model

Chun Zhao 4/12/2016 11:07 AM
Deleted: The model positive biases in AAOD in the warm months may be partly related to the constant anthropogenic BC emissions applied throughout the seasons while previous studies showed that anthropogenic BC emissions may have seasonal variation with lower values in the warm months (Lu et al

Chun Zhao 4/12/2016 11:07 AM
Moved down [3]: , 2010).

Chun Zhao 4/12/2016 11:07 AM
Deleted: ... [1]

Chun Zhao 4/12/2016 11:07 AM
Deleted: may indicate positive biases in the OMI SSA retrievals

Chun Zhao 4/12/2016 11:07 AM
Deleted: and

Chun Zhao 4/12/2016 11:07 AM
Deleted: that

Chun Zhao 4/12/2016 11:07 AM
Deleted: difference between

Chun Zhao 4/12/2016 11:07 AM
Deleted: simulation and

Chun Zhao 4/12/2016 11:07 AM
Deleted: retrievals

Chun Zhao 4/12/2016 11:07 AM
Deleted: Pacific

Chun Zhao 4/12/2016 11:07 AM
Deleted: partly due to negative biases in modeling SSA; however, it is noteworthy that the OMI retrievals may have difficulty in distinguishing

Chun Zhao 4/12/2016 11:07 AM
Deleted: ocean color effects from those of low aerosol concentrations in the UV spectral range and ignoring less-sufficient amounts of absorbing aerosols [

Chun Zhao 4/12/2016 11:07 AM
Moved up [2]: Veihelmann et al., 2007; Torres et al.,

Chun Zhao 4/12/2016 11:07 AM
Deleted: 2013]. In addition, the OMI retrievals may also have cloud contamination issue because of the large footprint

723 | distribution of aerosols. Previous studies have found that simulated aerosol vertical
724 | distributions differ significantly, which can affect the assessments of aerosol impacts on
725 | climate and air quality (e.g., Schulz et al., 2006; Textor et al., 2006). CALIPSO with the
726 | unique capability provides an opportunity to assess model simulation of aerosol vertical
727 | distributions (e.g., Huang et al., 2013). Figure 11 shows the vertical distributions of
728 | annual mean aerosol extinction coefficients for 2010-2014 averaged over the three sub-
729 | regions from the CALIPSO retrieval and the corresponding WRF-Chem simulation under
730 | cloud-free condition. The model results are sampled for averaging at the locations and
731 | times where and when retrievals are available. The CALIPSO retrieval shows clearly that
732 | aerosol extinction coefficients peak near several hundred meters above the surface and
733 | then decrease with the altitude over the three sub-regions. The extinction coefficients
734 | reduce from the West to East Pacific. The model generally reproduces the aerosol
735 | extinction vertical variation with correlation coefficients of 0.95-0.97. The simulated
736 | aerosol extinction coefficients are consistent with the retrievals around 0.5-1 km with
737 | difference within 15%. The difference increases in the free troposphere and below 0.5 km.
738 | The simulation is higher than the retrieval in the free troposphere (e.g., about a factor of 2
739 | around 4 km), which may be due to the reduced sensitivity of CALIPSO to tenuous
740 | aerosol layers above 4 km (Yu et al., 2010). The lower (up to 30% lower) simulated
741 | extinction coefficients below 0.5 km in all three sub-regions may indicate negative biases
742 | in estimating marine aerosol emissions and excessive wet scavenging of the model, as
743 | shown in Fig. 4. The in-situ measurements over the region are needed for further
744 | validating both remote sensing data and the simulation. The simulated mass fraction of
745 | each aerosol component (Fig. 12) shows that below 1 km, sea-salt dominates the total

Chun Zhao 4/12/2016 11:07 AM

Deleted: retrievals

Chun Zhao 4/12/2016 11:07 AM

Deleted: retrievals show

Chun Zhao 4/12/2016 11:07 AM

Moved (insertion) [3]

Chun Zhao 4/12/2016 11:07 AM

Deleted: distributions.

Chun Zhao 4/12/2016 11:07 AM

Deleted: show

750 aerosol mass over the Central and East Pacific, while the outflow of anthropogenic
751 aerosols and dust also makes significant contributions over the West Pacific. Above 4 km,
752 dust is the dominant aerosol over all three sub-regions.

753 The seasonal variation of aerosol extinction profiles averaged for 2010-2014 (Fig.
754 13) shows the spring maximum, particularly above 2 km, over all three sub-regions from
755 both the CALIPSO retrievals and the model simulation. This is likely due to the
756 seasonality of dust outflow over the Pacific (Fig. 14) that dominates the aerosol masses
757 above 2 km with a peak in spring (e.g., Huang et al. 2013). The model reasonably
758 reproduces the retrieved aerosol extinction vertical variation through the seasons over the
759 three sub-regions with the correlation coefficients of 0.93-0.98. Over the West Pacific,
760 the simulation has larger negative biases (up to 35%) below 1 km in DJF, when sea-salt
761 has a relatively larger contribution near the surface (Fig. 14) than other seasons (up to 15-
762 25%), and has positive biases above 1 km. At 1-4 km, the simulated aerosol extinction is
763 higher (up to a factor of 2) than the retrieval and the difference increases with the altitude.
764 The comparison between the simulation and retrieval at 1-4 km is the best in DJF with
765 the difference within 15%. In JJA, the aerosol mass has the largest contribution from the
766 anthropogenic pollutant outflow among the seasons with a peak at ~ 2 km above the
767 surface. Over the Central and East Pacific, the model has smaller negative biases (up to
768 20%) below 1 km than over the West Pacific and the maximum negative bias is in DJF.
769 Over these two regions, the seasonality of the vertical shape of each aerosol component
770 contribution is similar to that over the West Pacific, except that the sea-salt contribution
771 is larger near the surface (Fig. 14).

Chun Zhao 4/12/2016 11:07 AM

Deleted: make

Chun Zhao 4/12/2016 11:07 AM

Deleted: The simulation is a little higher than the retrievals in the free troposphere (e.g., >4 km) and at the surface. In the free troposphere, the difference may be due to the reduced sensitivity of CALIOP to tenuous aerosol layers above 4 km. At the surface, the lower CALIPSO aerosol extinction may result from a misclassification of polluted continental aerosol as marine aerosol when pollution outflow occurs near the surface and surface contamination during the retrievals (Yu et al., 2010). The model consistently underestimates the aerosol extinction coefficients between surface and 1 km in all three sub-regions, which may indicate that the model has negative biases for estimating marine aerosol emissions, as shown in Fig. 4.

Chun Zhao 4/12/2016 11:07 AM

Deleted: Over West Pacific, the

Chun Zhao 4/12/2016 11:07 AM

Deleted: profiles

Chun Zhao 4/12/2016 11:07 AM

Deleted: a relatively

Chun Zhao 4/12/2016 11:07 AM

Deleted: bias

Chun Zhao 4/12/2016 11:07 AM

Deleted: ,

Chun Zhao 4/12/2016 11:07 AM

Deleted: 14).

Chun Zhao 4/12/2016 11:07 AM

Deleted: similar amount of aerosols as that in MAM

Chun Zhao 4/12/2016 11:07 AM

Deleted: also well captures the vertical distributions with a relatively larger

Chun Zhao 4/12/2016 11:07 AM

Deleted: below 1 km

802 | **4.5 Aerosol surface mass concentrations over the West U.S.**

803 | For lack of in-situ observations of aerosol masses over the Pacific, measurements
804 | of surface fine aerosol (PM_{2.5}) component mass concentrations from the IMPROVE
805 | network over the western U.S. were widely used for model evaluation of trans-Pacific
806 | transport (e.g., Chin et al., 2007; Hadley et al., 2007). Daily variation of surface fine
807 | aerosols (dust, sulfate, nitrate, BC, and OC) averaged for 2010-2014 from the IMPROVE
808 | measurements and the monthly mean of measurements and corresponding model
809 | simulation are illustrated in Figure 15. The IMPROVE sites over the western U.S. (Fig. 1)
810 | that have measurements for the entire five years (2010-2014) and with less noisy values
811 | are divided at 40°N into two groups to represent the Northwest and Southwest U.S. The
812 | averaged values over the Northwest and Southwest sites are shown.

813 | At both Northwest and Southwest sites, the model generally captures the observed
814 | monthly variation of dust with the correlation coefficients of 0.61 and 0.55, respectively.
815 | Both the observation and simulation show the maximum dust mass concentration in
816 | MAM, and the minimum in DJF. The model simulates higher annual mean surface dust
817 | concentrations (0.25 μg m⁻³ and 0.56 μg m⁻³ over the Northwest and Southwest,
818 | respectively) than the observation (0.18 μg m⁻³ and 0.35 μg m⁻³, respectively). The
819 | observed surface sulfate concentrations are the lowest in the cold season (0.17 μg m⁻³ and
820 | 0.18 μg m⁻³ in DJF over the Northwest and Southwest, respectively) when
821 | photochemistry is least active, and the highest in the warm season (0.47 μg m⁻³ and 0.63
822 | μg m⁻³ in June-September, respectively) when the most active photochemistry occurs.
823 | This seasonality of sulfate may also be contributed by the seasonality of wet removal
824 | (much more precipitation in DJF). Over the Northwest and Southwest, the simulation

Chun Zhao 4/12/2016 11:07 AM

Deleted: US

Chun Zhao 4/12/2016 11:07 AM

Deleted: simulations

Chun Zhao 4/12/2016 11:07 AM

Deleted: the

Chun Zhao 4/12/2016 11:07 AM

Deleted: well

Chun Zhao 4/12/2016 11:07 AM

Deleted: seasonal

Chun Zhao 4/12/2016 11:07 AM

Deleted: .

Chun Zhao 4/12/2016 11:07 AM

Deleted: observations

Chun Zhao 4/12/2016 11:07 AM

Deleted: .

833 generally reproduces the magnitude and seasonality of sulfate with the minimum surface
834 concentrations of 0.17 $\mu\text{g m}^{-3}$ and 0.25 $\mu\text{g m}^{-3}$, respectively, in DJF and the maximum
835 surface concentrations of 0.49 $\mu\text{g m}^{-3}$ and 0.62 $\mu\text{g m}^{-3}$, respectively, in June-September,
836 and monthly correlation coefficients of 0.78 and 0.83, respectively. Nitrate shows a
837 seasonality that is opposite to that of sulfate, with a maximum surface concentration
838 occurring in the cold season (0.72 $\mu\text{g m}^{-3}$ and 1.22 $\mu\text{g m}^{-3}$ in DJ over the Northwest and
839 Southwest, respectively) and a minimum in the warm season (0.25 $\mu\text{g m}^{-3}$ and 0.35 $\mu\text{g m}^{-3}$
840 in JJA, respectively), which can be explained by the combined effects of temperature
841 and vertical turbulent mixing (Zhao et al., 2013a). The simulation generally reproduces
842 the seasonality of nitrate with a monthly correlation coefficient of 0.75 and 0.83 over the
843 Northwest and Southwest, respectively. Over the Northwest and Southwest, the model
844 simulates reasonably the maximum surface nitrate concentration of 0.69 $\mu\text{g m}^{-3}$ and 1.35
845 $\mu\text{g m}^{-3}$, respectively, in the cold season and the minimum with values of 0.18 $\mu\text{g m}^{-3}$ and
846 0.42 $\mu\text{g m}^{-3}$, respectively, in the warm season. The simulation has relatively larger
847 positive biases (a factor of 2) in months (February, March, October, and November)
848 between the cold and warm seasons, which may reflect the model deficiency in aerosol
849 thermodynamics (i.e., the partitioning of nitrate aerosol to the gas phase in these months
850 is too slow in the model). In general, both observation and simulation show higher
851 surface dust, sulfate, and nitrate concentrations over the Southwest than the Northwest.

852 A sensitivity simulation without dust, fire, and anthropogenic emissions over
853 North America (10°N-70°N and 170°W-60°W) indicates that the trans-Pacific
854 transported dust dominates the total dust amount in all seasons at the northern and
855 southern sites with the contribution of 80% and 60%, respectively, on annual mean,

Chun Zhao 4/12/2016 11:07 AM

Deleted: ,

Chun Zhao 4/12/2016 11:07 AM

Deleted: The simulation generally reproduces the magnitude and seasonality of both sulfate and nitrate. At the Southwest sites, the simulation is consistent with the observations on the magnitude and seasonality of surface concentrations of dust, surface, and nitrate.

Chun Zhao 4/12/2016 11:07 AM

Deleted: both

865 particularly in MAM, with the contribution of >90% and ~85%, respectively. At the
 866 southern sites, the trans-Pacific dust makes the lowest contribution of 19% in DJF. The
 867 large contribution of trans-Pacific dust indicates that the simulated overestimation of
 868 surface dust concentrations may be resulted from the excessive trans-Pacific transport of
 869 dust, which is also indicated in the comparison with the CALIPSO retrieval that shows
 870 the simulated aerosol extinction is overestimated above 1 km over the North Pacific. The
 871 difference may also be partly from the observation uncertainties. As described in Section
 872 3.2.2, the mass of soil dust is calculated from a linear combination of the measured
 873 elements associated predominantly with soil, including Al, Si, Ca, Fe, and Ti. The
 874 uncertainties associated with the reported dust values reflect the range and variation of
 875 mineral composition from a variety of soil types. The sensitivity simulation also shows
 876 that trans-Pacific transported sulfate can make significant contribution to its surface
 877 concentration over the western U.S., and the relative contributions are larger when the
 878 surface concentrations are lower with ~60% in DJF averaged at all sites and ~35% in JJA.
 879 The trans-Pacific nitrate contributes a relatively small amount (~15%) to the total nitrate
 880 surface concentration.

881 There is a significant difference in BC and OC surface concentrations between the
 882 observations and simulation. At the Northwest sites, the observed BC and OC show
 883 significant seasonal variation with the highest surface concentration in June-September
 884 (JJAS). The sensitivity simulation shows that the peak is dominated by the North
 885 American emission that is contributed by biomass burning with a maximum in JJAS
 886 (Chin et al., 2007). The simulation captures this seasonality to some extent with monthly
 887 correlation coefficients of 0.74 and 0.69 for BC and OC, respectively. However, the

Chun Zhao 4/12/2016 11:07 AM

Deleted: .

Chun Zhao 4/12/2016 11:07 AM

Deleted: North American

Chun Zhao 4/12/2016 11:07 AM

Deleted: a significant

Chun Zhao 4/12/2016 11:07 AM

Deleted: and nitrate

Chun Zhao 4/12/2016 11:07 AM

Deleted: their

Chun Zhao 4/12/2016 11:07 AM

Deleted: (i.e., cold seasons for sulfate and warm seasons for nitrate). During the cold seasons, the North American anthropogenic emissions determine the nitrate surface concentrations. Some differences in dust, sulfate, and nitrate surface concentrations also exist between the observations and simulation. These differences may reflect partly the modeling biases of trans-Pacific aerosols, and also the uncertainties in the North American dust and anthropogenic emissions. Another source of the difference may be from the sub-grid variability of emissions and surface concentrations that confounds the comparison of model simulation at one-degree horizontal grid resolution and the point measurements from the individual sites.

Chun Zhao 4/12/2016 11:07 AM

Deleted: This consistent

Chun Zhao 4/12/2016 11:07 AM

Deleted: of BC and OC surface concentrations

Chun Zhao 4/12/2016 11:07 AM

Deleted: likely due to

Chun Zhao 4/12/2016 11:07 AM

Deleted: that also reaches

Chun Zhao 4/12/2016 11:07 AM

Deleted: but

916 simulation significantly underestimates the JJAS peak with 0.05 $\mu\text{g m}^{-3}$ and 0.49 $\mu\text{g m}^{-3}$
 917 BC and 0.5 $\mu\text{g m}^{-3}$ and 4.5 $\mu\text{g m}^{-3}$ OC, from the simulation and observation, respectively.
 918 These significant negative biases in the model are likely from uncertainties in the
 919 GFEDv3 biomass burning inventory for the simulation period. The monthly mean
 920 emissions at a relatively coarse horizontal resolution may not be able to capture the
 921 strong local fire events. Mao et al. (2011) pointed out that the GFED inventory may
 922 underestimate the magnitude of biomass burning emissions in the western U.S. due to the
 923 issue of detecting small fires, for example, from prescribed and agricultural burning (e.g.,
 924 Randerson et al., 2012; Giglio et al., 2010). Mao et al. (2014) estimated that the biomass
 925 burning BC emissions inverted from the IMPROVE observations can be a factor of 5
 926 higher than the GFED inventory in July-September over the Western U.S. Another
 927 biomass burning emission inventory FINN (Fire INventory from Ncar) (Wiedinmyer et
 928 al., 2011) also shows a factor of 3 higher BC emissions than the GFED inventory over the
 929 Northwest U.S. (100°W-125°W and 40°N-50°N) in September 2011 (not shown).

930 At the Southwest sites, the impact of biomass burning on the BC and OC surface
 931 concentrations seems relatively small. The observations show the maximum BC surface
 932 concentration of 0.17 $\mu\text{g m}^{-3}$ in DJF and the minimum of 0.09 $\mu\text{g m}^{-3}$ in JJA, which is
 933 likely due to stronger vertical turbulent mixing in JJA compared with DJF. (Zhao et al.,
 934 2013a). The simulation can well capture the magnitude and seasonality of surface BC
 935 concentration with the monthly correlation coefficient of 0.78 and the maximum of 0.19
 936 $\mu\text{g m}^{-3}$ in DJF and the minimum of 0.10 $\mu\text{g m}^{-3}$ in JJA. The observed OC still shows the
 937 peak concentration of 1.27 $\mu\text{g m}^{-3}$ in JJA, and the model significantly underestimates the
 938 peak OC concentration with a value of 0.20 $\mu\text{g m}^{-3}$. The negative bias of OC over the

Chun Zhao 4/12/2016 11:07 AM
Deleted: for both
 Chun Zhao 4/12/2016 11:07 AM
Formatted: Superscript
 Chun Zhao 4/12/2016 11:07 AM
Deleted: . The sensitivity simulation shows that the peak is dominated by the North American emissions. This
 Chun Zhao 4/12/2016 11:07 AM
Deleted: bias
 Chun Zhao 4/12/2016 11:07 AM
Deleted: is

Chun Zhao 4/12/2016 11:07 AM
Deleted: The simulation can well capture the magnitude and seasonality of surface BC concentration that shows

Chun Zhao 4/12/2016 11:07 AM
Deleted: .

Chun Zhao 4/12/2016 11:07 AM
Deleted: concentrations

Chun Zhao 4/12/2016 11:07 AM
Deleted: concentrations. However, this

951 | Southwest seems not to be related to the underestimation of biomass burning because BC
952 | is reasonably simulated. This seasonal variability may be determined by the secondary
953 | production of OC, which peaks in JJA because photochemistry is more active and
954 | emissions of biogenic volatile organic compounds are higher in the warm season. The
955 | underestimation of secondary organic aerosol (SOA) may be due to the uncertainty of
956 | biogenic emissions (Zhao et al., 2016) and the outdated SOA mechanism used in the
957 | current version of WRF-Chem (Shrivastava et al., 2011). Besides the emission and model
958 | deficiency, another source of the difference between the simulation and observation may
959 | be from the sub-grid variability of emissions and surface concentrations that confounds
960 | the comparison of model simulation at one-degree horizontal grid resolution and the point
961 | measurements from the individual sites. On the other hand, it is also noteworthy that
962 | uncertainties in the IMPROVE carbonaceous aerosol data are also relatively high because
963 | they are inferred from optical/thermal measurements. The sensitivity simulation again
964 | shows that the peaks of BC and OC surface concentrations are dominated by the North
965 | American emissions.

966

967 | **5 Summary and conclusion**

968 | A fully coupled meteorology-chemistry model (WRF-Chem) has been configured
969 | to conduct quasi-global simulation for the 5 years of 2010-2014. The simulation results
970 | are evaluated for the first time with various reanalysis and observational datasets,
971 | including precipitation from GPCP, wind fields from MERRA, AOD, EAE, and AAOD
972 | from MODIS, MISR, OMI, and AERONET, aerosol extinction profiles from CALIPSO,
973 | and aerosol surface mass concentrations from IMPROVE. In this study, the evaluation

Chun Zhao 4/12/2016 11:07 AM

Deleted: of more active

Chun Zhao 4/12/2016 11:07 AM

Deleted: higher

Chun Zhao 4/12/2016 11:07 AM

Deleted: VOCs.

Chun Zhao 4/12/2016 11:07 AM

Deleted: 2015

Chun Zhao 4/12/2016 11:07 AM

Deleted: 2011).

979 and analysis focus on the trans-Pacific transport region for the purpose of demonstrating
980 the capability of using the quasi-global WRF-Chem simulation to provide consistent
981 lateral chemical boundaries for nested regional WRF-Chem simulations that can be used
982 to investigate the impact of trans-Pacific transported aerosols on the regional air quality
983 and climate over the western U.S. The main conclusion is summarized below:

984 ■ The comparison of simulated AOD with the satellite and AERONET retrievals
985 reveals that the model can well capture the spatial gradient of aerosol mass loading
986 decreasing from the West to East Pacific, resulting from the sea-salt loading and the
987 Asian pollutant outflow. The seasonal variation of aerosols across the Pacific with the
988 maximum AOD in MAM is also reproduced by the model. The model underestimates
989 AOD over the ocean to the south of 20°N and over the continent of North America
990 against the satellite retrievals. This discrepancy may reflect the model
991 underestimation of marine emissions and/or overestimation of aerosol wet removal or
992 the positive retrieval errors due to cloud-contamination. Compared with the
993 AERONET retrieval, the difference of AOD over the western U.S. between the
994 simulation and satellite retrievals may be due to the uncertainty in the satellite
995 retrievals over the continent.

996 ■ The assessment of simulated EAE indicates that the model generally captures the
997 observed smaller-size aerosols over the West Pacific contributed by the Asian
998 pollutant outflow compared to the relatively larger particles over the Central and East
999 Pacific with more contributions from sea-salt. The model also simulates the consistent
1000 seasonality of EAE with observations showing a minimum in DJF and a maximum in
1001 JJA due to the active production of small particles in warm seasons.

Chun Zhao 4/12/2016 11:07 AM
Deleted: US

Chun Zhao 4/12/2016 11:07 AM
Deleted: retrievals

Chun Zhao 4/12/2016 11:07 AM
Deleted: US

1005 ▪ The model reasonably simulates the decreasing gradient of OMI derived AAOD from
1006 the East to West of Pacific. The simulation shows a peak of AAOD in MAM due to
1007 the strong outflow of dust and anthropogenic pollutants. The comparison with
1008 AERONET retrieved AAOD over East Asia may indicate that the OMI SSA retrieval
1009 has positive biases over East Asia and also the West Pacific, particularly in JJA. Over
1010 East Asia, the model positive (negative) biases in AAOD in the warm (cold) months
1011 may be partly due to the neglect of the seasonal variability of anthropogenic BC
1012 emissions in this study.

Chun Zhao 4/12/2016 11:07 AM

Deleted: , and the seasonality with

Chun Zhao 4/12/2016 11:07 AM

Deleted: retrievals have

Chun Zhao 4/12/2016 11:07 AM

Deleted: that is significantly affected by the East Asian outflow

1013 ▪ The model generally captures the CALIPSO retrieved vertical gradient of aerosol
1014 extinction coefficients roughly decreasing with the altitude over the Pacific. Near the
1015 surface, the model biases in estimating marine aerosol emissions may contribute to
1016 the discrepancy between the simulation and retrievals. The difference between the
1017 simulation and retrievals in the free troposphere may be due to the reduced sensitivity
1018 of CALIPSO to the aerosol layers above 4 km. The model well captures the
1019 seasonality of aerosol extinction profiles with a maximum in MAM, which is largely
1020 controlled by the activity of dust outflow events over the Pacific.

Chun Zhao 4/12/2016 11:07 AM

Deleted: distributions

Chun Zhao 4/12/2016 11:07 AM

Deleted: retrieval uncertainties and

Chun Zhao 4/12/2016 11:07 AM

Deleted: both

Chun Zhao 4/12/2016 11:07 AM

Deleted: CALIOP

1021 ▪ Compared with the measurements from the IMPROVE sites over the western U.S.,
1022 the model simulates reasonable magnitudes and seasonality of the observed sulfate
1023 and nitrate surface concentrations with peaks in JJA and DJF, respectively. The
1024 simulation has relatively larger positive biases of nitrate surface concentrations in
1025 early spring and late fall, which may reflect the model deficiency in aerosol
1026 thermodynamics that the partitioning of nitrate aerosol to the gas phase in these
1027 months is too slow in the model. The simulation captures the observed seasonality of

Chun Zhao 4/12/2016 11:07 AM

Deleted: US, the model reproduces the observed magnitude and seasonality of dust, sulfate, and nitrate surface concentrations, with peaks in MAM, JJA, and DJF, respectively.

1041 dust surface concentrations with the maximum and minimum in MAM and DJF,
1042 respectively, but generally overestimates the observed dust surface concentrations,
1043 which may be due to the excessive trans-Pacific dust. The difference may also be
1044 partly from the observation uncertainties. Over the southwestern U.S., the simulation
1045 reproduces the magnitude and seasonality of surface BC concentrations that show the
1046 maximum in DJF, but significant underestimates the surface OC concentrations in
1047 JJA likely due to the negative biases in SOA production. Over the northwestern U.S.,
1048 the simulation significantly underestimates surface BC and OC concentrations likely
1049 due to the uncertainties in fire emissions that may not capture the strong local fire
1050 events. Another source of the difference may be due to the discrepancy in spatial
1051 scales between site observations and model outputs for the grid cell area of one-
1052 degree resolution. In addition, uncertainties in IMPROVE may also contribute to the
1053 discrepancy, in particular for carbonaceous aerosols that are inferred from
1054 optical/thermal measurements.

- 1055 ■ The sensitivity simulation shows that the trans-Pacific transported dust dominates the
1056 dust surface concentrations in the western U.S., particularly in MAM. The trans-
1057 Pacific transported sulfate and nitrate can also make significant contribution to their
1058 surface concentrations over the rural areas of the western U.S. The peaks of BC and
1059 OC surface concentrations over the western U.S. are dominated by the North
1060 American emissions. These sensitivity simulation results may be different to some
1061 extent from other models (e.g., Chin et al., 2007), which could result from the
1062 considerable differences in aerosol composition and vertical distributions due to
1063 differences in model treatments of emissions and removal processes as revealed by

Chun Zhao 4/12/2016 11:07 AM

Deleted: of which the monthly variation and the half-degree horizontal resolution may not be sufficient to

Chun Zhao 4/12/2016 11:07 AM

Deleted: output

Chun Zhao 4/12/2016 11:07 AM

Deleted: US,

Chun Zhao 4/12/2016 11:07 AM

Deleted: concentration

Chun Zhao 4/12/2016 11:07 AM

Deleted: US, in particular when their surface concentrations are relatively low

Chun Zhao 4/12/2016 11:07 AM

Deleted: US

1073 several inter-comparison studies (Barrie et al., 2001; Penner et al., 2002; Textor et al.,
1074 2006). More detailed model inter-comparison of the trans-Pacific transport of
1075 aerosols deserves further study.

1076 Although dust and biomass burning emissions in general have considerable year-
1077 to-year variations, the interannual variability of seasonal AOD for 2010-2014 averaged
1078 over the three sub-regions of the Pacific is small as indicated by the retrievals and
1079 simulation. It is noteworthy that the trans-Pacific aerosols identified in this study include
1080 not only the outflow of Asian pollutants and dust but also European pollutants and
1081 African dust that are transported to Asia and then merged with the Asian outflow. This
1082 has been recognized by previous studies (e.g., Chin et al., 2007). The evaluation in this
1083 study successfully demonstrates that the WRF-Chem quasi-global simulation with some
1084 improvements in emission inventories can be used for studying trans-Pacific transport of
1085 aerosols and providing reasonable inflow chemical boundaries for the western U.S. to
1086 further understand the impact of transported pollutants on the air quality and regional
1087 climate with high resolution nested regional modeling. It needs to be noted that the
1088 aerosol optical properties, such as AOD, AAOD, and EAE, derived from the retrievals
1089 and simulation have some different assumptions of the physical and optical parameters,
1090 so that the link between the model and the satellite data are only qualitative or semi-
1091 quantitative. Evaluation of model results with in-situ observations, would be informative.
1092 In-situ data even for specific events are valuable especially over Asia and the Pacific
1093 where public data are currently sparse or inaccessible, although some observations may
1094 be obtained through collaborations. Last but not least, the model biases against
1095 observations may be also partly contributed by the uncertainties in emissions. Some

Chun Zhao 4/12/2016 11:07 AM

Deleted:) and also our on-going research (Hu et al., 2015).

Chun Zhao 4/12/2016 11:07 AM

Deleted: simulations

Chun Zhao 4/12/2016 11:07 AM

Deleted: , particularly for a specific event may also be needed, especially over Asia and Pacific, where data are sparse or inaccessible.

1102 [recently updated anthropogenic emissions \(e.g., Janssens-Maenhout et al., 2015; Li et al.,](#)
1103 [2016\) and other biomass burning emissions with higher temporal and spatial resolutions](#)
1104 [\(e.g., Wiedinmyer et al., 2011\) may be used in future studies to investigate the impact of](#)
1105 [emission uncertainties on trans-Pacific aerosols over the West U.S.](#)

1106

1107 **Code availability**

1108 The WRF-Chem version 3.5.1 release can be obtained at
1109 http://www2.mmm.ucar.edu/wrf/users/download/get_source.html. A general WRF-Chem
1110 user's guide is also available online (<http://ruc.noaa.gov/wrf/WG11/>). [Code modifications](#)
1111 [include changes to the chemical boundary treatment using periodic boundary conditions](#)
1112 [in the zonal direction for quasi-global WRF-Chem simulation. Other changes to the](#)
1113 [model include the oceanic \(sea salt and dimethyl sulfide\) emission schemes and the](#)
1114 [convective transport and removal scheme of tracers that play a significant role in quasi-](#)
1115 [global WRF-Chem simulations of aerosols. These](#) modifications and model configuration
1116 for conducting quasi-global WRF-Chem simulations here are available upon request by
1117 contacting the corresponding author and will be incorporated in the future available
1118 release of WRF-Chem.

1119

1120 **Acknowledgements**

1121 This research was supported by the Office of Science of the U.S. Department of Energy
1122 (DOE) as part of the Regional & Global Climate Modeling (RGCM) program. J. Huang
1123 acknowledges support from the National Basic Research Program of China
1124 (2012CB955301). H. Yu was supported by NASA CALIPSO project (NNX14AB21G)

Chun Zhao 4/12/2016 11:07 AM

Deleted: Code

1126 managed by Dr. David Considine. This study used computing resources from the PNNL
1127 Institutional Computing. Pacific Northwest National Laboratory is operated by Battelle
1128 Memorial Institute for the DOE under contract DE-AC05-76RL01830. The CALIPSO
1129 data were obtained from the NASA Langley Research Center Atmospheric Sciences Data
1130 Center. MODIS and MISR data were obtained from the NASA Atmospheric Science
1131 Data Center. OMI data were obtained from the NASA Goddard Earth Sciences Data and
1132 Information Services Center.

1133

1134

1135 **Reference**

1136 Ahn, C., O. Torres, and P. K. Bhartia: Comparison of Ozone Monitoring Instrument UV
1137 Aerosol Products with Aqua/Moderate Resolution Imaging Spectroradiometer and
1138 Multiangle Imaging Spectroradiometer observations in 2006, 113, D16S27,
1139 doi:10.1029/2007JD008832, 2008.

1140 [Alizadeh-Choobari, O., P. Zawar-Reza, and A. Sturman: The global distribution of](#)
1141 [mineral dust and its impacts on the climate system: A review, Atmospheric Research](#)
1142 [138, 152–165, doi:10.1016/j.atmosres.2013.11.007, 2014.](#)

1143 [Alizadeh-Choobari, O., A. P. Sturman, and P. Zawar-Reza: Global distribution of mineral](#)
1144 [dust and its impact on radiative fluxes as simulated by WRF-Chem, Meteorology and](#)
1145 [Atmospheric Physics, 127\(6\), DOI: 10.1007/s00703-015-0390-4, 2015.](#)

1146 Anderson, T. L., Y. Wu, D. A. Chu, B. Schmid, J. Redemann, and O. Dubovik: Testing
1147 the MODIS satellite retrieval of aerosol fine-mode fraction, J. Geophys. Res., 110,
1148 D18204, doi:10.1029/2005JD005978, 2005.

1149 Angstrom, A. : On the atmospheric transmission of Sun radiation and on dust in the air,
1150 Geogr. Ann, 11, 156-166, 1929.

1151 Ault, A. P., C. R. Williams, A. B. White, P. J. Neiman, J. M. Creamean, C. J. Gaston, F.
1152 M. Ralph, and K. A. Prather: Detection of Asian dust in California orographic
1153 precipitation, J. Geophys. Res., 116, D16205, doi:10.1029/2010JD015351, 2011.

1154 Barnard, J. C., J. D. Fast, G. Paredes-Miranda, W. P. Arnott, and A. Laskin: Technical
1155 Note: Evaluation of the WRF-Chem “Aerosol Chemical to Aerosol Optical
1156 Properties” Module using data from the MILAGRO campaign, Atmos. Chem. Phys.,
1157 10, 7325-7340, doi:10.5194/acp-10-7325-2010, 2010.

1158 Barrie, L. A., Y. Yi, W. R. Leaitch, U. Lohmann, P. Kasibhatla, G. J. Roelofs, J. Wilson,
1159 F. McGovern, C. Benkovitz, M. A. Melieres, K. Law, J. Prospero, M. Kritz, D.
1160 Bergmann, C. Bridgeman, M. Chin, J. Christensen, R. Easter, J. Feichter, C. Land, A.
1161 Jeuken, E. Kjellstrom, D. Koch, and P. Rasch: A comparison of large-scale
1162 atmospheric sulphate aerosol models (COSAM): overview and highlights, *Tellus*,
1163 53B, 615-645, 2001.

1164 Binkowski, F. S., and Shankar, U.: The Regional Particulate Matter Model 1. Model
1165 description and preliminary results, *J. Geophys. Res.*, 100(D12), 26191-26209, 1995.

1166 Chapman, E. G., Gustafson Jr., W. I., Easter, R. C., Barnard, J. C., Ghan, S. J., Pekour,
1167 M. S., and Fast, J. D.: Coupling aerosol-cloud-radiative processes in the WRF-Chem
1168 model: Investigating the radiative impact of elevated point sources, *Atmos. Chem.*
1169 *Phys.*, 9, 945-964, doi:10.5194/acp-9-945-2009, 2009.

1170 Chen, S., J. Huang, C. Zhao, Y. Qian, L. R. Leung, and B. Yang: Modeling the transport
1171 and radiative forcing of Taklimakan dust over the Tibetan Plateau: A case study in the
1172 summer of 2006, *J. Geophys. Res.*, 118(2), 797-812, doi:10.1002/jgrd.50122, 2013.

1173 Chen, S., C. Zhao, Y. Qian, L. R. Leung, J. Huang, Z. Huang, J. Bi, W. Zhang, J. Shi, L.
1174 Yang, D. Li, J. Li: Regional modeling of dust mass balance and radiative forcing over
1175 East Asia using WRF-Chem, *Aeolian Research*, 15, 15-30,
1176 doi:10.1016/j.aeolia.2014.02.001, 2014.

1177 Chin, M., A. Chu, R. Levy, L. Remer, Y. Kaufman, B. Holben, T. Eck, P. Ginoux, and Q.
1178 Gao: Aerosol distribution in the Northern Hemisphere during ACE-Asia: Results
1179 from global model, satellite observations, and Sun photometer measurements, *J.*
1180 *Geophys. Res.*, 109, D23S90, doi:10.1029/2004JD004829, 2004.

1181 Chin, M., T. Diehl, P. Ginoux, and W. Malm: Intercontinental transport of pollution and
1182 dust aerosols: implications for regional air quality, *Atmos. Chem. Phys.*, 7, 5501–
1183 5517, 2007.

1184 Creamean, J. M., K. J. Suski, D. Rosenfeld, A. Cazorla, P. J. DeMott, R. C. Sullivan, A.
1185 B. White, F. M. Ralph, P. Minnis, J. M. Comstock, J. M. Tomlinson, and K. A.
1186 Prather: Dust and Biological Aerosols from the Sahara and Asia Influence
1187 Precipitation in the Western U.S., *Science*, 339, 1572, DOI:
1188 10.1126/science.1227279, 2013.

1189 Dentener, F., S. Kinne, T. Bond, O. Boucher, J. Cofala, S. Generoso, P. Ginoux, S. Gong,
1190 J. J. Hoelzemann, A. Ito, L. Marelli, J. E. Penner, J. P. Putaud, C. Textor, M. Schulz,
1191 G. R. van der Werf, and J. Wilson: Emissions of primary aerosol and precursor gases
1192 in the years 2000 and 1750 prescribed data-sets for AeroCom: *Atmos. Chem. Phys.*,
1193 6, 4321-4344, 2006.

1194 Diner, D. J., J. C. Beckert, T. H. Reilly, C. J. Bruegge, J. E. Conel, R. A. Kahn, J. V.
1195 Martonchik, T. P. Ackerman, R. Davies, S. A. W. Gerstl, H. R. Gordon, J. P. Muller,
1196 R. B. Myneni, P. J. Sellers, B. Pinty, and M. M. Verstraete: Multi-angle Imaging
1197 SpectroRadiometer (MISR) Instrument Description and Experiment Overview, *IEEE*
1198 *Trans, Geosci. Remote Sens*, 36, 1072-1087, 1998.

1199 Dubovik, O. and King, M. D.: A flexible inversion algorithm for retrieval of aerosol
1200 optical properties from Sun and sky radiance measurements, *J. Geophys. Res.*,
1201 105(16), 20673-20696, 2000.

1202 Dubovik, O., B. N. Holben, T. Lapyonok, A. Sinyuk, M. I. Mishchenko, P. Yang, and I.
1203 Slutsker: Non-spherical aerosol retrieval method employing light scattering by
1204 spheroids, *Geophys. Res. Lett.*, 29(10), 1415, 10.1029/2001GL014506, 2002.

1205 Easter, R. C., Ghan, S. J., Zhang, Y., Saylor, R. D., Chapman, E. G., Laulainen, N. S.,
1206 Abdul-Razzak, H., Leung, L. R., Bian, X., and Zaveri, R. A.: MIRAGE: Model
1207 Description and Evaluation of Aerosols and Trace Gases, *J. Geophys. Res.*, 109,
1208 D20210, doi:10.1029/2004JD004571, 2004.

1209 Eck, T. F., B. N. Holben, J. S. Reid, O. Dubovik, A. Smirnov, N. T. O'Neill, I. Slutsker,
1210 and S. Kinn: Wavelength dependence of the optical depth of biomass burning urban,
1211 and desert dust aerosols, , *J. Geophys. Res.*, 104(24), 31333-31349, 1999.

1212 Eguchi, K., I. Uno, K. Yumimoto, T. Takemura, A. Shimizu, N. Sugimoto, and Z. Liu:
1213 Trans-pacific dust transport: integrated analysis of NASA/CALIPSO and a global
1214 aerosol transport model, *Atmos. Chem. Phys.*, 9, 3137–3145, 2009.

1215 Fairlie, T. D., D. J. Jacob, and R. J. Park: The impact of transpacific transport of mineral
1216 dust in the United States: *Atmospheric Environment*, 41, 1251-1266, 2007.

1217 Fan, J., L. R. Leung, P. J. DeMott, J. M. Comstock, B. Singh, D. Rosenfeld, J. M.
1218 Tomlinson, A. White, K. A. Prather, P. Minnis, J. K. Ayers, and Q. Min: Aerosol
1219 impacts on California winter clouds and precipitation during CalWater 2011: local
1220 pollution versus long-range transported dust, *Atmos. Chem. Phys.*, 14, 81–101,
1221 doi:10.5194/acp-14-81-2014, 2014.

1222 Fan, J., D. Rosenfeld, Y. Yang, C. Zhao, L. R. Leung, and Z. Li: Substantial contribution
1223 of anthropogenic air pollution to catastrophic floods in Southwest China, *Geophys.*
1224 *Res. Lett.*, 42, 6066-6075, doi:10.1002/2015GL064479, 2015.

1225 Fast, J. D., W. I. Gustafson, R. C. Easter, R. A. Zaveri, J. C. Barnard, E. G. Chapman, G.
1226 A. Grell, and S. E. Peckham: Evolution of ozone, particulates, and aerosol direct
1227 radiative forcing in the vicinity of Houston using a fully coupled meteorology-
1228 chemistry- aerosol model, *J. Geophys. Res.*, 111, D21305,
1229 doi:10.1029/2005JD006721, 2006.

1230 Fast, J., A. C. Aiken, J. Allan, L. Alexander, T. Campos, M. R. Canagaratna, E.
1231 Chapman, P. F. DeCarlo, B. de Foy, J. Gaffney, J. de Gouw, J. C. Doran, L. Emmons,
1232 A. Hodzic, S. C. Herndon, G. Huey, J. T. Jayne, J. L. Jimenez, L. Kleinman, W.
1233 Kuster, N. Marley, L. Russell, C. Ochoa, T. B. Onasch, M. Pekour, C. Song, I. M.
1234 Ulbrich, C. Warneke, D. Welsh-Bon, C. Wiedinmyer, D. R. Worsnop, X. Y. Yu, and
1235 R. Zaveri: Evaluating simulated primary anthropogenic and biomass burning organic
1236 aerosols during MILAGRO: implications for assessing treatments of secondary
1237 organic aerosols, *Atmos. Chem. Phys.*, 9, 6191–6215, 2009.

1238 Fast, J. D., J. Allan, R. Bahreini, J. Craven, L. Emmons, R. Ferrare, P. L. Hayes, A.
1239 Hodzic, J. Holloway, C. Hostetler, J. L. Jimenez, H. Jonsson, S. Liu, Y. Liu, A.
1240 Metcalf, A. Middlebrook, J. Nowak, M. Pekour, A. Perring, L. Russell, A. Sedlacek,
1241 J. Seinfeld, A. Setyan, J. Shilling, M. Shrivastava, S. Springston, C. Song, R.
1242 Subramanian, J. W. Taylor, V. Vinoj, Q. Yang, R. A. Zaveri, and Q. Zhang:
1243 Modeling regional aerosol and aerosol precursor variability over California and its
1244 sensitivity to emissions and long-range transport during the 2010 CalNex and CARES
1245 campaigns, *Atmos. Chem. Phys.*, 14, 10013–10060, doi:10.5194/acp-14-10013-2014,
1246 2014.

1247 Fischer, E. V., N. C. Hsu, D. A. Jaffe, M.-J. Jeong, and S. L. Gong: A decade of dust:
1248 Asian dust and springtime aerosol load in the U.S. Pacific Northwest, *Geophys. Res.*
1249 *Lett.*, 36, L03821, doi:10.1029/2008GL036467, 2009.

1250 [Fonseca, R. M., T. Zhang, and K.-T. Yong: Improved simulation of precipitation in the](#)
1251 [tropics using a modified BMJ scheme in the WRF model, *Geosci. Model Dev.*, 8,](#)
1252 [2915–2928, 2015.](#)

1253 Forster, C., O. Cooper, A. Stohl, S. Eckhardt, P. James, E. Dunlea, D. K. Nicks, J. S.
1254 Holloway, G. Hubler, D. D. Parrish, T. B. Ryerson, and M. Trainer: Lagrangian
1255 transport model forecasts and a transport climatology for the Intercontinental
1256 Transport and Chemical Transformation 2002 (ITCT 2K2) measurement campaign, *J.*
1257 *Geophys. Res.*, 109, D07S92, doi:10.1029/2003JD003589, 2004.

1258 Gao, Y., X. Liu, C. Zhao, and M. Zhang: Emission controls versus meteorological
1259 conditions in determining aerosol concentrations in Beijing during the 2008 Olympic
1260 Games, *Atmos. Chem. Phys.*, 11, 12437–12451, doi:10.5194/acp-11-12437-2011,
1261 2011.

1262 Gao, Y., C. Zhao, X. H. Liu, M. G. Zhang, and L. R. Leung: WRF-Chem simulations of
1263 aerosols and anthropogenic aerosol radiative forcing in East Asia, *Atmospheric*
1264 *Environment*, 92, 250-266, 2014.

1265 Ginoux, P., M. Chin, I. Tegen, J. M. Prospero, B. Holben, O. Dubovik, and S. J. Lin:
1266 Sources and distributions of dust aerosols simulated with the GOCART model, *J.*
1267 *Geophys. Res.*, 106(17), 20255-20273, 2001.

Chun Zhao 4/12/2016 11:07 AM
Moved (insertion) [4]

1268 Gong, S. L.: A parameterization of sea-salt aerosol source function for sub- and super-
1269 micron particles, *Global Biogeochemical Cycle*, 17(4), 1097,
1270 doi:10.1029/2003GB002079, 2003.

1271 Grell, G. A., S. E. Peckham, R. Schmitz, S. A. McKeen, G. Frost, W. C. Skamarock, and
1272 B. Eder: Fully coupled “online” chemistry within the WRF model, *Atmospheric*
1273 *Environment*, 39, 6957-6957, doi:10.1016/j.atmosenv.2005.04.027, 2005.

1274 Gustafson, W. I., E. G. Chapman, S. J. Ghan, R. C. Easter, and J. D. Fast: Impact on
1275 modeled cloud characteristics due to simplified treatment of uniform cloud
1276 condensation nuclei during NEAQS 2004, *Geophys. Res. Lett.*, 34, L19809,
1277 doi:10.1029/2007GL030021, 2007.

1278 [Guenther, A; Zimmerman, P; & Wildermuth, M.: Natural volatile organic compound](#)
1279 [emission rate estimates for U.S. woodland landscapes. *Atmospheric Environment*,](#)
1280 [28\(6\), 1197 - 1210. doi: 10.1016/1352-2310\(94\)90297-6, 1994.](#)

1281 Hadley, O. L., V. Ramanathan, G. R. Carmichael, Y. Tang, C. E. Corrigan, G. C.
1282 Roberts, and G. S. Mauger: Trans-Pacific transport of black carbon and fine aerosols
1283 ($D < 2.5 \text{ }\mu\text{m}$) into North America, *J. Geophys. Res.*, 112, D05309,
1284 doi:10.1029/2006JD007632, 2007.

1285 Hadley, O. L., C. E. Corrigan, T. W. Kirchstetter, S. S. Cliff, and V. Ramanathan:
1286 Measured black carbon deposition on the Sierra Nevada snow pack and implication
1287 for snow pack retreat, *Atmos. Chem. Phys.*, 10, 7505-7513, doi:10.5194/acp-10-
1288 7505-2010, 2010.

1289 [Hagos, S. M., Z. Feng, C. D. Burleyson, C. Zhao, M. N. Martini, and L. K. Berg: Moist](#)
1290 [Process Biases in Simulations of the Madden–Julian Oscillation Episodes Observed](#)

1291 | [during the AMIE/DYNAMO Field Campaign, J. Climate, DOI:](#)
1292 | <http://dx.doi.org/10.1175/JCLI-D-15-0349.1>, 2016.

1293 Hand, J., S. A. Copeland, D. E. Day, A. M. Dillner, H. Indresand, W. C. Malm, C. E.
1294 McDade, C. T. Moore, Jr, M. L. Pitchford, B. A. Schichtel, and J. G. Watson: Spatial
1295 and seasonal patterns and temporal variability of haze and its constituents in the
1296 United States: Report V, June, 2011, available from
1297 <http://vista.cira.colostate.edu/improve/Publications/Reports/2011/2011.htm>, 2011.

1298 Heald, C. L., D. J. Jacob, R. J. Park, B. Alexander, T. D. Fairlie, R. M. Yantosca, and D.
1299 A. Chu: Transpacific transport of Asian anthropogenic aerosols and its impact on
1300 surface air quality in the United States, *J. Geophys. Res.*, 111, D14310,
1301 doi:10.1029/2005JD006847, 2006.

1302 Hess, M., P. Koepke, and I. Schult: Optical Properties of Aerosols and Clouds: The
1303 Software Package OPAC, *Bull. Am. Meteorol. Soc.*, 79(5), 831-844, 1998.

1304 Holben, B. N., T. F. Eck, I. Slutsker, D. Tanre', J. P. Buis, A. Setzer, E. Vermote, J. A.
1305 Reagan, Y. J. Kaufman, T. Nakajima, F. Lavenue, I. Jankowiak, and A. Smirnov:
1306 AERONET - A Federated Instrument Network and Data Archive for Aerosol
1307 Characterization, *Remote Sens. Environ.*, 66, 1-16, 1998.

1308 Holben, B. N., D. Tanr, A. Smirnov, T. F. Eck, I. Slutsker, N. Abuhassan, W. W.
1309 Newcomb, J. S. Schafer, B. Chatenet, F. Lavenue, Y. J.Kaufman, J. V. Castle, A.
1310 Setzer, B. Markham, D. Clark, R. Frouin, R. Halthore, A. Karneli, N. T. O'Neill, C.
1311 Pietras, R. T. Pinker, K. Voss, and G. Zibordi: An emergingground-
1312 basedaerosolclimatology: Aerosol optical depth from AERONET, *J. Geophys. Res.*,
1313 106(11), 12067-12097, 2001.

1314 Hsu, N. C., S. C. Tsay, M. D. King, and J. R. Herman: Deep Blue Retrievals of Asian
1315 Aerosol Properties During ACE-Asia, *IEEE Trans, Geosci. Remote Sens.*, 44(11),
1316 3180-3195, 2006.

1317 Hsu, N. C., M.-J. Jeong, and C. Bettenhausen: Enhanced Deep Blue aerosol retrieval
1318 algorithm: The second generation, *J. Geophys. Res. Atmos.*, 118 (16): 9296–9315,
1319 2013.

1320 Hu, Y., M. Vaughan, Z. Liu, B. Lin, P. Yang, D. Flittner, B. Hunt, R. Kuehn, J. Huang,
1321 D. Wu, S. Rodier, K. Powell, C. Trepte, and D. Winker, The depolarization-
1322 attenuated backscatter relation: CALIPSO lidar measurements vs. theory, *Optics*
1323 *Express*, 15 (9), 5327-5332, 2007.

1324 Hu, Y., D. Winker, M. Vaughan, B. Lin, A. Omar, C. Trepte, D. Flittner, P. Yang, S.
1325 Nasiri, B. Baum, W. Sun, Z. Liu, Z. Wang, S. Young, K. Stamnes, J. Huang, R.
1326 Kuehn, and R. Holz, CALIPSO/CALIOP cloud phase discrimination algorithm,
1327 *Journal of Atmospheric and Oceanic Technology*, 26 (11) (2009), 2293-2309,
1328 doi:10.1175/2009JTECHA1280.1, 2009.

1329 Huang, J., B. Lin, P. Minnis, T. Wang, X. Wang, Y. Hu, Y. Yi, and J. Ayers, Satellite-
1330 based assessment of possible dust aerosols semi-direct effect on cloud water path over
1331 East Asia, *Geophysical Research Letters*, 33 (19), L19802,
1332 doi:10.1029/2006GL026561, 2006.

1333 Huang, J., P. Minnis, B. Chen, Z. Huang, Z. Liu, Q. Zhao, Y. Yi, and J. Ayers, Long-
1334 range transport and vertical structure of Asian dust from CALIPSO and surface
1335 measurements during PACDEX, *Journal of Geophysical Research*, 113 (D23),
1336 D23212, doi:10.1029/2008JD010620, 2008.

Chun Zhao 4/12/2016 11:07 AM

Deleted: Z., C. Zhao, J. Huang, L. R. Leung, and Y. Qian: Transpacific transport and evolution of aerosols: Source contribution analysis, manuscript in preparation

Chun Zhao 4/12/2016 11:07 AM

Formatted: Font:Bold

1342 [Huang, J., T. Wang, W. Wang, Z. Li, and H. Yan, 2014: Climate effects of dust aerosols](#)
1343 [over East Asian arid and semiarid regions, *Journal of Geophysical Research:*](#)
1344 [Atmospheres, 119, 11398–11416, doi:10.1002/2014JD021796, 2014.](#)

1345 Huang, L., J. H. Jiang, J. L. Tackett, H. Su, and R. Fu: Seasonal and diurnal variations of
1346 aerosol extinction profile and type distribution from CALIPSO 5-year observations, *J.*
1347 *Geophys. Res. Atmos.*, 118, 4572–4596, doi:10.1002/jgrd.50407, 2013.

1348 Huffman, G. J., R. F. Adler, M. M. Morrissey, D. T. Bolvin, S. Curtis, R. Joyce, B.
1349 McGavock, and J. Susskind: Global Precipitation at One-Degree Daily Resolution
1350 from Multisatellite Observations. *J. Hydrometeor.*, 2, 36–50, doi:
1351 [http://dx.doi.org/10.1175/1525-7541\(2001\)002<0036:GPAODD>2.0.CO;2](http://dx.doi.org/10.1175/1525-7541(2001)002<0036:GPAODD>2.0.CO;2), 2001.

1352 Iacono, M. J., E. J. Mlawer, S. A. Clough, and J. J. Morcrette: Impact of an
1353 improved longwave radiation model, RRTM, on the energy budget and thermodynamic
1354 properties of the NCAR community climate model, CCM3, *J. Geophys. Res.*,
1355 105(11), 14873–14890, 2000.

1356 Jaegle, L., P. K. Quinn, T. S. Bates, B. Alexander, and J. T. Lin: Global distribution of
1357 sea salt aerosols: new constraints from in situ and remote sensing observations,
1358 *Atmos. Chem. Phys.*, 11, 3137–3157, doi:10.5194/acp-11-3137-2011, 2011.

1359 Jaffé, D., T. Anderson, D. Covert, R. Kotchenruther, B. Trost, J. Danielson, W. Simpson,
1360 T. Berntsen, S. Karlsdottir, D. Blake, J. Harris, G. Carmichael, and I. Uno: Transport
1361 of Asian Air Pollution to North America, *Geophys. Res. Lett.*, 26(6), 711–714, 1999.

1362 [Janssens-Maenhout, G., Crippa, M., Guizzardi, D., Dentener, F., Muntean, M., Pouliot,](#)
1363 [G., Keating, T., Zhang, Q., Kurokawa, J., Wankmüller, R., Denier van der Gon, H.,](#)
1364 [Kuenen, J. J. P., Klimont, Z., Frost, G., Darras, S., Koffi, B., and Li, M.: HTAP_v2.2:](#)

1365 [a mosaic of regional and global emission grid maps for 2008 and 2010 to study](#)
1366 [hemispheric transport of air pollution, Atmos. Chem. Phys., 15, 11411-11432,](#)
1367 [doi:10.5194/acp-15-11411-2015, 2015.](#)

1368 Jethva, H., O. Torres, and C. Ahn: Global assessment of OMI aerosol single-scattering
1369 albedo using ground-based AERONET inversion, *J. Geophys. Res. Atmos.*, 119,
1370 9020–9040, doi:10.1002/2014JD021672, 2014.

1371 Kahn, R. A., D. L. Nelson, M. J. Garay, R. C. Levy, M. A. Bull, D. J. Diner, J. V.
1372 Martonchik, S. R. Paradise, E. G. Hansen, and L. A. Remer: MISR Aerosol Product
1373 Attributes and Statistical Comparisons With MODIS, *IEEE Trans, Geosci. Remote*
1374 *Sens*, 47(12), 4095-4114, 2009.

1375 Kaufman, Y. J., D. Tanré, L. A. Remer, E. F. Vermote, A. Chu, and B. N. Holben:
1376 Operational remote sensing of tropospheric aerosol over land from EOS moderate
1377 resolution imaging spectroradiometer, *J. Geophys. Res.*, 102(D14), 17051-17067,
1378 1997.

1379 Kaufman, Y. J., O. Boucher, D. Tanre, M. Chin, L. A. Remer, and T. Takemura: Aerosol
1380 anthropogenic component estimated from satellite data, *Geophys. Res. Lett.*, 32,
1381 L17804, doi:10.1029/2005GL023125, 2005a.

1382 Kaufman, Y. J., I. Koren, L. A. Remer, D. Rosenfeld, and Y. Rudich: The effect of
1383 smoke, dust, and pollution aerosol on shallow cloud development over the Atlantic
1384 Ocean, *Proc. Natl. Acad. Sci. USA*, 102(32), 11207-11212,
1385 Doi/10.1073/pnas.0505191102, 2005b.

Chun Zhao 4/12/2016 11:07 AM
Moved (insertion) [5]

1386 King, M. D., Y. J. Kaufman, D. Tanre, and T. Nakajima: Remote Sensing of
1387 Tropospheric Aerosols from Space: Past, Present, and Future, *Bull. Am. Meteorol.*
1388 *Soc.*, 80(11), 2229-2259, 1999.

1389 Kok, J. F.: A scaling theory for the size distribution of emitted dust aerosols suggests
1390 climate models underestimate the size of the global dust cycle, *Proc. Natl. Acad. Sci.*
1391 *USA*, 108(3), 1016-1021, doi/10.1073/pnas.1014798108, 2011.

1392 Koren, I., Y. J. Kaufman, D. Rosenfeld, L. A. Remer, and Y. Rudich: Aerosol
1393 invigoration and restructuring of Atlantic convective clouds, *Geophys. Res. Lett.*, 2,
1394 L14828, doi:10.1029/2005GL023187, 2005.

1395 [Lau, K., V. Ramanathan, G. Wu, Z. Li, S. Tsay, C. Hsu, R. Sikka, B. Holben, D. Lu, G.](#)
1396 [Tartari, M. Chin, P. Koudelova, H. Chen, Y. Ma, J. Huang, K. Taniguchi, and R.](#)
1397 [Zhang, The joint aerosol-monsoon experiment: A new challenge for monsoon climate](#)
1398 [research, *Bulletin of American Meteorological Society*, 89 \(3\), 369-383, 2008.](#)

1399 Levy, R. C., L. A. Remer, R. G. Keidman, S. Mattoo, C. Ichoku, R. Kahn, and T. F. Eck:
1400 Global evaluation of the Collection 5 MODIS dark-target aerosol products over land,
1401 *Atmos. Chem. Phys.*, 10, 10399–10420, doi:10.5194/acp-10-10399-2010, 2010.

1402 Levy, R. C., S. Mattoo, L. A. Munchak, L. A. Remer, A. M. Sayer, F. Patadia, and N.
1403 Hsu: The Collection 6 MODIS Aerosol Products over Land and Ocean, *Atmos. Meas.*
1404 *Tech.*, 6, 2989-3034 doi:10.5194/amt-6-2989-2013, 2013.

1405 [Li, M., Q. Zhang, J. Kurokawa, J. H. Woo, K. B. He, Z. Lu, T. Ohara, Y. Song, D. G.](#)
1406 [Streets, G. R. Carmichael, Y. F. Cheng, C. P. Hong, H. Huo, X. J. Jiang, S. C. Kang,](#)
1407 [F. Liu, H. Su, and B. Zheng \(2015\), MIX: a mosaic Asian anthropogenic emission](#)

Chun Zhao 4/12/2016 11:07 AM

Deleted:

Chun Zhao 4/12/2016 11:07 AM

Moved (insertion) [6]

1409 [inventory for the MICS-Asia and the HTAP projects, Atmos. Chem. Phys. Discuss.,](#)
1410 [15\(23\), 34813-34869, doi:10.5194/acpd-15-34813-2015.](#)

1411 Liang, Q., L. Jaegle, D. A. Jaffe, P. Weiss-Penzias, A. Heckman, and J. A. Snow: Long-
1412 range transport of Asian pollution to the northeast Pacific: Seasonal variations and
1413 transport pathways of carbon monoxide, *J. Geophys. Res.*, 109, D23S07,
1414 doi:10.1029/2003JD004402, 2004.

1415 Liu, Z., M. A. Vaughan, D. M. Winker, C. A. Hostetler, L. R. Poole, D. Hlavka, W. Hart,
1416 abd M. McGill: Use of probability distribution functions for discriminating between
1417 cloud and aerosol in lidar backscatter data, *J. Geophys. Res.*, 109, D15202,
1418 doi:10.1029/2004JD004732, 2004.

1419 [Liu, Z., D. Liu, J. Huang, M. Vaughan, I. Uno, N. Sugimoto, C. Kittaka, C. Trepte, Z.](#)
1420 [Wang, C. Hostetler, and D. Winker, Airborne dust distributions over the Tibetan](#)
1421 [Plateau and surrounding areas derived from the first year of CALIPSO lidar](#)
1422 [observations, Atmospheric Chemistry and Physics, 8 \(16\), 5045-5060, 2008.](#)

1423 [Lu, Z., Q. Zhang, and D. G. Streets: Sulfur dioxide and primary carbonaceous aerosol](#)
1424 [emissions in China and India, 1996–2010, Atmos. Chem. Phys., 11, 9839-9864,](#)
1425 [doi:10.5194/acp-11-9839-2011, 2011.](#)

1426 Malm, W. C., J. F. Sisler, D. Huffman, R. A. Eldred, and T. A. Cahill: Spatial and
1427 seasonal trends in particle concentration and optical extinction in the United States,
1428 99(D1), 1347-1370, 1994.

1429 [Mao, Y. H., Li, Q. B., Zhang, L., Chen, Y., Randerson, J. T., Chen, D., and Liou, K. N.:](#)
1430 [Biomass burning contribution to black carbon in the Western United States Mountain](#)

Chun Zhao 4/12/2016 11:07 AM

Deleted: Lu, Z., D. G. Streets, Q. Zhang, S. Wang, G.

Chun Zhao 4/12/2016 11:07 AM

Moved up [6]: R. Carmichael, Y. F. Cheng, C.

Chun Zhao 4/12/2016 11:07 AM

Moved up [4]: T.

Chun Zhao 4/12/2016 11:07 AM

Moved up [5]: Chem.

Chun Zhao 4/12/2016 11:07 AM

Deleted: Wei, M. Chin,

Chun Zhao 4/12/2016 11:07 AM

Deleted: Diehl, and Q. Tan: Sulfur dioxide emissions in China and sulfur trends in East Asia since 2000, *Atmos.*

Chun Zhao 4/12/2016 11:07 AM

Deleted: Phys., 10, 6311-6331, doi:10.5194/acp-10-6311-2010, 2010. .

1443 [Ranges, Atmos. Chem. Phys., 11, 11253–11266, doi:10.5194/acp-11- 11253-2011,](#)
1444 [2011.](#)

1445 [Mao, Y. H., Li, Q. B., Chen, D., Zhang, L., Hao, W.-M., and Liou, K.-N.: Top-down](#)
1446 [estimates of biomass burning emissions of black carbon in the Western United States,](#)
1447 [Atmos. Chem. Phys., 14, 7195-7211, doi:10.5194/acp-14-7195-2014, 2014.](#)

1448 Martonchik, J. V., David J. D., Kathleen A. C., and M. A. Bull: Regional Aerosol
1449 Retrieval Results From MISR, IEEE Trans, Geosci. Remote Sens, 40(7), 1520-1531,
1450 2002.

1451 McKeen, S. A., G. Wotawa, D. D. Parrish, J. S. Holloway, M. P. Buhr, G. Hubler, F. C.
1452 Fehsenfeld, and J. F. Meagher: Ozone production from Canadian wildfires during
1453 June and July of 1995, J. Geophys. Res., 107(D14), 4192, 10.1029/2001JD000697,
1454 2002.

1455 Mlawer, E. J., S. J. Taubman, P. D. Brown, M. J. Iacono, and S. A. Clough: Radiative
1456 transfer for inhomogeneous atmospheres: RRTM, a validated correlated-k model for
1457 the longwave, J. Geophys. Res., 102(D14), 16663-16682, 1997.

1458 Painter, T. H., J. S. Deems, J. Belnap, A. F. Hamlet, C. C. Landry, and B. Udall:
1459 Response of Colorado River runoff to dust radiative forcing in snow, Proc. Natl.
1460 Acad. Sci. USA, 107(40), 17125-17130, doi/10.1073/pnas.0913139107, 2010.

1461 Penner, J. E., S. Y. Zhang, M. Chin, C. C. Chuang, J. Fechter, Y. Feng, I. V.
1462 Geogdzhayev, P. Ginoux, M. Herzog, A. Higurashi, D. Koch, C. Land, U. Lohmann,
1463 M. Mischecko, T. Nakajima, G. Pitari, B. Soden, I. Tegen, and L. Stowe: A
1464 Comparison of Model- and Satellite-Derived Aerosol Optical Depth and Reflectivity,
1465 J. Atmos. Sci., 59, 441-460, 2002.

1466 Qian, Y., W. I. Gustafson, L. R. Leung, and S. J. Ghan: Effects of soot-induced snow
1467 albedo change on snowpack and hydrological cycle in western United States based on
1468 Weather Research and Forecasting chemistry and regional climate simulations, *J.*
1469 *Geophys. Res.*, 114, D03108, doi:10.1029/2008JD011039, 2009.

1470 Qian, Y., W. I. Gustafson Jr. and J. D. Fast: An investigation of the sub-grid variability of
1471 trace gases and aerosols for global climate modeling, *Atmos. Chem. Phys.*, 10, 6917-
1472 6946, doi:10.5194/acp-10-6917-2010, 2010.

1473 Qian, Y., H. Yan, Z. Hou, C. Johannesson, S. Klein, D. Lucas, R. Neale, P. Rasch, L.
1474 Swiler, J. Tannahill, H. Wang, M. Wang, and C. Zhao: Parametric sensitivity analysis
1475 of precipitation at global and local scales in the Community Atmosphere Model
1476 CAM5, *J. Adv. Model. Earth Syst.*, 7, 382-411, doi:10.1002/2014MS000354, 2015.

1477 Remer, L. A., Y. J. Kaufman, D. Tanre, S. Mattoo, D. A. Chu, J. V. Martins, R. R. Li, C.
1478 Ichoku, R. C. Levy, R. G. Kleidman, T. F. Eck, E. Vermote, and B. N. Holben: The
1479 MODIS aerosol algorithm, products and validation, *J. Atmos. Sci.*, 62, 947-973,
1480 2005.

1481 Remer, L. A. and Kaufman, Y. J.: Aerosol direct radiative effect at the top of the
1482 atmosphere over cloud free ocean derived from four years of MODIS data, *Atmos.*
1483 *Chem. Phys.*, 6, 237–253, 2006.

1484 Rienecker, M. M., M. J. Suarez, R. Gelaro, R. Todling, J. Bacmeister, E. Liu, M. G.
1485 Bosilovich, S. D. Schubert, L. Takacs, G.-K. Kim, S. Bloom, J. Chen, D. Collins, A.
1486 Conaty, A. da Silva, W. Gu, J. Joiner, R. D. Koster, R. Lucchesi, A. Molod, T.
1487 Owens, S. Pawson, P. Pegion, C. R. Redder, R. Reichle, F. R. Robertson, A. G.
1488 Ruddick, M. Sienkiewicz, and J. Woollen: MERRA: NASA's Modern-Era

1489 Retrospective Analysis for Research and Applications. *J. Climate*, 24, 3624–3648.
1490 doi: <http://dx.doi.org/10.1175/JCLI-D-11-00015.1>, 2011.

1491 Sassen, K.: Indirect climate forcing over the western US from Asian Dust storm,
1492 *Geophys. Res. Lett.*, 29(10), 1465, 10.1029/2011GL014051, 2002.

1493 Schulz, M., C. Textor, S. Kinne, Y. Balkanski, S. Bauer, T. Berntsen, T. Berglen, O.
1494 Boucher, F. Dentener, S. Guibert, I. S. A. Isaksen, T. Iversen, D. Koch, A. Kirkevag,
1495 X. Liu, V. Montanaro, G. Myhre, J. E. Penner, G. Pitari, S. Reddy, Ø. Seland, P.
1496 Stier, and T. Takemura: Radiative forcing by aerosols as derived from the AeroCom
1497 present-day and pre-industrial simulations, *Atmos. Chem. Phys.*, 6, 5225–5246, 2006.

1498 Schuster, G. L., O. Dubovik, and B. N. Holben: Angstrom exponent and bimodal aerosol
1499 size distributions, *J. Geophys. Res.*, 111, D07207, doi:10.1029/2005JD006328, 2006.

1500 Shrivastava, M., J. Fast, R. Easter, W. I. Gustafson, R. A. Zaveri, J. L. Jimenez, P. Saide,
1501 and A. Hodzic: Modeling organic aerosols in a megacity: comparison of simple and
1502 complex representations of the volatility basis set approach, 11, 6639–6662,
1503 doi:10.5194/acp-11-6639-2011, 2011.

1504 Skamarock, W. C. and Klemp, J. B.: A time-split nonhydrostatic atmospheric model for
1505 weather research and forecasting applications, *J. Com. Phy.*, 227, 3456–3485,
1506 doi:10.1016/j.jcp.2007.01.037, 2008.

1507 [Smirnov, A., B. N. Holben, T. F. Eck, O. Dubovik, and I. Slutsker: Effect of wind speed](#)
1508 [on columnar aerosol optical properties at Midway Island, *J. Geophys. Res.*, 108,](#)
1509 [4802, doi:10.1029/2003JD003879, D24, 2003.](#)

1510 Stauffer, D. R. and Seaman, N. L.: Use of Four-Dimensional Data Assimilation in a
1511 Limited_Area Mesoscale Model. Part I: Experiments with Synoptic-Scale Data, Mon.
1512 Wea. Rev., 118, 1250-1277, 1990.

1513 [Takemura T, Nakajima T, Dubovik O, Holben BN, Kinne S. Single-scattering albedo and](#)
1514 [radiative forcing of various aerosol species with a global three-dimensional model. J](#)
1515 [Climate,15:333–52,2002.](#)

1516 Tao, Z., H. Yu, and M. Chin, Impact of transpacific aerosol on air quality over the United
1517 States: A perspective from aerosol-cloud-radiation interactions, Atmos. Environ.,
1518 125, 48-60, 2016.

1519 Textor, C., M. Schulz, S. Guibert, S. Kinne, Y. Balkanski, S. Bauer, T. Berntsen, T.
1520 Berglen, O. Boucher, M. Chin, F. Dentener, T. Diehl, R. Easter, H. Feichter, D.
1521 Fillmore, S. Ghan, P. Ginoux, S. Gong, A. Grini, J. Hendricks, L. Horowitz, P.
1522 Huang, I. Isaksen, T. Iversen, S. Kloster, D. Koch, A. Kirkevåg, J. E. Kristjansson,
1523 M. Krol, A. Lauer, J. F. Lamarque, X. Liu, V. Montanaro, G. Myhre, J. Penner, G.
1524 Pitari, S. Reddy, Ø. Seland, P. Stier, T. Takemura, and X. Tie: Analysis and
1525 quantification of the diversities of aerosol life cycles within AeroCom, Atmos. Chem.
1526 Phys., 6, 1777–1813, 2006.

1527 Torres, O., C. Ahn, and Z. Chen: Improvements to the OMI near-UV aerosol algorithm
1528 using A-train CALIOP and AIRS observations, Atmos. Meas. Tech., 6, 3257–3270,
1529 doi:10.5194/amt-6-3257-2013, 2013.

1530 [Uno, I., K. Eguchi, K. Yumimoto, T. Takemura, A. Shimizu, M. Uematsu, Z. Liu, Z.](#)
1531 [Wang, Y. Hara, and N. Sugimoto: Asian dust transported one full circuit around the](#)
1532 [globe, Nature Geoscience, 557-560, doi:10.1038/ngeo583, 2009.](#)

1533 [Uno, I., Eguchi, K., Yumimoto, K., Liu, Z., Hara, Y., Sugimoto, N., Shimizu, A., and](#)
1534 [Takemura, T.: Large Asian dust layers continuously reached North America in April](#)
1535 [2010, Atmos. Chem. Phys., 11, 7333-7341, doi:10.5194/acp-11-7333-2011, 2011.](#)

1536 VanCuren, R. A.: Asian aerosols in North America: Extracting the chemical composition
1537 and mass concentration of the Asian continental aerosol plume from long-term
1538 aerosol records in the western United States, *J. Geophys. Res.*, 108, NO. D20, 4623,
1539 doi:10.1029/2003JD003459, 2003.

1540 van der Werf, G. R., J. T. Randerson, L. Giglio, G. J. Collatz, M. Mu, P. S. Kasibhatla, D.
1541 C. Morton, R. S. DeFries, Y. Jin, and T. T. van Leeuwen: Global fire emissions and
1542 the contribution of deforestation, savanna, forest, agricultural, and peat fires (1997–
1543 2009), *Atmos. Chem. Phys.*, 10, 11707–11735, doi:10.5194/acp-10-11707-2010,
1544 2010.

1545 Veihelmann, B., P. F. Levelt, P. Stammes, and J. P. Veefkind: Simulation study of the
1546 aerosol information content in OMI spectral reflectance measurements, *Atmos.*
1547 *Chem. Phys.*, 7, 3115–3127, 2007.

1548 [Wiedinmyer, C., S. K. Akagi, R. J. Yokelson, L. K. Emmons, J. A. Al-Saadi, J. J.](#)
1549 [Orlando, and A. J. Soja. "The Fire Inventory from Near \(Finn\): A High Resolution](#)
1550 [Global Model to Estimate the Emissions from Open Burning." *Geoscientific Model*](#)
1551 [Development 4, no. 3 \(2011\): 625-41, 2011.](#)

1552 Winker, D. M., W. H. Hunt, and M. J. McGill: Initial performance assessment of
1553 CALIOP, *J. Geophys. Res.*, 34, L19803, doi:10.1029/2007GL030135, 2007.

1554 Winker, D. M., M. A. Vaughan, A. Omar, Y. Hu, K. A. Powell, Z. Liu, W. H. Hunt, and
1555 S. A. Young: Overview of the CALIPSO Mission and CALIOP Data Processing

1556 Algorithms, J. Atmos. Oceanic Technol., 26, 2310–2323, doi:
1557 <http://dx.doi.org/10.1175/2009JTECHA1281.1>, 2009.

1558 Yu, H. B., R. E. Dickinson, M. Chin, Y. J. Kaufman, B. N. Holben, I. V. Geogdzhayev,
1559 and M. I. Mishchenko: Annual cycle of global distributions of aerosol optical depth
1560 from integration of MODIS retrievals and GOCART model simulations, J. Geophys.
1561 Res.,108, NO. D3, 4128, doi:10.1029/2002JD002717, 2003.

1562 Yu, H. B., R. E. Dickinson, M. Chin, Y. J. Kaufman, M. Zhou, L. Zhou, Y. Tian, O.
1563 Dubovik, and B. N. Holben: Direct radiative effect of aerosols as determined from a
1564 combination of MODIS retrievals and GOCART simulations, J. Geophys. Res.,109,
1565 D03206, doi:10.1029/2003JD003914, 2004.

1566 Yu, H. B., R. Fu, R. E. Dickinson, Y. Zhang, M. Chen, and H. Wang, Interannual
1567 variability of smoke and warm cloud relationships in the Amazon as inferred from
1568 MODIS retrievals, Remote Sens. Environ., 111, 435-449,
1569 doi:10.1016/j.rse.2007.04.003, 2007.

1570 Yu, H. B., L. A. Remer, M. Chin, H. S. Bian, R. G. Kleidman, and T. Diehl: A satellite-
1571 based assessment of transpacific transport of pollution aerosol, J. Geophys. Res., 113,
1572 D14S12, doi:10.1029/2007JD009349, 2008.

1573 Yu, H., M. Chin, L. A. Remer, R. G. Kleidman, N. Bellouin, H. Bian, and T. Diehl:
1574 Variability of marine aerosol fine-mode fraction and estimates of anthropogenic
1575 aerosol component over cloud-free oceans from MODIS, J. Geophys. Res., 114,
1576 D10206, doi:10.1029/2008JD010648, 2009.

1577 Yu, H. B., M. Chin, D. M. Winker, A. H. Omar, Z. Y. Liu, C. Kittaka, and T. Diehl:
1578 Global view of aerosol vertical distributions from CALIPSO lidar measurements and

1579 GOCART simulations: Regional and seasonal variations, *J. Geophys. Res.*, 115,
1580 D00H30, doi:10.1029/2009JD013364, 2010.

1581 Yu, H., L. A. Remer, M. Chin, H. Bian, Q. Tan, T. Yuan, and Y. Zhang: Aerosols from
1582 Overseas Rival Domestic Emissions over North America, *Science*, 337, 566-569,
1583 2012.

1584 Yu, H., M. Chin, H. Bian, T. L. Yuan, J. M. Prospero, A. H. Omar, L. A. Remer, D. M.
1585 Winker, Y. Yang, Y. Zhang, and Z. Zhang: Quantification of trans-Atlantic dust
1586 transport from seven-year (2007-2013) record of CALIPSO lidar measurements,
1587 *Remote Sens. Environ.*, 159, 232-249, <http://dx.doi.org/10.1016/j.rse.2014.12.010>,
1588 2015.

1589 Zaveri, R. A. and Peters, L. K.: A new lumped structure photochemical mechanism for
1590 large-scale applications, *J. Geophys. Res.*, 104(D23), 30387-30415, 1999.

1591 Zaveri, R. A., R. C. Easter, J. D. Fast, and L. K. Peters: Model for Simulating Aerosol
1592 Interactions and Chemistry (MOSAIC), *J. Geophys. Res.*, 113, D13204,
1593 doi:10.1029/2007JD008782, 2008.

1594 Zhang, J. and Reid, J. S.: MODIS aerosol product analysis for data assimilation:
1595 Assessment of over-ocean level 2 aerosol optical thickness retrievals, *J. Geophys.*
1596 *Res.*, 111, D22207, doi:10.1029/2005JD006898, 2006.

1597 Zhang, Q., D. G. Streets, G. R. Carmichael, K. B. He, H. Huo, A. Kannari, Z. Klimont, I.
1598 S. Park, S. Reddy, J. S. Fu, D. Chen, L. Duan, Y. Lei, L. T. Wang, and Z. L. Yao:
1599 Asian emissions in 2006 for the NASA INTEX-B mission, *Atmos. Chem. Phys.*, 9,
1600 5131–5153, 2009.

1601 Zhao, C., X. Liu, L. R. Leung, B. Johnson, S. A. McFarlane, W. I. Gustafson, J. D. Fast,
1602 and R. Easter: The spatial distribution of mineral dust and its shortwave radiative
1603 forcing over North Africa: modeling sensitivities to dust emissions and aerosol size
1604 treatments, *Atmos. Chem. Phys.*, 10, 8821–8838, doi:10.5194/acp-10-8821-2010,
1605 2010a.

1606 Zhao, C., Y. Wang, Q. Yang, R. Fu, and Y. Choi: Impact of East Asia summer monsoon
1607 on the air quality over China: view from space, *J. Geophys. Res.*, 115, D09301,
1608 doi:10.1029/2009JD012745, 2010.

1609 Zhao, C., X. Liu, L. R. Leung, and S. Hagos: Radiative impact of mineral dust on
1610 monsoon precipitation variability over West Africa, *Atmos. Chem. Phys.*, 11, 1879-
1611 1893, doi:10.5194/acp-11-1879-2011, 2011.

1612 Zhao, C., X. Liu, and L. R. Leung: Impact of the Desert dust on the summer monsoon
1613 system over Southwestern North America, *Atmos. Chem. Phys.*, 12, 3717–3731, d
1614 oi:10.5194/acp-12-3717-2012, 2012.

1615 Zhao, C., L. R. Leung, R. Easter, J. Hand, and J. Avise: Characterization of speciated
1616 aerosol direct radiative forcing over California, *J. Geophys. Res.*, 118, 2372–2388,
1617 doi:10.1029/2012JD018364, 2013a.

1618 Zhao, C., S. Chen, L. R. Leung, Y. Qian, J. F. Kok, R. A. Zaveri, and J. Huang:
1619 Uncertainty in modeling dust mass balance and radiative forcing from size
1620 parameterization, *Atmos. Chem. Phys.*, 13, 10733–10753, doi:10.5194/acp-13-10733-
1621 2013, 2013b.

1622 Zhao, C., Z. Hu, Y. Qian, L. R. Leung, J. Huang, M. Huang, J. Jin, M. G. Flanner, R.
1623 Zhang, H. Wang, H. Yan, Z. Lu, and D. G. Streets: Simulating black carbon and dust

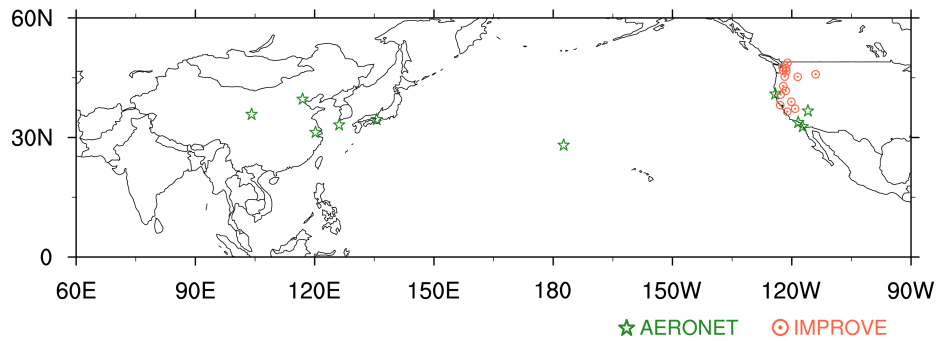
1624 and their radiative forcing in seasonal snow: a case study over North China with field
1625 campaign measurements, Atmos. Chem. Phys., 14, 11475–11491, doi:10.5194/acp-
1626 14-11475-2014, 2014.

1627 Zhao, C., M. Huang, J. Fast, L. Berg, Y. Qian, A. Guenther, D. Gu, M. Shrivastava, Y.
1628 Liu, S. Walters, G. Pfister, J. Jin: Sensitivity of biogenic volatile organic compounds
1629 (BVOCs) to land surface processes and vegetation distributions in California, Geosci.
1630 Model Dev. [Discuss.](#), doi:10.5194/gmd-2015-266, in review, 2016.

1631

Chun Zhao 4/12/2016 11:07 AM
Deleted: submitted to
Chun Zhao 4/12/2016 11:07 AM
Formatted: Font:Not Italic

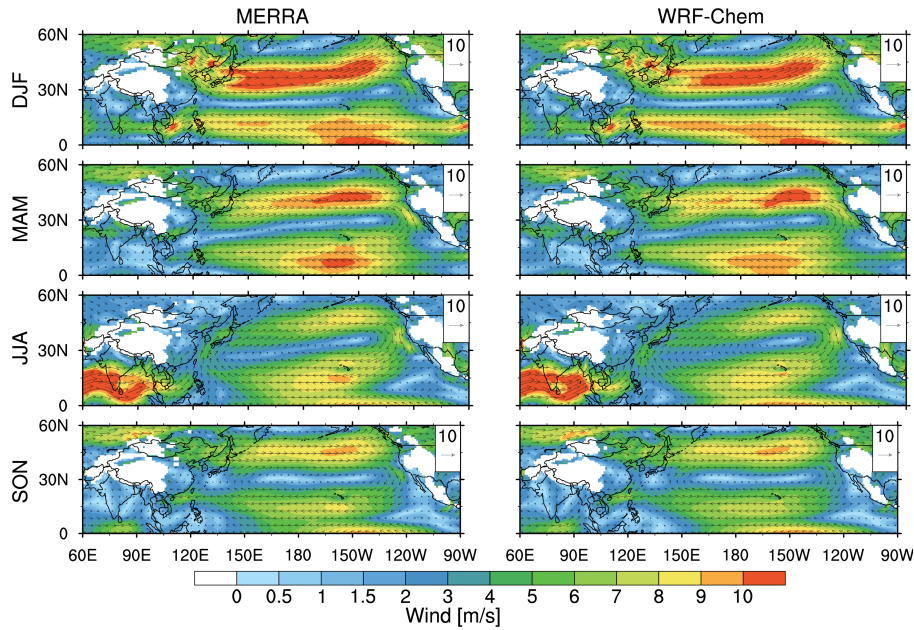
1633
1634
1635
1636
1637



1638
1639
1640
1641
1642
1643
1644
1645
1646
1647
1648
1649
1650

Figure 1 Observation sites for the AERONET (green stars) and IMPROVE (red dot circle) networks used in this study.

1651
1652
1653
1654



1655
1656
1657
1658
1659
1660
1661
1662
1663

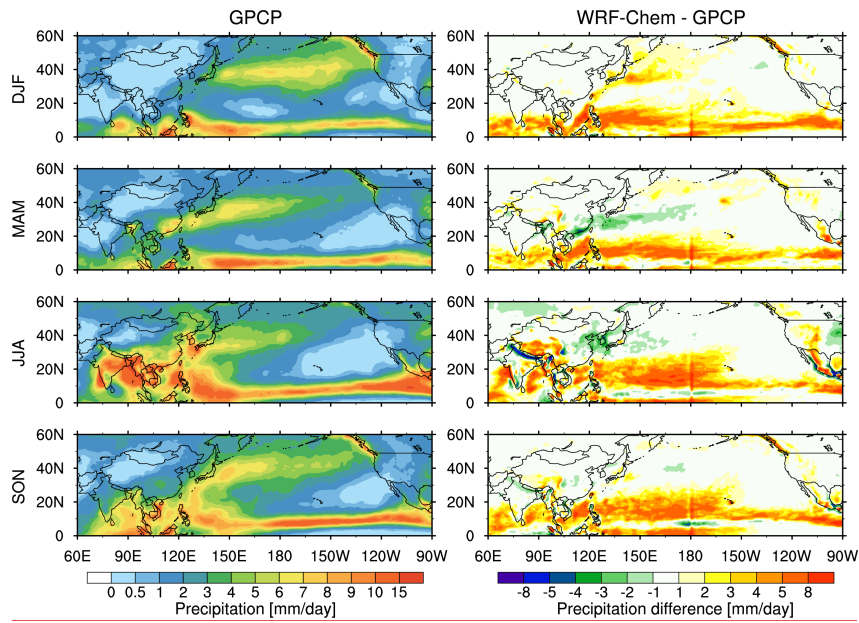
Figure 2 Spatial distributions of seasonal averaged wind fields at 850hPa from [the MERRA reanalysis](#) and [the WRF-Chem simulation](#) for the period 2010-2014.

Chun Zhao 4/12/2016 11:07 AM
Deleted: simulations
Chun Zhao 4/12/2016 11:07 AM
Deleted: of

1666

1667

1668



1669

1670

1671

1672

1673

1674

1675

1676

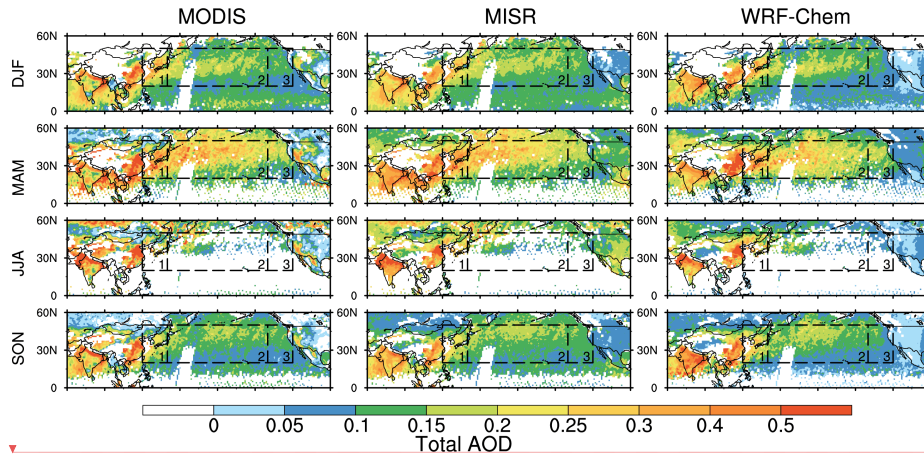
1677

1678

Figure 3 Spatial distributions of seasonal averaged precipitation from the GPCP observation and the difference between GPCP and the WRF-Chem simulation for the period 2010-2014.

- Chun Zhao 4/12/2016 11:07 AM
Deleted: observations
- Chun Zhao 4/12/2016 11:07 AM
Deleted: simulations
- Chun Zhao 4/12/2016 11:07 AM
Deleted: of

1682
1683
1684
1685



1686

1687 **Figure 4** Spatial distributions of seasonal mean 550 nm AOD from the retrievals of
1688 MODIS and MISR onboard Terra and the WRF-Chem simulation for the period 2010-
1689 2014. The daily results from MISR, MODIS, and WRF-Chem are only sampled for
1690 averaging when all of them have valid values at the same location and time. Three sub-
1691 regions are denoted by the black boxes: Region 1 (20° N-50° N and 120° E-140° E),
1692 Region 2 (20° N-50° N and 140° E-140° W), and Region 3 (20° N-50° N and 140° W-120°
1693 W).

1694
1695
1696
1697

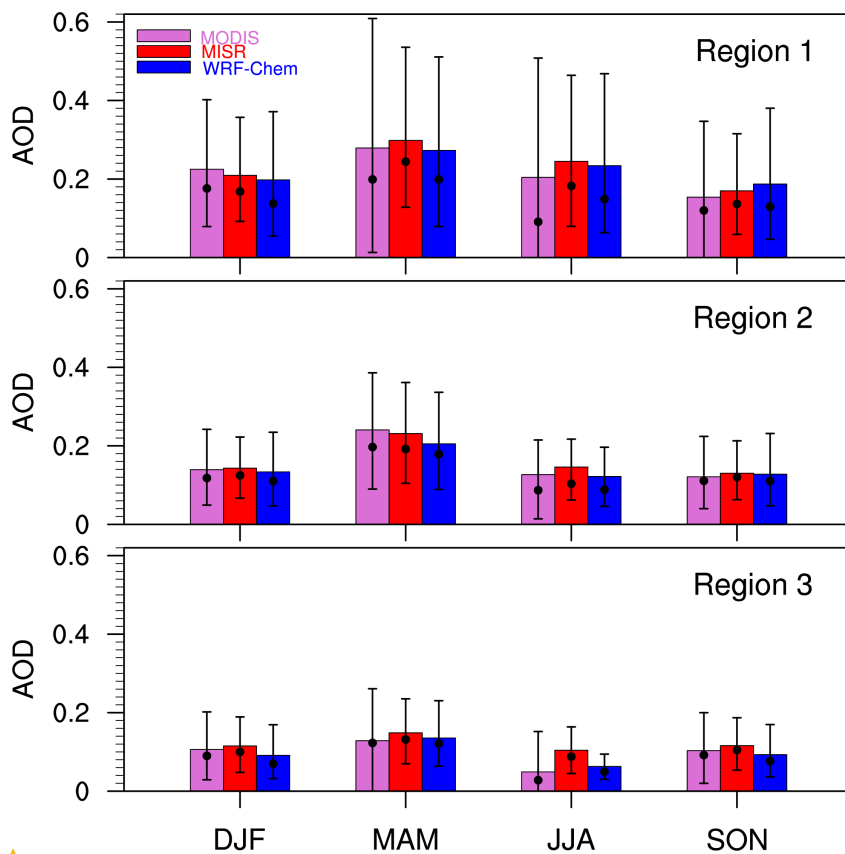
Chun Zhao 4/12/2016 11:07 AM
Deleted: -

Chun Zhao 4/12/2016 11:07 AM
Deleted: simulations

Chun Zhao 4/12/2016 11:07 AM
Deleted: of

Chun Zhao 4/12/2016 11:07 AM
Deleted: average

1702
1703



1704
1705
1706
1707
1708
1709
1710

Figure 5 Seasonal mean 550nm AOD from MISR and MODIS retrievals, and the corresponding WRF-Chem simulation averaged for the period 2010-2014, over the three sub-regions shown in Fig. 4. The values of bars represent the mean. The vertical lines represent 10th and 90th percentile values, and the black dots represent the median values.

Chun Zhao 4/12/2016 11:07 AM

Formatted: Font:Times New Roman, 16 pt

Chun Zhao 4/12/2016 11:07 AM

Formatted: Justified

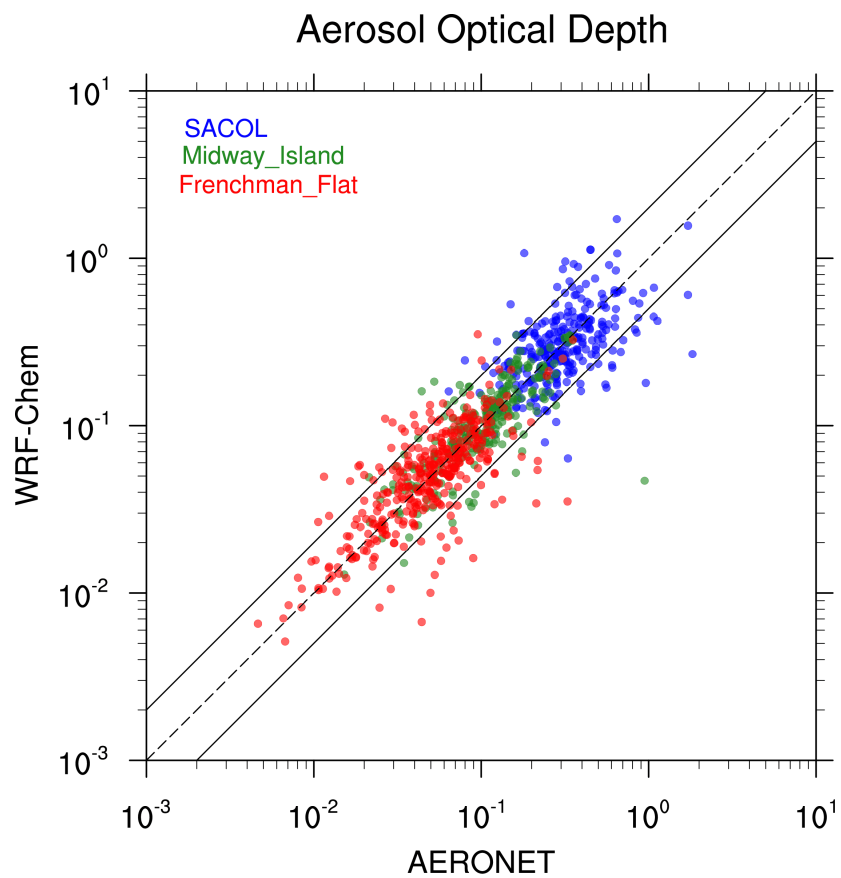
Unknown

Formatted: Font:(Default) Times New Roman, Bold

Chun Zhao 4/12/2016 11:07 AM

Deleted: simulations

1712



1713

1714 **Figure 6** The AERONET observations of daily AOD at 550 nm at the three sites
1715 (SACOL, Midway Island, and Frenchman Flat) versus the corresponding WRF-Chem
1716 simulation for the period 2010-2014.

1717

1718

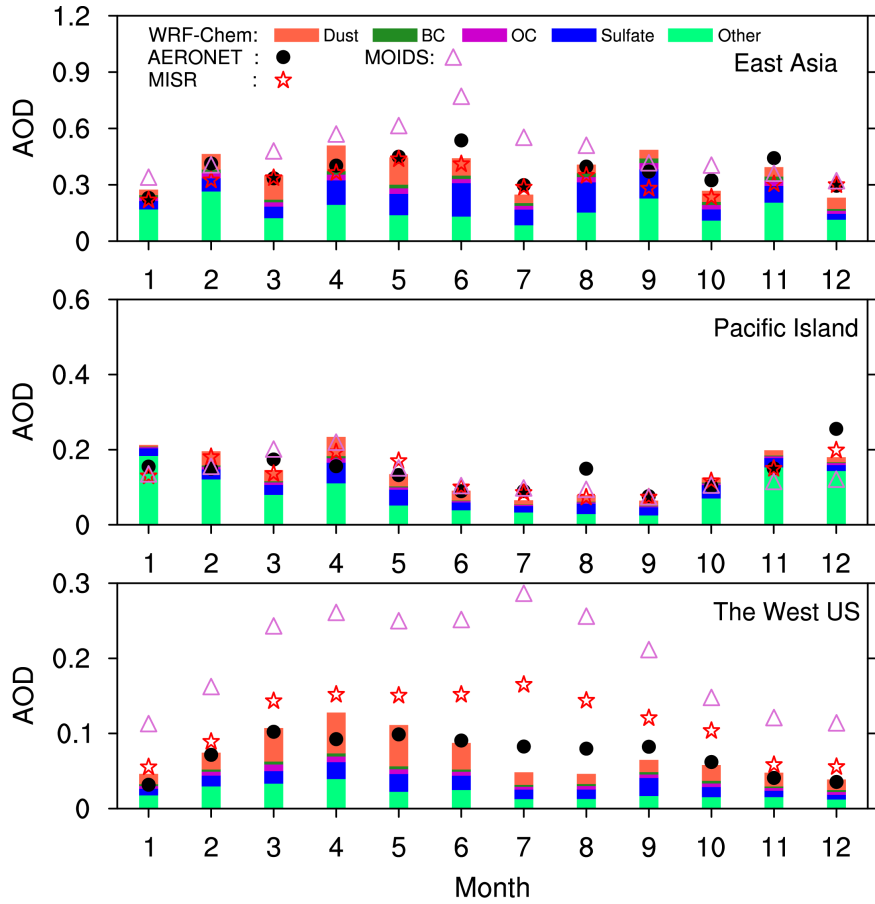
1719

1720

Chun Zhao 4/12/2016 11:07 AM
Deleted: simulations

1722

1723



1724

1725 **Figure 7** Monthly mean 550nm AOD from AERONET (black dots), MODIS (purple
 1726 triangles), MISR (red five-pointed stars) and the corresponding WRF-Chem simulation
 1727 (histogram) averaged for the period 2010-2014 at the East Asian sites, the Pacific island,
 1728 and the West U.S. sites as shown in Fig. 1.

1729

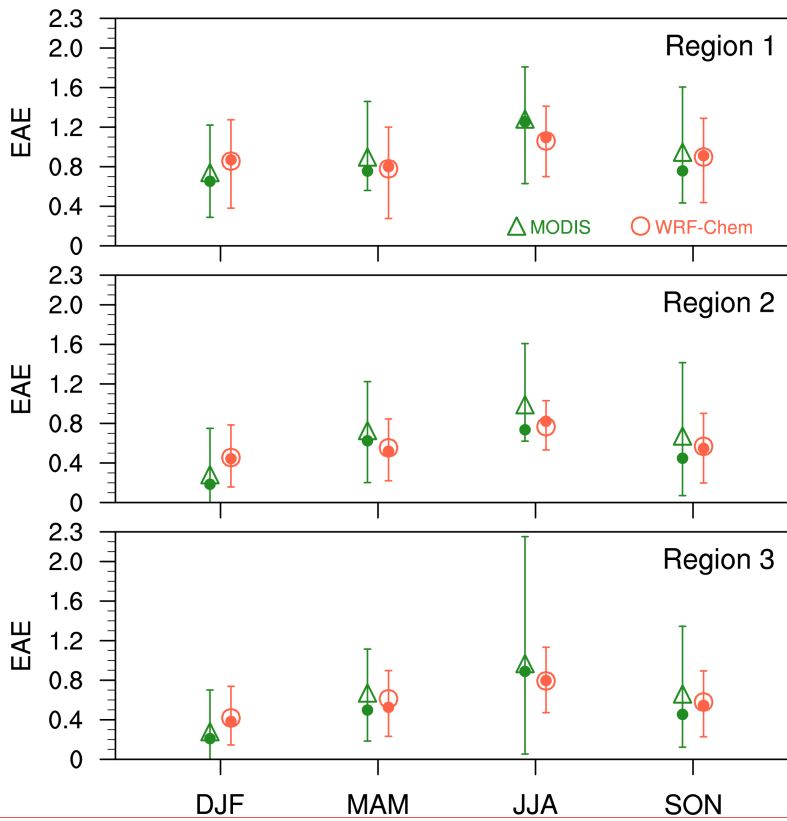
1730

Chun Zhao 4/12/2016 11:07 AM
 Deleted: simulations

Chun Zhao 4/12/2016 11:07 AM
 Formatted: Font:+Theme Body

1732

1733



1734

1735 **Figure 8** Seasonal mean EAE from the MODIS retrievals and the corresponding WRF-

1736 Chem simulation averaged for the period 2010-2014, over the three sub-regions shown in

1737 Fig. 4. The vertical bars represent 10th and 90th percentile values, the filled dots represent

1738 the median values, and the triangles and circles represent the mean values.

1739

1740

1741

Chun Zhao 4/12/2016 11:07 AM

Deleted: simulations

Chun Zhao 4/12/2016 11:07 AM

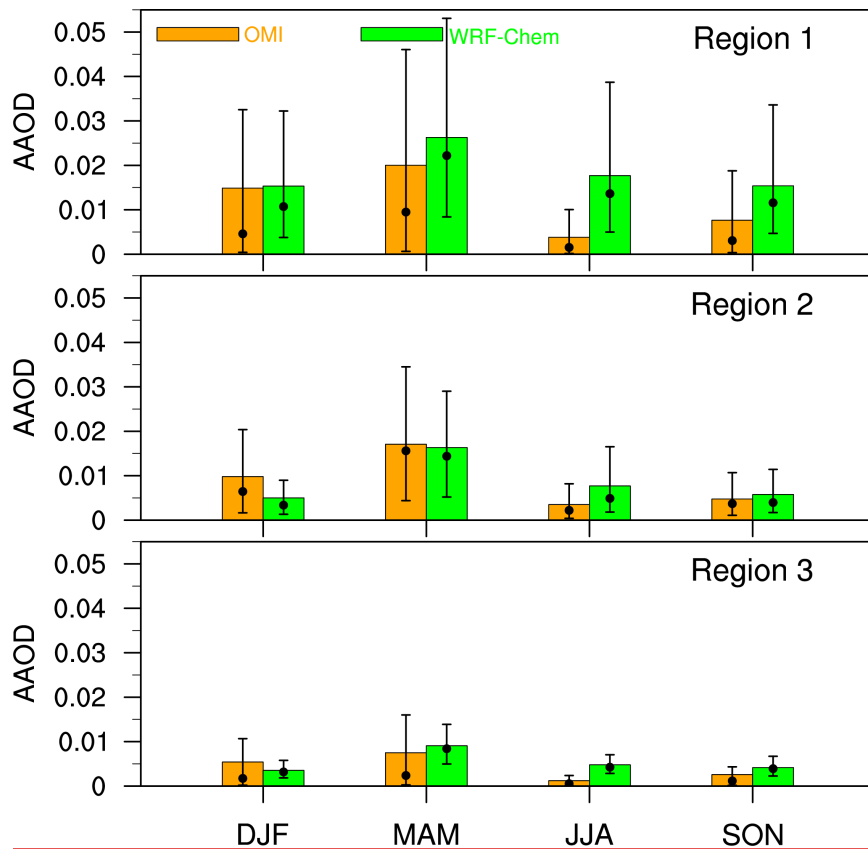
Deleted: and

Chun Zhao 4/12/2016 11:07 AM

Deleted: black

1745

1746



1747

1748

1749

1750

1751

1752

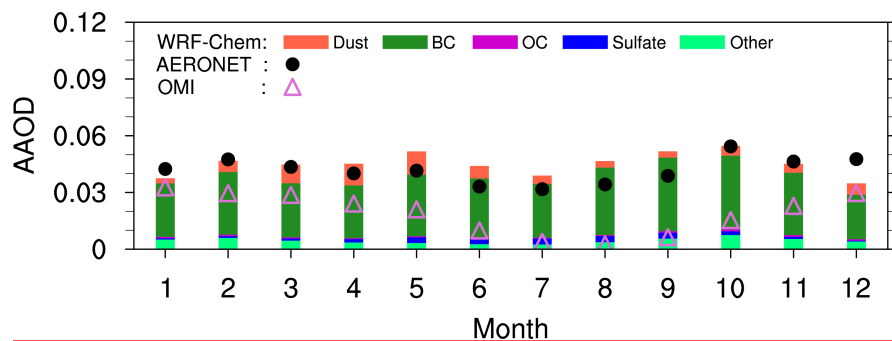
1753

1754

Figure 9 Seasonal mean AAOD at 500 nm from the OMI retrievals and the corresponding WRF-Chem simulation averaged for the period 2010-2014, over the three sub-regions shown in Fig. 4. The values of bars represent the mean. The vertical lines represent 10th and 90th percentile values, and the black dots represent the median values.

Chun Zhao 4/12/2016 11:07 AM
Deleted: simulations

1756
1757
1758
1759
1760
1761

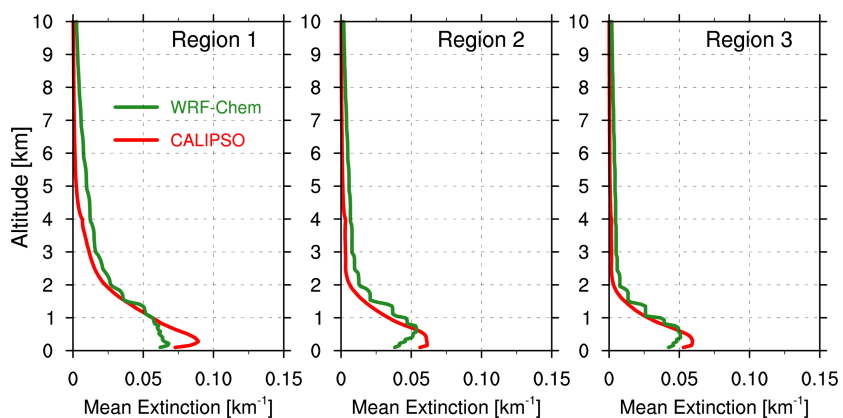


1762
1763
1764
1765
1766
1767
1768
1769
1770
1771

Figure 10 Monthly AAOD from the retrievals of AERONET and OMI and the corresponding WRF-Chem simulation averaged for the period 2010-2014 over the East Asia sites as shown in Fig. 1.

Chun Zhao 4/12/2016 11:07 AM
Deleted: simulations

1773
1774
1775
1776
1777



1778

1779 **Figure 11** Annual vertical distributions of extinction from CALIPSO observations and
1780 the corresponding WRF-Chem simulation averaged for the period 2010-2014, over the
1781 three sub-regions shown in Fig. 4.

1782
1783
1784
1785
1786

Chun Zhao 4/12/2016 11:07 AM

Deleted: simulations

Chun Zhao 4/12/2016 11:07 AM

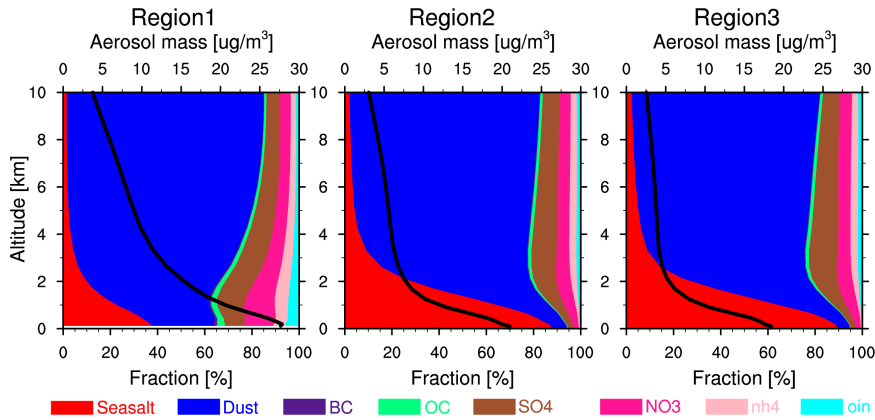
Deleted: ,

1789

1790

1791

1792



1793

1794

1795

1796

1797

1798

1799

1800

1801

1802

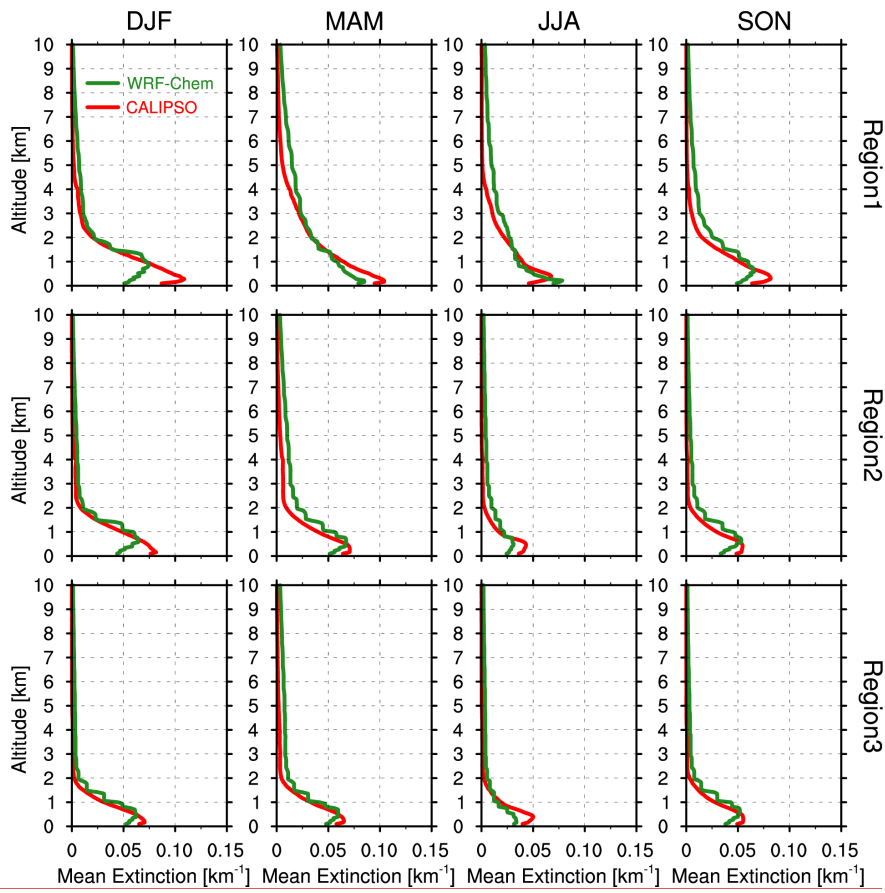
1803

Figure 12 Vertical distributions of mean aerosol mass (black solid line) and its composition fractions (colored shade-contour) from the WRF-Chem simulation averaged for the period 2010-2014 over three sub-regions as shown in Fig. 4.

Chun Zhao 4/12/2016 11:07 AM
Deleted: simulations

1805

1806



1807

1808 **Figure 13** Vertical distributions of seasonal mean aerosol extinction from the CALIPSO

1809 retrievals and the corresponding WRF-Chem simulation averaged for the period 2010-

1810 2014 over three sub-regions as shown in Fig. 4.

1811

1812

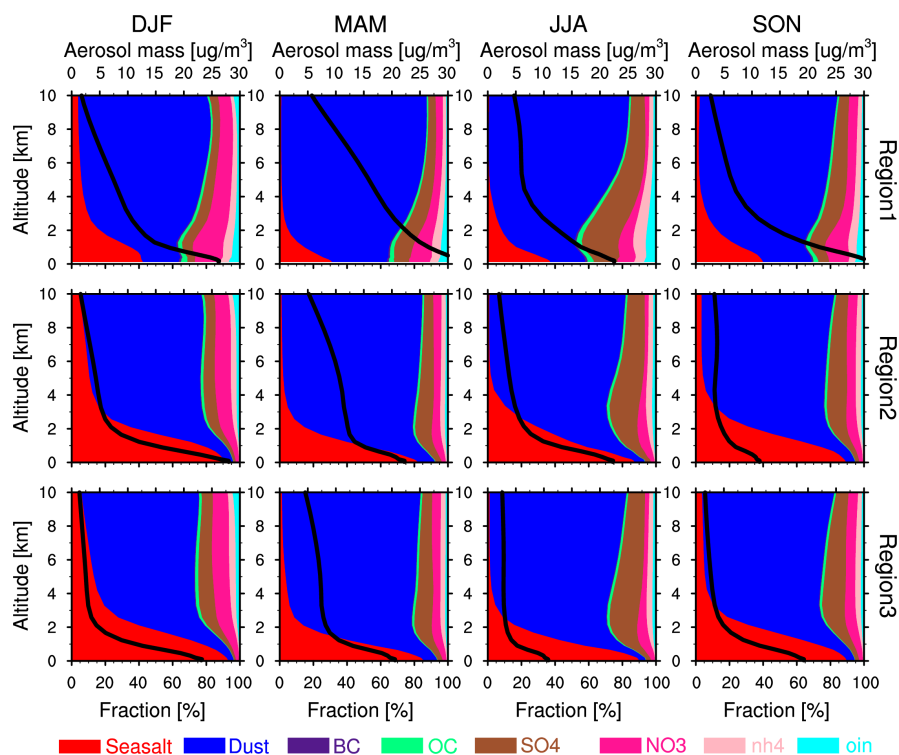
1813

Chun Zhao 4/12/2016 11:07 AM

Deleted: simulations

1815

1816



1817

1818 **Figure 14** Vertical distributions of seasonal mean aerosol mass (black solid line) and its
1819 composition fraction (colored shade-contour) from the WRF-Chem simulation averaged
1820 for the period 2010-2014 over three sub-regions as shown in Fig. 4.

1821

1822

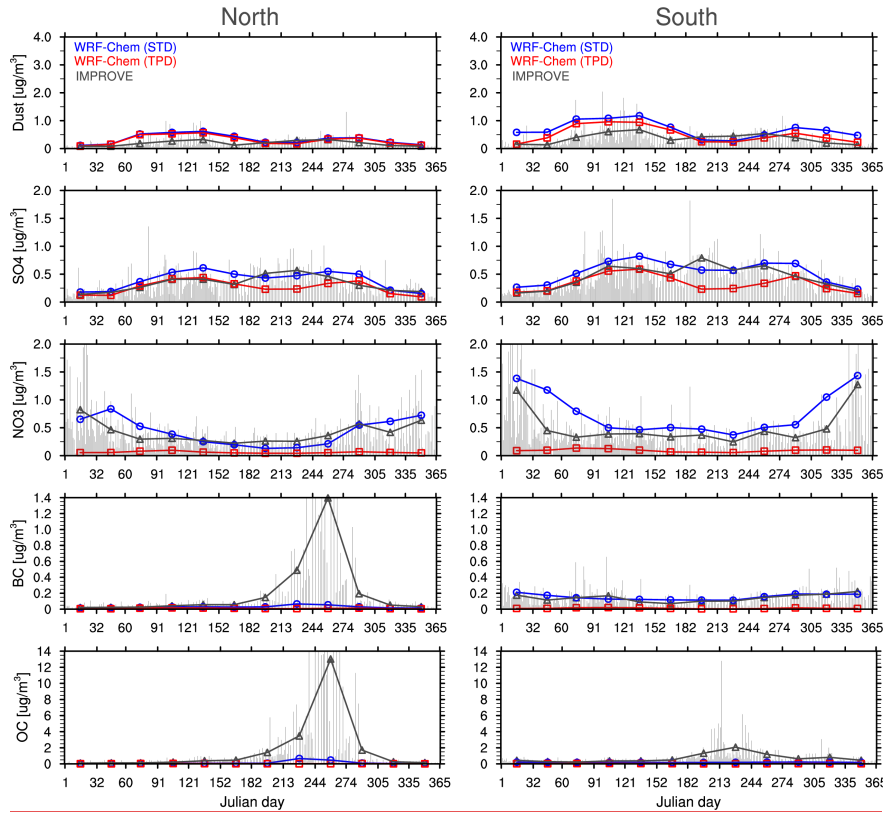
1823

1824

1825

Chun Zhao 4/12/2016 11:07 AM

Deleted: simulations



1828

1829 **Figure 15** Daily mass concentrations of fine-mode ($PM_{2.5}$) dust, sulfate, nitrate, BC, and
 1830 OC averaged for the period 2010-2014 at the IMPROVE sites over the Northwest and
 1831 Southwest U.S. (shown in Fig. 1) from the IMPROVE observations (vertical gray bars)
 1832 and the monthly average of the IMPROVE observations (gray triangles) and the
 1833 corresponding WRF-Chem standard simulation (STD; blue dots) and the sensitivity
 1834 simulation without North American emissions (TPD; red dots).

1835

Chun Zhao 4/12/2016 11:07 AM
 Deleted: US

Chun Zhao 4/12/2016 11:07 AM
 Deleted: simulations

Chun Zhao 4/12/2016 11:07 AM
 Deleted: simulations